A Novel Extension of Assisted History Matching to Honour Geological Constraints

Doctoral thesis (Dissertation)

to be awarded the degree

Doctor of Engineering (Dr.-Ing.)

submitted by

Dipl.-Ing. Bettina Jenei

from Debrecen, Hungary

approved by the

Faculty of Energy and Management Science at Clausthal University of Technology

oral examination date: February 17, 2022

Institute of Subsurface Energy Systems (ITE)

Clausthal University of Technology

Dean
Prof. Dr.mont. Leonhard Ganzer

Chairperson of the board of examiners
Prof. Dr Inge Wulf

Chief reviewer
Prof. Dr.mont. Leonhard Ganzer

External Advisor
Assoc. Prof. Dr Hussein Almuallim

Reviewer
Prof. Dr.-Ing. habil. Philip Jaeger

Acknowledgement

I would like to thank for the opportunity given to me to pursue a PhD degree at TU Clausthal in the Institute of Subsurface Energy Systems. I want to express my sincere gratitude to my Professors and Colleagues for their support! I would like to thank Leonhard Ganzer for inviting me to Clausthal, supervising me during my doctoral studies and being an outstanding role model in teaching! Special thanks to my friend, Roman Manasipov, for his dedicated moral support in all sorts of circumstances, for his exceptional skills in mathematics and for valuable consultations. I would like to thank HOT Firmsoft Solutions for providing me with the main workflow and the constant feedback from my external Professor, Hussein Almuallim. I hope to have the chance to work together in the future too! I would like to mention my dear office mate, Ke Li. We started our journey together in Germany and completed our doctoral defence on the same day! I am grateful to know him because he is the nicest and most tolerant person I know. I am grateful to Philip Jaeger for his contribution and interest in my topic and for introducing me to an amazing person, colleague, and now one of my closest friends, Hanin Samara. She showed me new ways of looking at life and work differently.

Last but not least, I would like to thank all my family, friends and acquaintances for teaching me something professionally or personally during this time.

EIDESSTATTLICHE ERKLÄRUNG - Declaration of Authorship

Hiermit erkläre ich an Eides Statt, dass ich die bei der Fakultät für Energie- und Wirtschaftwissenschaften der Technischen Universität Clausthal eingereichte Dissertation selbsständig und ohne unerlaubte Hilfe angefertigt habe. Die benutzten Hilfsmittel sind vollständig angegeben.

I confirm that I have prepared this doctoral thesis independently by myself. All information taken from other sources is clearly referenced.

Signature:

Date: 10.01.2022

Abstract

Most gradient-based history matching (HM) tools consider only the minimum and maximum geological constraints in the algorithm and the applied calculations. As a result, the crucial link connecting geological, petrophysical and reservoir engineering data is diminished or, at times, completely lost. Therefore, an iteratively created model suffers significantly from the subsequent inconsistencies, e.g., porosity/permeability relations do not honour their petrophysical constraints. This leads to questionable admissibility of the entire model and, thus, calls for the necessity of removing or minimalising these inconsistencies.

This dissertation focuses on finding an innovative solution to suggest better and more plausible results. It investigates a new workflow that improves the geological consistency and suggests automation of the process of assisted history matching with a strong consideration of different geological constraints with respect to the different rock type definitions. The new workflow is provided as an external tool using available libraries in Python that can be applied as an extension for existing assisted history matching workflows. The rock typing coupled with the adjoint method is proposed to maintain the relationship between model parameters to different rock types, which are then iteratively updated during the history matching procedure. The rock types have different porosity and permeability ranges, relative permeability curves, and different connate water and residual oil

saturation. The rock type is changed with corresponding parameters at the grid-block level based on the porosity and horizontal permeability change. The so-called rock-typing extension of the history matching workflow allows parameters to be modified co-dependently according to the rock type definition after the permeability adjustment suggested by adjoint-based sensitivity calculations.

As proof of the concept, the simulation was carried out for the synthetic model with the same parameter distribution with and without the extended workflow. The results show obvious improvements in history matching quality in terms of geological consistency with fewer iterations or within the same amount of iterations with favourable objective function (OF) values. The simulation output achieves the target observed production profiles driven by the automatic joint correction of the saturation functions, including the initial saturations due to the rock type adjustments.

Properly including the porosity-permeability correlations, priorities and model-specific details, the rock type can bind all the geological properties together, allowing consistent parameter changes for an improved history matching process. Since the base case is a product of geostatistical modelling, the level of certainty needs to be accounted for. Therefore a statistical distance is applied, which is the Mahalanobis distance. The Mahalanobis distance is associated with each rock type; it helps to guide the validation and correction step and determines the appropriate rock type based on the underlying statistical information. It also serves as the basis for the calculation to prove the concept.

Overall, the novel approach has successfully managed to improve the geological consistency of the models during the history matching process, thereby improving the quality and reliability of the reverse simulation. Moreover, this extension includes workflow automation. It is an excellent practical standalone achievement that can potentially reduce the previously required work hours for the iterations to find the right set of data.

List of Figures

List of Tables

TABLE OF CONTENTS

"Essentially, all models are wrong, but some are useful."

- George E. P. Box

Chapter 1 Introduction

A reservoir model's history matching (HM) is a significant and often time-consuming task in every field study. History matching can be broadly described as the calibration of a static model until it produces the closest possible match in dynamic results to the observed history (Oliver, Reynolds and Liu, 2008). In order to achieve a realistic reservoir behaviour that matches historical observations, the engineer in charge needs to change the static parameters in the model. This time-consuming and complex iterative process is described as a mathematical problem(Oliver, Reynolds and Liu, 2008). Therefore it can be a computer-assisted or automated procedure.

History matching can be formulated as an ill-posed inverse problem, where the output is known while the input is an unknown variable. Therefore adjustments must be made to the input(Oliver, Reynolds and Liu, 2008). The input data of the static model is provided in a limited amount, which leads to a high amount of uncertainty (Pyrcz and Deutsch, 2014). Thus, appropriate alterations to the input data must be made to iterate the result closer to the target. However, multiple

parameter combinations can provide the same result. The input is the petrophysical data; the output is the production and pressure data observed over a certain period. Automated, accurate, and fast methods that consider the geological constraints are already developed (Zakirov *et al.*, 2017). However, these computer-assisted history matching tools only apply minimum and maximum bounding geological constraints on the considered input variables (Almuallim *et al.*, 2018).

During history matching, the link between lithology, petrophysics, and special core analysis (SCAL) is often lost. Therefore, the iteratively created models can suffer considerable geological inconsistencies; for instance, a rock type is not honoured by petrophysical properties(Bentley, 2016). Since these models are used to predict future performance, physical consistency needs to be improved. To tackle the problem of geological inconsistency during history matching, typically, an approach of combining the geostatistical modelling and history matching is applied (Schulze-Riegert *et al.*, 2013). A variety of papers were published on that topic using different optimization techniques, such as ensemble methods (Liu and Oliver, 2005), (Maschio, Vidal and Schiozer, 2008), gradient-based optimization (Bukshtynov *et al.*, 2015), deep learning methods (Caers, 2002), (Mosser, Dubrule and Blunt, 2019). However, not much attention has been paid to the significance of the link between SCAL saturation functions and rock types during the history matching process.

The crucial point of not diverging from the original static model is to avoid decoupling the data. The static model coming from geostatistical modelling is a complex system, as the data comes from different sources of many disciplines (Pyrcz and Deutsch, 2014). The input for reservoir characterization (Pyrcz and Deutsch, 2014), in fact, is coming from petrophysics (Tiab and Donaldson, 2015), seismic interpretations, geological study, well test analysis, flow simulations (Helmig, 1997) and geostatistics(Johnson, 1996; Pyrcz and Deutsch, 2014; Pyrcz, 2018c). The geomodel, hence, contains the essential connection between different data types coming from the branches mentioned above. Therefore the correlation between other parameters as well as the constitutive relation needs to be maintained and honoured. In this work, the link between model parameters is recovered iteratively based on the rock type adjustment defined by the corresponding regions in ϕ-k diagrams in an automated way.

Understanding and characterising the subsurface fluid flow and its system is not only the primary concern of petroleum engineering. It also has enormous importance in several other practical applications in subsurface energy systems, such as the exponentially developing underground storage of energy and gases, one of which is carbon capture and storage (CCS) (Class *et al.*, 2009) or hydrogen storage (Panfilov, 2010). Due to the radically increasing global warming issue, the need for CCS has jumped to a higher level. Understanding the flow and transport behaviour of the earth's subsurface can answer many questions, such as the safety of CCS and other underground storage of energy and gases.

One should also not forget about hydrogeological considerations (Michael and Voss, 2009), such as drink water formations and geothermal reservoirs. Finally, a better understanding of underground fluid flow can solve the current problem related to the transportation of different types of pollutants in the aqueous phase, thereby affecting the environment (Mosser, Dubrule and Blunt, 2019). That being so, the improved history matching tool has a great potential to be widely used in the future outside of classical petroleum engineering.

Profound convening research proved that implementing co-dependent geological constraints can improve assisted history matching (AHM). The improvement can be achieved by extending the presently available tools by introducing an external workflow and the knowledge gained from the results of Mr Awofodu's work (Awofodu, 2019). It aimed to develop advanced techniques for calibrating reservoir simulation models to available observed data using the adjoint method (Almuallim *et al.*, 2010). Subsequently, algorithms and workflows for improving reservoir characterization by detecting hidden reservoir features (Awofodu, Ganzer and Almuallim, 2018) in reservoir simulation models have been developed throughout that research project using the adjoint technique.

This work developed an integrated and automated workflow using state-of-the-art optimization techniques combined with the adjoint method (Almuallim *et al.*, 2010) for history matching. The developed workflow was ascertained through nine reservoir simulation models varying in reservoir heterogeneity complexities and reservoir physics. The aim is to

improve reservoir characterization within the history matching framework. In the past, the history matching de facto was rather impairing the reservoir characterization from geoscientific aspects because the priority was given to matching the dynamic data without necessarily maintaining geological realism(Bentley, 2016). The workflow (Jenei *et al.*, 2020) established in this study improves the model in terms of dynamic and prediction performance and improves or at least does not harm the static model in its established relations. The workflow uses the results of the adjoint-based history matching tool and automatically validates or corrects the rock types with the utilisation of Mahalanobis distance (Mahalanobis, 1936) calculation.

1.1 Definitions

Throughout the entire dissertation, there are two significant definitions often used. These are the rock type and the geological consistency. Since these terms can have flexibility in their meaning, the used definitions need to be clarified.

Rock type

The rock type is a geological formation that can be identified and characterised through the rock properties, namely the porosity and the absolute permeabilities and the rock fluid interactions, so-called saturation functions. In the scope of this work, the interest in differentiating rock type extends to the level of details satisfying the

proper distinction between the different rocks in terms of flow properties. Therefore the rock type is utilised to differentiate the flow behaviour. Only the parameters directly affecting the dynamic simulation characterise the rock types in this research. The mineral composition, compaction, geological age, depositional environment, and other factors from a geological point of view are not investigated. A detailed review of rock type and facies modelling can be found in Chapter 3.

Geological consistency

In this research, the geological consistency means that the preliminarily established connection during geostatistical modelling is maintained through the history matching phase of the reservoir characterisation, avoiding the introduction of physically and geologically contradicting data and sudden changes in the reservoir properties. The rock types are modelled after stratigraphic layering and large-scale modelling within the reservoir characterisation process. Within the identified rock types, each rock type has its porosity, permeability distributions, established porosity-permeability ($\boldsymbol{\phi}$-k) relationships and corresponding saturation functions which are the relative permeability and capillary pressure. In the scope of this research, the geological consistency is when the defined parameter ranges and distributions are not violated, and the link between the different rock type-dependent parameters is not lost during history matching. In addition, the uncertainty of the model parameters directly relates to the tolerance of the deviation. Details about the

relationship between uncertainty and geological consistency are summarised in Chapter 3.

1.2 Motivation and importance of improved geologically consistent history matching workflows

History matching processes have significant importance in the management decisions of projects. Accurate and rapid methods and tools to process history matching, which considers the geological constraints, are already developed (Almuallim *et al.*, 2018). However, not enough attention is paid to the relationship between the model parameters during the history matching process.

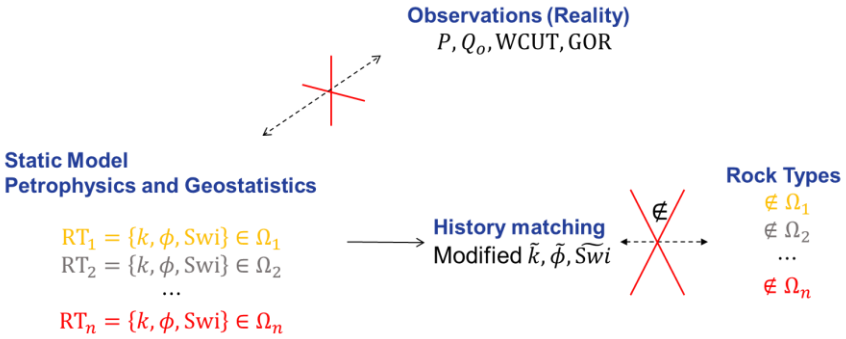

Fig. 1.1.: The conflicting indicators in reservoir characterisation workflow (Jenei et al., 2020)

In other words, they do not honour the rock type, so the relationship between lithology, petrophysics, and SCAL is substantially lost. Fig. 1.1 represents the mentioned issues. This dissertation aims to optimize, improve and test the available Assisted History Matching (AHM) tools to perform reliable, fast, and practical history matching within engaged geological constraints (Jenei *et al.*, 2020). The core of this new investigation is an explicit consideration of the geological constraints that automatically conserve the relationship between petrophysical and lithological information through the rock type parameter. When the reservoir model is initialized at reservoir conditions, the base case forward simulation model honours the geological details consistently (Ertekin, Abou-Kassem and King, 2001).

The process of the standard history matching is the adjustment of the model parameters until the simulation model reproduces the actual observed reservoir behaviour within an acceptable range (Oliver and Chen, 2010). In the applied gradient-based assisted history matching, the model parameters are modified according to computed sensitivities, and it allows parameter changes at the grid block level in efficient computational time (Almuallim *et al.*, 2010). The parameter constraints are honoured individually without their correlation. The minimum and maximum limits are defined for each parameter, but the changes of the model parameters are independent, meaning that their relationship is ignored. Therefore, the iteratively created model suffers from certain geological inconsistencies. These models then are used to predict the

future performance of the reservoir through the geologically inconsistent model.

In the new workflow (Jenei *et al.*, 2020), the link between model parameters is to be recovered iteratively based on complex criteria, including rock type distribution and rock-type dependent properties, such as permeability and porosity (ϕ-k) correlation, relative permeability, capillary pressure and irreducible saturation.

Although various methods of performing proper history matching are available on the market, they try to preserve the geological consistency, but none considers the relationship between the model parameters within the same integrated workflow like this research does. In stochastic approaches, geological consistency is achieved by creating new model realisations. While, in gradient approaches using one realisation, the preliminarily defined porosity and permeability constraints during reservoir characterisation and the geostatistical modelling are honoured individually without their correlations. The presented workflow includes the correlations where the rock type binds all the properties together so that every parameter changes automatically in a continuous and connected fashion, within the same realisation.

Generally, history matching is conducted in a sequence; the process is divided into different stages, global-level and well-level. Fluid production/injection rates such as reservoir rate or individual well-rates

and pressures such as average reservoir pressure or bottom hole flowing pressure can also be separately matched within the global and well-levels. The history matching sequence is usually not automated; therefore, the secondary goal is to provide the automated history matching process for the general sequence as an option, which can be more efficient than manually setting up the different stages one by one after each stage.

This research investigates an automated workflow that improves the process of assisted history matching with a strong consideration of different geological constraints and respect for their relations. It is also of great benefit that developing an external tool is possible, which improves the results and the efficiency of existing assisted history matching tools regarding geological consistency.

1.3 Objectives

Most state-of-the-art history matching approaches are good at global level history matching, but they are not fulfilling in terms of local optimisation. Most of them are even automated, but they lack geological consistency. Therefore, the most fundamental objectives of this research topic are defined as the following first two:

- Geological consistency: One of the main objectives is to achieve geological consistency to a higher level than already available. The

geological consistency should be maintained through rock type definition.

- Automated-extended workflow: Implement a general, robust workflow, which can be applied to any simulation software to perform automated history matching.

    - Proof of Concept Model: Develop a proof-of-concept model, which could serve the fundamental purpose of proving the concept within realistic data ranges and distribution.

    - Sensitivity Analysis: Analyse the performance of the extended workflow concerning the parameters which characterise different rock types, namely porosity, permeability, relative permeability, and capillary pressure functions. Demonstrate the advantages of the created workflow compared to the conventional approach through the different history matching cases - representing the advantages of the rock type adjusting workflow.

Not included in this work

The work combines different disciplines: numerical reservoir simulation, history matching (numerical optimization), geology, petrophysics, geostatistics and algebra. Therefore, each topic is described to the extent sufficient for the application and the understanding of the presented approach.

The simulation software specifics and numerical methods are not included in this work. Therefore, the solvers are not discussed in detail because there were no modifications/implementation in the simulator since the work instead focuses on the applied engineering solution.

The idea of performing computer-assisted history matching employing a post-processing tool is not new. Therefore, the workflow description does not provide a detailed insight into the adjoint-based gradient approach implementation. A detailed review describes the reason behind the selection of method, including the practical and fundamental understanding of the advantages and disadvantages of its application compared to the other methods.

The geostatistical reservoir modelling is not covered to the greatest extent in this work. The dissertation only presents the relevant fundamentals applied in this research and information to help understand the geological consistency.

1.4 State of the Art

Due to its importance in management decisions, different methods were developed to create assisted history matching tools. Assisted history matching tools are beneficial since the manual history matching process is less accurate and requires more man-hours. In assisted history matching, the mismatch is minimized precisely, while it is only based on the engineer's judgment in the manual process. In addition, most of the time, the manual way violates the geological constraints of the model due to the generally applied box multipliers. The bigger the size of the model, the higher the level of complexity and the more details the models have. Therefore it becomes more and more difficult, if not impossible, to handle them only with a human brain during a manual history matching procedure. With assisted approaches, the sensitivity of the model parameters to the mismatch is quantified precisely, accounting for every single influence of the model parameter. Therefore, with assisted tools, matching large models with a significant amount of complexity and details is more accurate than with a manual approach and, most importantly, feasible.

History matching is static model calibration until the model reproduces the closest possible dynamic result to the observed history. From the mathematical point of view, it is an ill-posed inverse problem. The geologically consistent spatial distribution of the petrophysical properties underground needs to be found, which gives simulation results in good agreement with the historically observed dynamic data

(Oliver, Reynolds and Liu, 2008). The history matching problem can be analysed solved with different mathematical approaches.

Several commercial tools are available on the market with assisted history matching and uncertainty analysis features. The most widely used ones by far, but not limited to, are MEPO (Schlumberger, 2021), ResX (Resoptima, 2021), tNavigator (Rock Fluid Dynamics, 2021), CMOST (Computer Modelling Group, 2021), 3DSL (Streamsim Technologies, 2021), Tempest ENABLE (EMERSON, 2021), Raven (Christie, Arnold and Winton, 2021), CougarFlow (BeicipFranlab, 2021), SenEx (HOT Engineering, 2021). They all attempt to honour the geological constraints, but none of them does it in a linked, integrated, and fully automated way yet.

For instance, MEPO is a Multiple Realization Optimizer, which uses modern optimization and experimental design techniques. It allows the user to explore better the solution space of the problem. The stochastic method determines different simulation runs depending on the probability of the parameters included in the model with known minimum and maximum values. These methods can create various parameter distributions based on geostatistical information. In contrast to the advantages, this method is neither convenient in its computational time nor considers the relationship between the model parameters.

Additionally, proxy (Zubarev, 2009) and dimensionality reduction models (Crevillén-García, 2018) help to reduce the computational costs of the history matching process. It still faces some difficulties in terms of the complex relationship of the model parameters, which are still not considered.

The other example, SenEx, is a gradient-based assisted history matching tool. The model parameters are modified according to computed sensitivities. The adjoint method allows parameter changes at the grid-block level in efficient computational time (Almuallim *et al.*, 2010). The changes of the model parameters are also independent, meaning that their relationship is ignored.

In joint research to utilise the benefits of the stochastic and gradient technique, a combination of both methods to improve history matching on a reservoir model was implemented and published (Schulze-Riegert *et al.*, 2013). However, the resulting model does not honour the geological constraints to the greatest extent. To avoid geological inconsistency, a research paper (Mosser, Dubrule and Blunt, 2019) presents a developed tool that allows history matching to consider correlations between the model parameters and uses rock type as a model parameter on a synthetic case study for single-phase flow.

The principal objective of this work is to combine the statistical and adjoint-based gradient methods with the potential of future extension of its application for real cases. Nonetheless, it should apply to

commercial tools or at least easy to be adapted to other history matching workflows.

1.5 Outline of Thesis

The particular focus of this work is thoroughly discussed in the following chapters, i.e., Chapters 2-7.

Chapter 2 - Literature Review of History Matching – State-of-the-Art

Chapter 2 provides a literature review on the history matching procedure in theory and application. It gives the necessary overview of the fundamentals and different history matching techniques, including basic concepts, manual and computer-aided assisted history matching methods. This section summarizes the fundamentals of history matching techniques that are most commonly used in the industry. In addition, it provides a short overview of a typical history matching sequence as well.

In detail, this chapter compares the adjoint and direct formulation of the gradient approach, and as well it presents the application of the adjoint method. It discusses the advantages of the applied assisted history matching approach and the mathematical description of the application. It gives a clear picture of the impact of reservoir characterization on history matching through the role of history

matching in reservoir characterization and vice versa. Furthermore, the chapter lists the utilised tools and software applications in this research.

Chapter 3 - Rock Typing

The main message of Chapter 3 is how to identify a sufficient amount of rock types, which are beneficial for subsurface flow simulation and history matching as well. It describes and provides the necessary fundamentals of rock typing, also known as facies modelling. It highlights the theoretical importance of reservoir characterization in history matching, especially considering the established connections of different model parameters from geostatistical modelling. It shows the importance and definition of varying facies categories.

Moreover, it describes the identification of the right amount of rock types in a geological model. It summarises the different facies definitions and modelling techniques and clarifies the used meaning in this work. The fundamental properties which are dependent on the various rock types are listed and explained. These are the porosity, absolute permeability and their relationship, and saturation functions, which play an essential role, are relative permeability and capillary pressure functions. Additionally, the commonly used parameterisations of these functions are presented.

Chapter 4 - Methodology and Rock Typing Workflow

This chapter consists of two main parts: methodology and the rock type adjusting history matching workflow. It summarises the applied methodology of preparing the proof of concept model with a simple synthetic case and the designed workflow.

Therefore, it describes the design and construction of a synthetic model to extend the history matching tool that allows for assessment, validation, and correction within engaged reservoir geological constraints focusing on reservoir pressure, oil, and water rate match with liquid rate control.

As a second part, the developed workflow is explained in detail. The optimised workflow is based on multiple test cases and automation of it integrating into the inner loop for the black oil simulator ECLIPSE and tNavigator. Furthermore, it describes the theory behind the extended workflow completed for integration into various user interfaces.

The following most valuable concept of the rock type adjusting history matching workflow is described in this chapter with details.

- Constraints – Set Up
- Automation - Multiple Set-Up combinations
- Adjustment of Rock Type

- Python workflow

Then the main parts are the Mahalanobis calculation, and the confidence interval is defined to understand the reason behind using it.

- Distance Calculation - Application of Mahalanobis distance and the conditions of application
- Application of Confidence Ellipse Calculation
- Rock Type Selection
- Conditions of application of the Mahalanobis distance

Chapter 5 – Proof of Concept – Simple Quarter-Five-Spot Model and Chapter 6 - Results

In Chapter 5 and 6, the results of the nine test cases are summarized and presented. It contains the model descriptions of "TRUTH" and BASE cases, including the initial and boundary conditions of the simulation cases. It lists the model description with the different parameter setups in Chapter 5. Chapter 6 consists of a comprehensive summary of the results of all nine cases conducted using the nine variations of the simple model. The results of the "PERMKR" case is presented with the details and thoroughly analysed. The comprehensive summary of results in each case is shown separately, comparing the

required number of iterations, the objective function and the geological consistency indicators in both multi setup combinations "BESTPARENT" and "ITERNUM". The history matching setups are performed without (standard workflow) and with the rock typing workflow.

Chapter 7 – Summary

Chapter 7 summarizes the significant aspects of this work and provides an overview of the conclusions, including suggestions for future investigations and further other research activities on the topic of improved history matching.

Chapter 2 Literature Review of History Matching – State-of-the-Art

This chapter provides a comprehensive overview of the fundamentals considered in this dissertation. It covers the topic of reservoir characterization workflow from the geostatistical modelling through the facies definition to the post-processing tools, mainly focusing on the utilised history matching approach. In addition, it lists and briefly explains the state-of-the-art and most widely used history matching techniques and algorithms(Oliver and Chen, 2010). The used methods and their mathematical background are discussed and described in this chapter. It is focused and limited to the parts necessary for the work performed in this dissertation. The chapter also shows the advantages, benefits and reasons of the utilization of the adjoint approach in comparison to the direct one; however, the implementation of the used gradient approach is not described. The software tools used in this dissertation are summarized and listed in Chapter 2.4. Lastly, the geostatistical reservoir modelling (Pyrcz and Deutsch, 2014) is covered with the relevant information to help understand the geological consistency.

2.1 Theory and application of History Matching

The history matching is an iterative and, therefore, time-consuming procedure. The key is the calibration of the geological model to reproduce the realistic reservoir behaviour (Oliver, Reynolds and Liu, 2008). It can be conducted either manually or with the help of a computer program(Oliver and Chen, 2010). Considerably extensive experience and engineering judgement are required in both cases.

Assisted history matching is widely used due to its efficiency and improved computational power compared to the technical capabilities in the past. History matching can be mathematically defined as an inverse problem since the output is known, but there is limited information about the input. There is no unique solution to these problems. Thus, the history matching needs to be well constrained and controlled in order to create a reliable model of the underlying formation (Oliver, Reynolds and Liu, 2008).

The final models are often used in decision-making and future predictions. Therefore honouring the geological features and interconnected petrophysical details is crucial (Liu and Oliver, 2003). Particularly, vast consideration should be given to the relationships established during reservoir characterization. This procedure involves a complex, thorough, and well-structured geological modelling effort in order to build a static model, which serves as the input for the base case simulation (Pyrcz and Deutsch, 2014). Consequently, the basic details

of the initial model should not be ignored or forgotten during further model alterations, such as reverse simulation iterations.

The history matching procedure can be limited by the type and characteristics of a given problem to be solved(Oliver and Chen, 2010). For example, the complexity of the model, the scale of the model, the number of wells, and the applied fluid model define the chosen approach. The objective of the history matching is pretty the same in terms of minimization of the mismatch, but the realisation of it, the methods can vary over large ranges. The choice of approach is dependent on several factors. Primarily, the application of one particular minimization method highly depends on the difficulty of the implementation (Oliver and Chen, 2010).

On the other hand, the history matching problem itself defines the required optimization method(Oliver and Chen, 2010). For instance, a smaller and simpler model can be easily matched manually within a reasonable amount of time, while a larger, more complex model might require computer-assisted optimization. Therefore, the complexity of the model, i.e., the size of the reservoir, compartmentalisation, geological features, the number of wells, and fluid models, always need to be considered to select an optimization tool.

The most common history matching techniques are listed and summarized in the following subchapter. The adjoint technique is

explained in detail, as this research is developed based on the utilization of the adjoint algorithm.

2.1.1 Overview of the Algorithms for History Matching

The development of different history matching methods and algorithms has increased exponentially in the last 25 years. A detailed review has been conducted by D.S Oliver about all the existing and most often used tools. These methods are briefly listed below before the detailed explanation of the adapted method(Oliver and Chen, 2010).

The most widely applied techniques, history matching methods:

- Manual History Matching: It has a high range of flexibility in terms of the parameters and the data set. Hence, it poorly assesses the uncertainty and consumes significant investment in human/engineering work. Since it is extremely time consuming, it is not suitable for large reservoirs with a high amount of variables.

- Evolutionary algorithms: It is suitable for discrete parameters and highly non-Gaussian distributions. Unfortunately, these algorithms have slow convergence; therefore, it is not robust. Along with the manual history matching, the evolutionary algorithms are weak in uncertainty assessment and are not advisable for large and complex models.

- Ensemble Kalman Filter (EnKF): This technique generally underestimates uncertainty. On top of that, additional parametrisation is required to take in the discrete variables. EnKF is highly parallelizable and is also well-suitable for models with a large number of variables. Moreover, the algorithm has high flexibility, as it can be used with all model variables and adapted to different simulator programs.

- Adjoint approach: The primary advantage of this method is its robustness due to its considerably fast convergence rate. This method provides a single history match with a high-efficiency level in terms of computation time and effort in total. It takes more computational time than other methods per iteration because, on top of the simulation, the calculation of derivates takes additional time, but in return, it takes fewer iterations to reach the optimal solution. In comparison to the direct approach, the adjoint formulation is still faster. Moreover, with several history matches, uncertainty estimation becomes possible. Nonetheless, with its great benefits, the adjoint method is not the most flexible approach, as it is not simply adaptable to all simulators and variables.

The following section further describes the manual and assisted history matching approaches, including those as mentioned above widely used techniques.

2.1.2 History Matching Phases/Sequence of History Matching

In general, the history matching process, independently from manual or automated/assisted, can be divided into two main phases: the global (field-level) and the local (well-level) performance. On top of that, the global and local phases need to be separated into smaller steps. The typical sequence of history matching procedure is the following (Aziz and Settari, 1979), (Ertekin, Abou-Kassem and King, 2001):

1. Match the global (field level) average reservoir pressure (Pr): This step assures that the overall reservoir energy is matched.

2. Match the individual fluid rates at field-level, such as oil rate(q_o) and water rate(q_w), which includes water-cut (WCUT). In case gas production is present, the gas rate (q_g) and the gas-oil ratio (GOR) need to be matched as well. This phase assures that the liquid production rate is distributed correctly within the different phases.

3. Match the different fluid rates (q_o, q_w, q_g) at the well-level: this assures the correct fluid distribution in the reservoir by correctly dividing the liquid production rate into individual fluid rates at every well.

4. Match the bottom hole flowing pressure at each well (p_{wf}): with this stage, the local energy is matched in the drainage area of the wells, including near-wellbore effects, i.e., skin factor.

5. Match the water breakthrough: Complete matching of the breakthrough times at the well-level is the most difficult if not impossible in some cases. Sometimes this is not a target, for example, when we have high uncertainty of this data. High uncertainty of the production data could happen in cases where we have a rough estimate for the breakthrough time, for instance, when we have the production data from production allocation.

The above-described sequence is typically recommended to follow, but the main focus of the history matching is always unique and defined by the purpose of the model. The sequence can be varied when needed for practical reasons because, in the end, the final models should always serve the original purpose.

The rule of thumb (Aziz and Settari, 1979) in history matching is first to change the parameter that has the most significant influence on the simulated result and has the highest uncertainty. Changing the relative permeability data is the last resort in conventional history matching because it hugely affects the simulated data (Ertekin, Abou-Kassem and King, 2001). Therefore, it must be defined accurately before history matching as an input parameter. Last but not least, preferably, several

scenarios have to be created to provide a range of models with different probabilities (Pyrcz and Deutsch, 2014), (Ringrose and Bentley, 2015).

With the consideration of the rules of the history matching sequence, automation is conducted as part of the improved workflow. The rock type adjustment and the sequence of the different history matching steps listed above can be automatized through the developed workflow. The effort for the automation of the mentioned steps is relatively small, while the value of the automation is way higher. Two significant factors make the automation of the history matching sequence certainly conductible. The main factor is the flexibility of the application of the adjoint method, and the second factor is the structure of the rock typing workflow, which is wrapping up the adjoint method without the need of modifying it but instead utilising the results and expanding the list of functionalities.

Typical reservoir data to adjust (parameters to modify)

During history matching, there could be an almost infinite amount of reservoir data to be adjusted in the reservoir model. Based on the uncertainty and the sensitivity of these parameters, the list of variables can be shortened uniquely. The most typical data to be modified during the history matching are the size and strength of the aquifer, vertical barriers, $k_h h$ product (absolute horizontal permeability), the ratio of horizontal and vertical permeabilities, pore-volume, relative permeability and capillary pressure.

In this dissertation, the directly modified parameters are the porosity and the absolute permeability. In addition, in the rock typing workflow, not only the porosity and the absolute permeability are modified, but the relative permeability and capillary pressure functions are indirectly adjusted according to the rock type validation. The indirect change means that the changes are not done conventionally (scaling) but through the rock type link.

First of all, the modifications of relative permeability should always be the last resort in history matching. Second of all, when it is modified, it is done by the scaling of relative permeabilities. The scaling means that the curves are shifted along the saturation axis by changing the connate water, and residual oil saturation or the end-points of the relative permeability curves are modified or the combination of these two.

In this dissertation, the relative permeabilities stay untouched; the developed workflow keeps the original values as it is interpreted but changes jointly with the rock type change. When the rock types are adjusted, the corresponding saturation tables are used for the calculations, so practically, the saturation functions are not modified but switched.

An extensive summary of all the parameters and their contribution to the match is shown in Fig. 2.1.

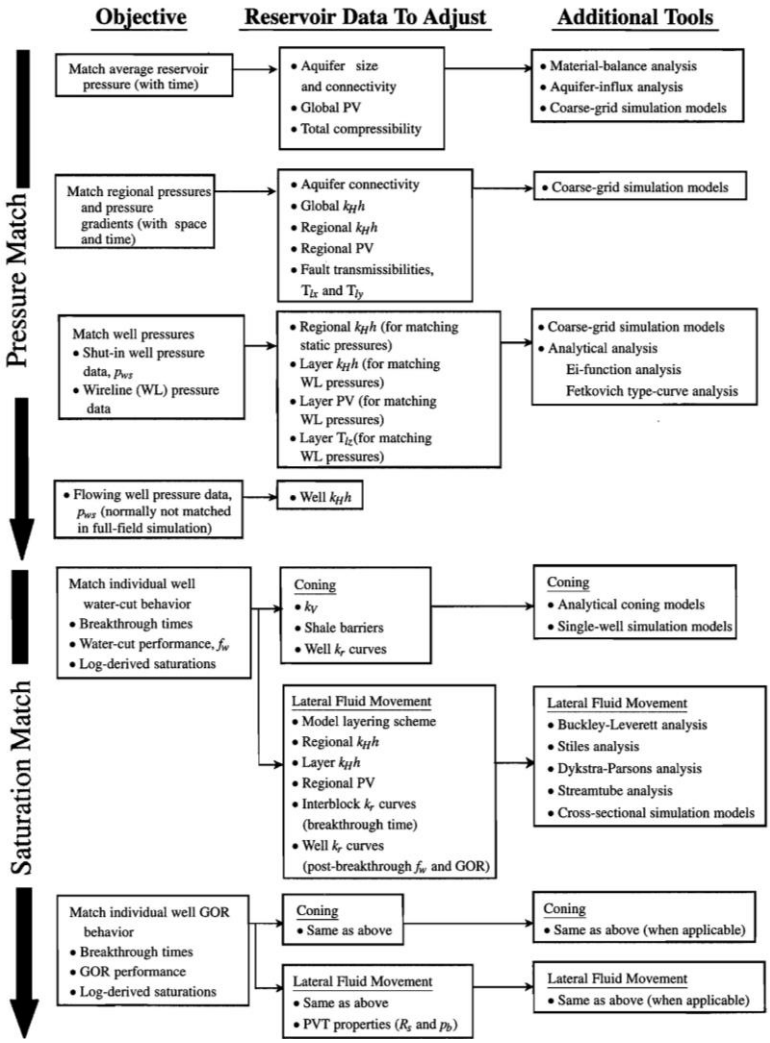

Fig. 2.1: Typical reservoir data to adjust during history matching (Ertekin et al., 2001)

2.2 Manual History Matching

The basic concept of manual history matching (Ertekin, Abou-Kassem and King, 2001) is to adjust the input parameters of the built static model, manually one by one, parameter by parameter for numerical simulation until the simulated data is in good agreement with the historical data. In conventional or manual history matching, commonly observed data is the same as in the assisted way: water-cut, gas-oil-ratio, average reservoir pressure (static, shut-in pressure), flowing well pressure, oil production rates breakthrough time, and others.

The inverse modelling approach (Oliver, Reynolds and Liu, 2008)allows the engineer to determine numerical parameters of the corresponding input variable based on the known output results. In other words, the purpose of history matching is to manually find the best set of input data to reproduce the historically observed data. Inverse problems do not have unique solutions. It does not have a unique solution because many different sets of input data can reproduce the same outcome performance. On the one hand, it is impossible to try all the realistic combinations manually with a trial and error process. On the other hand, the quantification of the mismatch and the model parameter modification is less accurate than in computer-assisted history matching approaches.

Typically, the engineer runs the simulations with different parameter combinations in several iterations and monitors the simulated data

changes regarding the changed parameters. As a start, in order to understand the model and find the sensitivities of the model, the parameters are changed separately. It is not efficient to change parameters on grid-block level by hand. Therefore box multipliers can be applied, which breaks the continuity of the underlying geological parameters.

The quality of the outcome of the history matching is not limited to the degree of matching. On top of the unknown rock properties and saturation functions, the dynamic input parameters may include a certain level of uncertainty to the results. As such, inaccurate, insufficient, and inconsistent measured fluid properties and historical production data, i.e. production rates, reservoir pressure, and well-flowing pressure, may contribute negatively to the overall precision of the history matching procedure.

The history matching is time-consuming. It takes a large portion of a reservoir study, especially when it is only completed manually. The process is repetitive/iterative and takes an enormous amount of time only by the trial-and-error approach. Conventionally, the manual history matching is segregated into two phases, where globally observed data is matched first, and only then the observed data is matched on the local-scale or so-called well-scale.

The typical sequence of history matching is described in subchapter 2.1.2, which is also applicable in manual model adjustments. The typically adjusted parameters are summarised in subchapter 2.1.2.

2.3 Assisted History Matching Methods

The computer-assisted or automated history matching approaches pursue the same goal as the manual history matching techniques (Oliver and Chen, 2010). The methodology is the same, but the realisation can be different. From the perspective of this research topic, it is essential to highlight that the assisted history matching tools can be divided into two main groups. The first group comprises the gradient-free, mainly stochastic or statistical and simplex methods, and the second consists of gradient approaches. While discussing the gradient approach, it is essential to point out the differences between the direct and the adjoint approaches, as the latter method is adopted in this work. Both direct and adjoint approaches are gradient-based algorithms, but the underlying difference exists in the formulations of the equations. Before moving forward to the comparison of the two gradient-based approaches, a short note on the most widely used algorithms is summarized below.

Trial and error approaches, such as manual history matching techniques, are impractical due to the high computational cost of each simulation and the significant amount of model parameters. Today,

complex and large models are more feasible and, thus, popular. Therefore, the need for accurate and precise automated history matching tools is constantly growing. Moreover, the approach to honour all the parameter constraints and their relationship is required.

The arising system of modelling equations that describe the reservoir fluid flow is the incompressible two-phase flow system Eq. 2.1 (Aziz and Settari, 1979). Such a system can be written in the following way (Oliver, Reynolds and Liu, 2008):

$$L(\boldsymbol{p}, \boldsymbol{m}) = L(\boldsymbol{p}(\boldsymbol{m}), \boldsymbol{m}) = 0$$

Eq. 2.1

, where

$\boldsymbol{L(p, m)}$ – set of discretised flow equations,

$\boldsymbol{p}$ – primary variables (pressure, saturation),

$\boldsymbol{m}$ – model parameters (porosity, permeability, parameterization of k_r and P_c)

2.3.1 Objective Function

The following equation Eq. 2.2, represents the calculation of the objective function. The objective function quantifies the mismatch between simulated results and observed production history (Oliver, Reynolds and Liu, 2008).

$$J(p,m) = \frac{1}{2} \sum_{i=1}^{N_{observed}} \omega_i (d^{calculated}(p) - d^{observed})^2$$

Eq. 2.2

, where

$J(p,m)$ – objective function,

ω_i – weighting factor,

$d^{calculated}(p)$ – simulation results,

$d^{observed}$ – production history.

In the optimization workflow, the goal is to find the minimum of the objective function subject to the discretised flow equation (Oliver, Reynolds and Liu, 2008).

$$\min_{m} J(p,m) => \nabla J(p,m) = 0$$

Eq. 2.3

The minimization problem of described type can be solved by various methods, among which the stochastic approaches and gradient-based methods are the most popular choices. Each method has its advantages and disadvantages. A good review of recent developments in history matching is published(Oliver and Chen, 2010). The stochastic approaches like EnKF (Ensemble Kalman Filter) and EnRML (Ensemble Randomised Maximum Likelihood) (Li and Reynolds, 2009) are attractive because they do not require the calculation of the gradient of an objective function, but on the other hand, gradient approaches have a higher rate of convergence.

2.3.2 **Gradient Free Algorithms**

The first group of algorithms that needs to be mentioned is the gradient-free stochastic methods. The most widely used ones are the evolutionary algorithm (Bäck, 1996) and the EnKF (Kalman, 1960; Evensen, 1994; Liu and Oliver, 2005; Aanonsen *et al.*, 2009; Li and Reynolds, 2009; Chen and Ollver, 2010; Oliver and Chen, 2010; Schulze-Riegert *et al.*, 2013; Thiele and Batycky, 2016; Wang and Oliver, 2021). The used methods in practice are not limited to those. There are numerous other gradient-free approaches available. Simplex methods such as the Nelder-Mead optimization algorithm (Nelder and Mead, 1965) can be used for

relatively minor problems, meaning a small number of model parameters (model with a small number of grid blocks). It is a generalized bi-section unconstraint optimization approach for high-dimensional parameter spaces. This method is robust, does not require any Hessian matrix calculation (Nocedal and Wright, 2006), and applies to a wide range of functions. Another category is the swarm intelligence algorithms, the most popular are the Particle Swarm Optimization (PSO) (Kennedy and Eberhart, 1995) and the Ant Colony Optimisation (ACO) (Dorigo and Gambardella, 1997). In both cases, the algorithm tries to replicate the behaviour of insects, birds, and fish populations. In nature, their goal is to arrive at a particular location of their interest, so, therefore, modelling this behaviour in every iteration, the direction and the velocity of movement are defined. These algorithms have growing popularity and have a high chance to dominate in the future with a combination of machine learning techniques (Mosser, Dubrule and Blunt, 2019). Nevertheless, the most widely used ones are the following two described below.

Evolutionary algorithm

Evolutionary algorithms are based on the ideas of biological processes such as natural selection, mutation, reproduction. The most popular methods from this category are the Genetic algorithms (Romero and Carter, 2001) and Differential evolution (Storn and Price, 1997). Each model/realization in the terminology of the evolutionary algorithms is called population. After generating the initial population at random,

every new population is generated by selecting the most potent members, survivors and applying one or several genetic functions on them, such as mutation and recombination. The selection process is performed using the fitness function, equal to the mismatch between the model prediction and observed data. The process continues till the desired fitness or maximum allowed number of iterations is reached. In differential evolution, the difference between members is used together with the random differential weight to produce a new candidate solution. Although the evolutionary algorithms are very general in their formulation and can be applied to different types of problems and do not require gradient calculation, the convergence rate is prolonged for these algorithms.

One great example of the widely used software where the application of Evolutionary algorithm is available amongst others, but not limited to, is tNavigator (Rock Fluid Dynamics, 2021).

Ensemble Kalman Filter (EnKF)

The widely used method ensemble Kalman filter is named after Dr Rudolf Kalman, a Hungarian mathematician who introduced a Kalman filter in 1960 (Kalman, 1960). Further on, the ensemble Kalman filter (EnKF) approach, exploiting the Monte-Carlo method (Hastings, 1970) and Bayesian formulation, was introduced in the petroleum industry in 1994 (Evensen, 1994). An excellent overview of different EnKF methods can be found in publication(Aanonsen *et al.*, 2009).

The EnKF method is a sequential data assimilation approach consisting of forecast and assimilation steps, which modify model parameters and so-called state variables, such as pressure, saturation, and observed data. First, the ensemble of models is generated using underlying statistics of model parameters, or in other words, different model realizations are considered an initial guess. Further, two main steps, forecast and assimilation, are applied to modify current model parameters and state variables (primary variables and production data). During the forecast step, the simulation is performed given the current model parameters. Therefore the predictions are made with the help of a simulator. Afterwards, the assimilation of the measured data observed at the forecast step is performed. In the assimilation step, the update of model parameters and the state variables is done using the so-called Kalman gain matrix. The assimilation step does not require the use of a simulator. Hence it is computationally cheap to perform. This advantage made EnKF method trendy(Oliver, Reynolds and Liu, 2008).

On the other hand, EnKF approaches suffer from various drawbacks. Firstly, it is inaccurate for non-Gaussian distributed parameters and highly non-linear problems. Secondly, the assimilation step, which relies on applying the Kalman gain matrix, can produce non-physical solutions while modifying state variables (Oliver, Reynolds and Liu, 2008).

The most widely used software where the application of the EnKF algorithm is available amongst others, but not limited to, is MEPO (Schlumberger, 2021).

2.3.3 Gradient Approach (Adjoint vs Direct formulation)

In this dissertation, the solution of inverse problems with a gradient approach based on adjoint formulation is introduced (Almuallim *et al.*, 2010) and extended (Jenei *et al.*, 2020). All inverse problems are characterized by many model parameters that have to be defined based on the observed response of the modelling system.

The observed data always contain measurement errors. It is impossible to correctly estimate all the model parameters from inaccurate, insufficient and inconsistent data. This issue causes the non-uniqueness of the inverse problem solution. The plausibility of models is ensured by applied bounds and constraints on the model parameters.

The gradient approaches are well known to be dependent on the initial guess. In order to successfully minimise the objective function with any gradient approach, the initial model has to be selected carefully. The solution of the gradient approach is strongly affected by the starting point, the initial guess. If the initial parameter distribution is far from the solution, the approach might never arrive at the correct values. Therefore, the artefact of the approach is that during reservoir history matching, the base case model needs to be close enough to the final solution for it to work (Nocedal and Wright, 2006).

To successfully minimize the objective function with a gradient approach, applying an accurate gradient calculation is of great

importance. There are three typical methods of how to calculate gradients for performing optimization. One of the simplest but least accurate ways to calculate the gradient of an objective function is by the finite difference method(Oliver, Reynolds and Liu, 2008):

$$\frac{dJ(m)}{dm} = \frac{J(m + \Delta m) - J(m - \Delta m)}{2\Delta m}$$

Eq. 2.4

In order to achieve better accuracy in the solution, the direct approach or the adjoint approach can be used. Since the objective function is a function of primary variables and model parameters, its derivative can be calculated by chain rule:

$$\frac{dJ}{dm} = \frac{\partial J}{\partial p} \cdot \frac{dp}{dm} + \frac{\partial J}{\partial m}$$

Eq. 2.5

$$\frac{dJ}{dm} = \frac{\partial J}{\partial p} \cdot \frac{dp}{dm} + \frac{\partial J}{\partial m} = 0$$

Eq. 2.6

And the derivative of primary variables with respect to model parameters $\frac{dp}{dm}$ can be obtained directly by differentiating the constraints:

$$\frac{\partial L}{\partial m} + \frac{\partial L}{\partial p} \cdot \frac{dp}{dm} = 0$$

Eq. 2.7

Therefore, one needs to solve the corresponding system (Eq. 2.8):

$$\frac{\partial L}{\partial p} \cdot \frac{dp}{dm} = -\frac{\partial L}{\partial m}$$

Eq. 2.8

The algebraic explanation for the difference between the direct and adjoint gradient approach is the following, introducing the following system (Oliver, Reynolds and Liu, 2008).

$$u = \frac{dp}{dm}$$

Eq. 2.9

$$A = \frac{\partial L}{\partial p}$$

Eq. 2.10

$$f = -\frac{\partial L}{\partial m}$$

Eq. 2.11

$$g^T = \frac{\partial J}{\partial p}$$

Eq. 2.12

, where

u – a variable which needs to be solved for ($N_p \times N_m$ matrix, where N_p is the number of primary variables, N_m is the number of model parameters),

A – $N_p \times N_p$ matrix,

f – right-hand side, $N_p \times N_m$ matrix,

g^T – $1 \times N_p$ vector.

The dimensionality of such a system depends on the number of model parameters. In the case of a large number of model parameters, it is worth considering another method rather than the direct approach. In the direct method, the linear system $A \cdot u = f$ is solved, and, afterwards, $g^T \cdot u$ product is calculated.

Solved:

$$A \cdot u = f$$

Eq. 2.13

Calculated:

$$g^T \cdot u$$

Eq. 2.14

In the adjoint method, the system of $A^T \cdot \lambda = g$ is proposed to be solved, and the calculated product is $\lambda^T \cdot f$, which is equal to $g^T \cdot u = (A^T \cdot \lambda)^T \cdot u = \lambda^T \cdot (A \cdot u) = \lambda^T \cdot f$.

Solved:

$$A^T \cdot \lambda = g$$

Eq. 2.15

Calculated:

$$\lambda^T \cdot f$$

Eq. 2.16

$$g^T \cdot u = (A^T \cdot \lambda)^T \cdot u = \lambda^T \cdot (A \cdot u) = \lambda^T \cdot f$$

Eq. 2.17

In this case, the product $g^T \cdot u = \frac{\partial J}{\partial p} \cdot \frac{dp}{dm}$ is equivalent to the calculation of $\lambda^T \cdot f = \lambda^T \cdot \left(-\frac{\partial L}{\partial m}\right)$ after the following system is solved:

$$\left(\frac{\partial L}{\partial p}\right)^T \cdot \lambda = \left(\frac{\partial J}{\partial p}\right)^T$$

Eq. 2.18

This comparison clearly shows that, while for the direct approach, the dimensionality of the arisen linear system is proportional to the number of model parameters, the computational effort of the adjoint formulation is not dependent on the number of model parameters. Therefore it is a more suitable solution for reservoir engineering optimization problems.

Steepest Gradient Descent

In order to understand the parameter modifications in the adjoint-based workflow, the steepest gradient descent algorithm needs to be clarified. The gradient of function $\nabla J(\boldsymbol{p}, \boldsymbol{m})$ gives the direction of maximum change. Hence, for the minimization problem, the direction of minimization is done along the negative gradient direction -$\nabla J(\boldsymbol{p}, \boldsymbol{m})$. In the following expression, the following applies $\boldsymbol{x} = (\boldsymbol{p}, \boldsymbol{m})$.

$$\boldsymbol{x}_{k+1} = \boldsymbol{x}_k - \alpha_k \cdot \nabla \mathrm{J}(\boldsymbol{x}_k)$$

Eq. 2.19

, where

k - is the iteration step

α_k - is the step size.

The choice of α_k at each iteration-step depends on the minimization algorithm. Steepest gradient descent (Debye, 1909) makes the choice of step size based on the condition of minimum achievable function value:

$$\alpha_k = \arg\min_{\alpha \geq 0} J(\boldsymbol{x}_k - \alpha \cdot \nabla J(\boldsymbol{x}_k))$$

Eq. 2.20

The gradient direction, which is the direction of maximum function change, is described as follows. First, the direction in which function changes most rapidly must be found. For that, one may use the directional derivative $\nabla_{\boldsymbol{v}} J(\boldsymbol{x})$, where $\boldsymbol{v}$ is the directional vector of unit norm $\|\boldsymbol{v}\| = 1$

In the small vicinity of point $\boldsymbol{x}$, the multivariate function can be represented using the Taylor expansion demonstrated below.

$$\begin{aligned} J(\boldsymbol{x} + \varepsilon \cdot \boldsymbol{v}) &= J(\boldsymbol{x}) + \nabla J^T(\boldsymbol{x}) \cdot (\boldsymbol{x} + \varepsilon \cdot \boldsymbol{v} - \boldsymbol{x}) + o(\varepsilon) \\ &= J(\boldsymbol{x}) + \varepsilon \cdot \nabla J^T(\boldsymbol{x}) \cdot \boldsymbol{v} + o(\varepsilon) \end{aligned}$$

Eq. 2.21

Hence, the derivate in the direction $\boldsymbol{v}$ is the scalar product of gradient $\nabla J(\boldsymbol{x})$ and directional vector $\boldsymbol{v}$:

$$\nabla_{\boldsymbol{v}} J(x) = \lim_{\varepsilon \to 0} \frac{J(\boldsymbol{x} + \varepsilon \cdot \boldsymbol{v}) - J(\boldsymbol{x})}{\varepsilon} = \nabla J^T(\boldsymbol{x}) \cdot \boldsymbol{v}$$

Eq. 2.22

The maximum of direction can be defined from the definition of the scalar product.

$$\max_{\boldsymbol{v}} \nabla_{\boldsymbol{v}} J(x) = \max_{\boldsymbol{v}} \nabla J^T(\boldsymbol{x}) \cdot \boldsymbol{v} = \|\nabla \mathrm{J}(\boldsymbol{x})\| \cdot \|\boldsymbol{v}\| \cdot \max_{\boldsymbol{v}} \cos(\nabla \mathrm{J}(\boldsymbol{x}), \boldsymbol{v}) = \|\nabla \mathrm{J}(\boldsymbol{x})\|$$

Eq. 2.23

Maximum function change is achieved when $\max_{\boldsymbol{v}} \cos(\nabla J(\boldsymbol{x}), \boldsymbol{v}) = 1$, i.e., $\boldsymbol{v}$ is collinear to gradient direction $\boldsymbol{v} \parallel \nabla J(\boldsymbol{x})$ (Nocedal and Wright, 2006).

Apart from the steepest descent algorithm, other gradient optimization approaches such as Levenberg-Marquardt (Levenberg, 1944; Marquardt, 2006), L-BFGS-B (Broyden-Fletcher-Goldfarb-Shanno algorithm) (Liu and Nocedal, 1989) can be applied. L-BFGS-B is a quasi-Newton method (Nocedal and Wright, 2006) because it uses approximated Hessian matrix from the provided gradient of the function of interest (objective function). It uses a line search procedure to find an appropriate step by bi-section approach. At any next iteration, the vector of parameters is being changed according to new steps and directions. This method is a relatedly accurate algorithm with bounding constraints.

Almost all of the applications mentioned previously in the 1.4 State of the Art section have at least one form of gradient-based algorithm

available, for example, CMOST, SimOpt and SenEx. In this thesis, SenEx was chosen to exploit the functionality of sensitivity calculations.

2.4 The applied software: Numerical simulation, optimization, post-processing

In this subchapter of the dissertation, the applied software is listed, defined, and disclosed during this research.

2.4.1 The applied software: SenEx, tNavigator, ECLIPSE and Python

The main assisted history matching workflow, the sensitivity explorer (*SenEx*), supports the two primary players in commercial simulation. Therefore, the improved and extended history matching tool is designed in a way that it is capable of handling both tNavigator and ECLIPSE simulation run decks. The SenEx workflow currently supports the black oil simulators. Hence, the extended history matching workflow is designed and tested for the black-oil simulator of both computer programs from RFD and Schlumberger.

tNavigator software is developed by Rock Flow Dynamics (RFD), a Russian based company. The software has been under development and fine-tuning for 15 years, releasing four software updates per year. It is a high-performance tool for integrated static and dynamic modelling from

the reservoir to the surface networks. From the various modules suggested in the software by RFD, the particular feature of interest is the "Black Oil Simulator". The feature works with fully implicit and adaptive implicit algorithms. It supports all industry-standard functionality, including three-phase flow and temperature extensions (Rock Flow Dynamics, 2021).

Eclipse is a software package developed by Schlumberger Ltd., which is historically known as a French oil field company founded in 1926. ECLIPSE 100 was used in this dissertation, which is part of the package offered by ECLIPSE. It is a fully implicit integrated finite difference three-phase general purpose black oil simulator (Schlumberger, 2020a).

Petrel is a complex geomodelling software widely used in the industry and also in research. It has a broad number of functionalities, from basic seismic interpretation to comprehensive visualisation of the simulation results. The tool is developed and distributed by Schlumberger Ltd. In this dissertation, Petrel was used to design the synthetic models, including static and dynamic datasets. Petrel Workflows were implemented as a proof of concept before writing the Python scripts to prove the method's validity (Schlumberger, 2020b).

Python is listed within the applied software, but it is a non-commercial open-source programming language. It is used to extend the history matching workflow because it is powerful, fast and adaptable to other software or languages, flexible, and relatively easy to use. Another

reason for choosing Python is the availability of the libraries, which are integrated. The principal used libraries are the following: SciPy (Virtanen *et al.*, 2020), Pandas (pandas development team, 2020), NumPy (Harris *et al.*, 2020), Bokeh (Bokeh Development Team, 2021), which means that already available developed functions are used together from different sources.

2.5 Application of Adjoint Method – Sensitivity Explorer (SenEx)

The reasons described above led to selecting the adjoint method for the engine of the extension of the history matching workflow introduced in this dissertation. Sensitivity Explorer is unique computer software that is based on the adjoint-driven history matching approach. The highlight of the workflow is the automated sensitivity analysis followed by input data alteration for the sole purpose of reducing the mismatch. The parameters are adjusted repetitively in traditional or manual history matching until the mismatch results reach the desired quality. It can be concluded that computer-assisted automation is heavily required considering a large number of parameters in the models and the increasing expectations for resulting efficiency from the industry.

The general workflow of the adjoint-based algorithm of Sensitivity Explorer is represented in Fig. 2.2. The base workflow has five significant stages or actions. The first two steps require assistance from

the engineer and simulator. The latter three ones are automatically performed within the Sensitivity Explorer. Below, the conventional workflow (Sensitivity Explorer's) introduced in Fig. 2.2. is described.

Sensitivity Explorer Loop (one optimization iteration) contains and executes the following steps:

1. Initialize Sensitivity Explorer Case (This step requires engineering assistance.)

2. Simulation (The simulation part is conducted outside, calling a simulator software program.)

3. Mismatch calculation (Objective Function is estimated in this stage, from simulation results with primary set weighting factors.)

4. Sensitivity coefficients calculation (The derivatives are calculated automatically utilizing the calculated OF with respect to the model parameters.)

5. Model parameters modification (This step executes the export of the new parameter arrays, based on the sensitivity coefficients.)

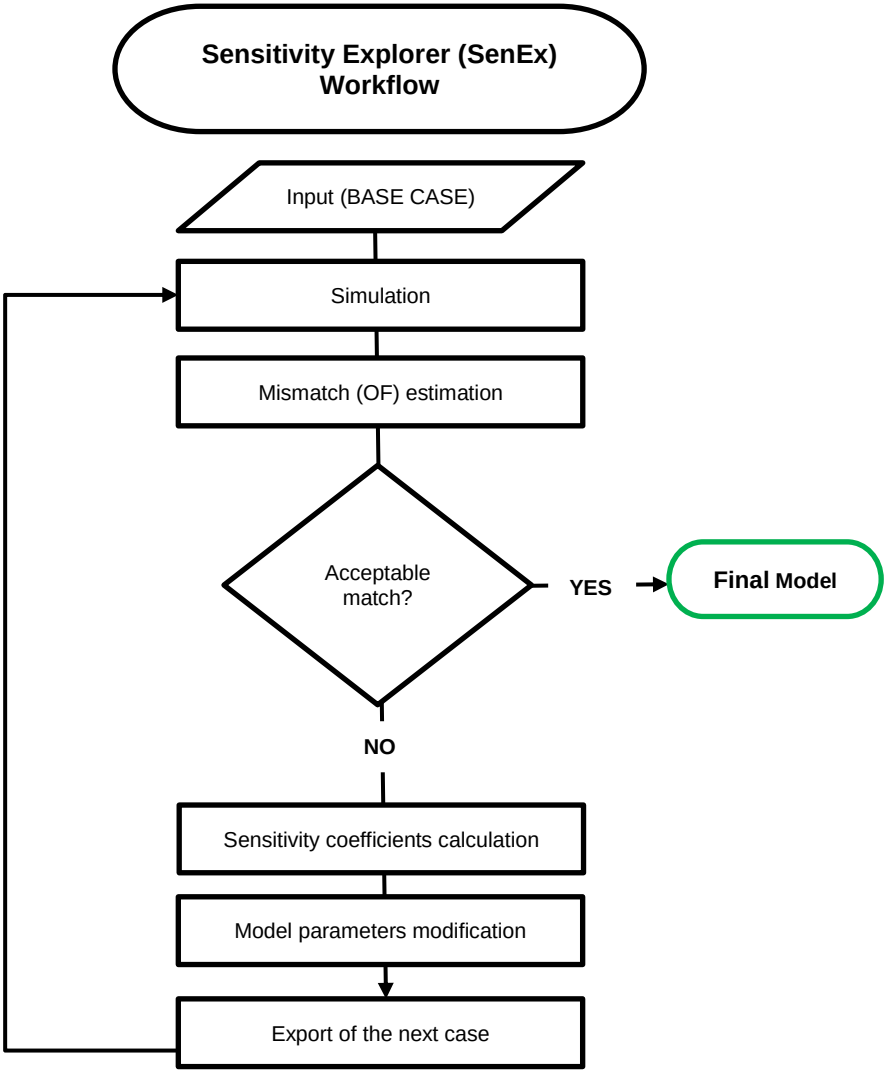

Fig. 2.2: The Sensitivity Explorer Workflow

The sensitivity explorer works with a technique based on the analytical computation of objective function and sensitivity coefficients. The objective function measures or quantifies the mismatch of the model. The sensitivity coefficients are computed using partial derivatives. The partial derivatives are calculated for an appropriate objective function with respect to the model parameters.

The objective function is calculated in the applied adjoint-based workflow using the following formula:

$$OF = J\,(p,m) = \sum_i \omega_i \cdot M_i$$

Eq. 2.24

$$M_i = \sum_t \left[\frac{\alpha_o \left(O_{i,t}^{computed} - O_{i,t}^{observed}\right)^2}{\beta_{L,i}} + \frac{\alpha_w \left(W_{i,t}^{computed} - W_{i,t}^{observed}\right)^2}{\beta_{L,i}} + \frac{\alpha_g \left(G_{i,t}^{computed} - G_{i,t}^{observed}\right)^2}{\beta_{g,i}} + \frac{\alpha_p \left(p_{i,t}^{computed} - p_{i,t}^{observed}\right)^2}{\beta_{p,i}} \right]$$

Eq. 2.25

, where

OF – Objective function,

i – well index,

α_i; ω_i – weighting factors at well i,

M_i – mismatch at well i,

β_i – standard deviation,

o, w, g – oil, water and gas index.

The goal of the presented workflow (SenEx) is to minimise the objective function. In order to minimise the objective function, one needs to know how the parameters are contributing to the mismatch. The sensitivity coefficients help to quantify that. These coefficients are calculated with the computation of the partial derivatives.

The partial derivatives are calculated with the following equation (Oliver, Reynolds and Liu, 2008):

$$\frac{\partial J\,(p,m)}{\partial m}$$

Eq. 2.26

, where

$J(p, m)$ – Objective function,

m – model parameter.

The model parameters are the porosity *(ϕ)* and the absolute permeability *(k)* in both horizontals *(k_x, k_y)* and vertical *(k_z)* directions. In order to generate new property arrays, the initial sensitivity calculation is followed by the parameter modifications at the grid-block level accordingly.

The optimization during history matching is specified within parameter bounds through multipliers. These are the ratio of the new values updated by the gradient of the objective function and the initial value:

$$\boldsymbol{x}_{k+1} = \boldsymbol{x}_k - \alpha_k \cdot \nabla \mathrm{J}(\boldsymbol{x}_k)$$

Eq. 2.27

, where

α_k – step size,

$\nabla \mathrm{J}(\boldsymbol{x}_k)$ – gradient of the objective function.

It is necessary to mention that all together, four parameters can be modified at the grid block level, namely the porosity (ϕ) and the absolute permeability (k) in both horizontal (k_x, k_y) and vertical (k_z) directions. In contrast to other assisted history matching approaches, this method allows modifying the parameters grid cell by grid cell. The box multipliers are not required. Therefore the changes in grid-block properties are minimised, and the final model remains more continuous and preserves the geological features to a greater extent. The parameter modifications are iterative, and it is a non-linear problem; following the partial derivative, we can expect a change in the mismatch. The workflow is repeated until an acceptable match is reached. The new arrays should stay within realistic ranges, which are unique in every reservoir model. Internally, in order to stay within these preliminary defined desirable parameter ranges, the $\frac{x^{k+1}}{x^0}$ multiplication factor is used.

The aforementioned adjoint-based history matching approach used for the new history matching workflow has already been implemented and introduced by H. Almuallim(Almuallim *et al.*, 2010). This post-processing method, built on the adjoint approach, is already of enormous significance compared to the manual history matching procedure. The benefits of an adjoint-based computer-assisted history matching procedure can be seen in the paper published by H. Almuallim (Almuallim *et al.*, 2018).

In this dissertation, the achievements mentioned above of H. Almuallim are taken as the basis. The objective was to extend his work by improving the adjoint-based tool concerning geological consistency. A thorough description of the extension of the algorithm is presented in Chapter 4.

The workflow extension is developed outside of the domain of SenEx software, making it flexible to adapt to any other optimization tools. The independent extension is done to exclude the limitations of applicability.

2.6 Closed-loop reservoir characterization role in history matching workflow

Prior to performing a history matching procedure, there must be an available base case model of the subsurface formation. This initial model must contain the closest realisation of the reservoir characteristics. In order to achieve the best static and dynamic representation of the reservoir, one must rely on the availability of the required data.

The data come in from several different sources, presented in Fig. 2.3 on the left side. The sources are namely laboratory experiments (routine core analysis (RCA), special core analysis (SCAL)), seismic data, well testing data and production history. As a result of so many different available input data, reservoir characterization is a complex, tedious,

and time-consuming procedure. This work focuses on the flow simulation and post-processing of a geomodel. Hence, in order to keep the final product of the history matching consistent with the reservoir characteristics and reliable for further use, the development of the reservoir model needs to be fully understood.

The reservoir characterisation process is complex as it generally combines data from multiple disciplines and establishes relationships between the different geological and petrophysical parameters. In order to preserve the quality of the reservoir model over the history matching procedure, the essentials of the geological model construction procedure need to be given fair consideration. The quality, not only in terms of prediction performance but the geological consistency, must be maintained for a better and more precise reservoir representation and, ultimately, better decision making in future operations. The most crucial input data and processes concerning reservoir characterization are shown in Fig. 2.3.

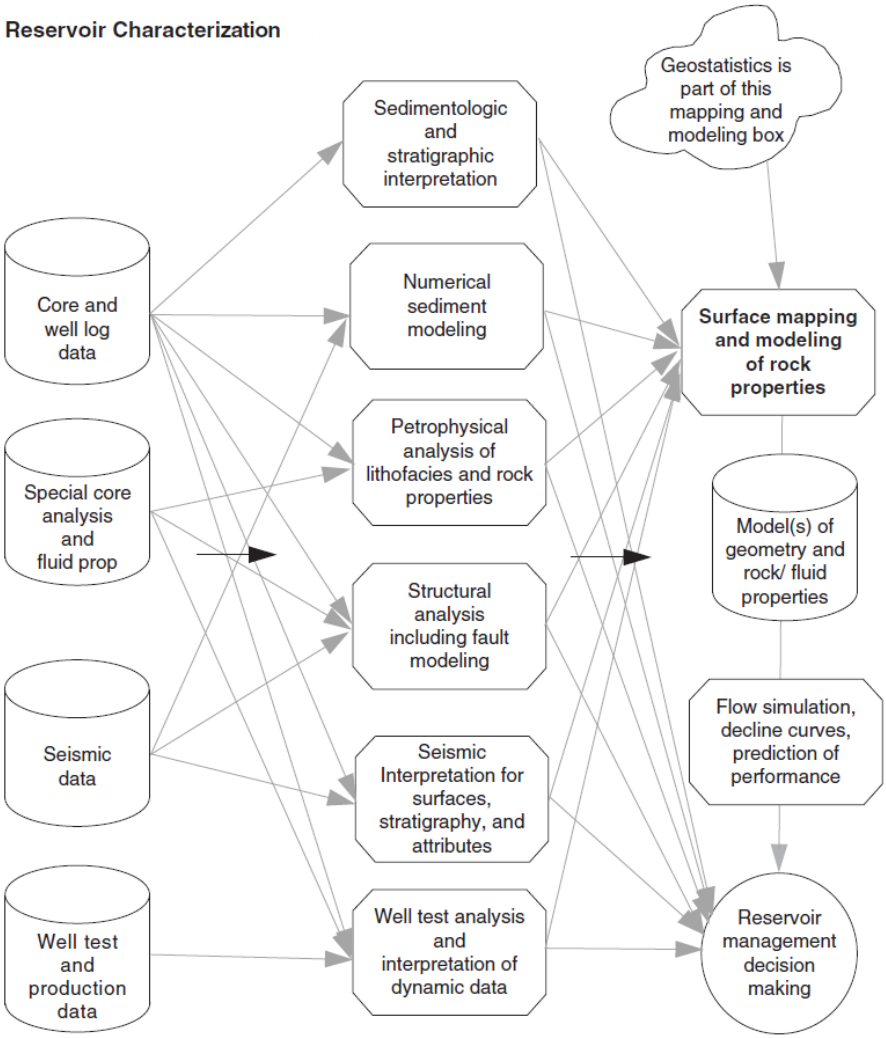

Fig. 2.3.: Summary of the significant input and operations of reservoir characterization workflow (Pyrcz and Deutsch, 2014)

It is important to note that history matching and reservoir characterization have a mutual relationship in this work. In general, the reservoir characterization workflow should contain history matching, but most commonly, the reservoir characterization is conducted through geostatistical modelling. The contribution of history matching is well known as a reservoir model adjustment to reproduce the historical data. In this research, the focus is to conduct the history matching to mimic the dynamic behaviour and improve the quality of reservoir characterization. The workflow extension keeps the preliminarily established connection instead of introducing physically and geologically inconsistent data and sudden changes in the reservoir properties.

The operation of the Reservoir Characterization is multidisciplinary and complex and, therefore, is a time-consuming and tedious process. It engages data from petrophysics, seismic interpretation, well-test analysis and production history. The geo- and petrophysical data come from well-logs and core flooding analysis. These data are then integrated into all the modelling operations starting from the sedimentologic and stratigraphic interpretation, modelling through the petrophysical analysis of facies and rock properties, and the structural and fault modelling based on the seismic interpretation of surfaces, to the flow simulation and dynamic data interpretation. In Fig. 2.3:

- The fluid flow simulation uses the results of SCAL as well, which serves as one of the most significant inputs for fluid flow dynamics through constitutive equations.

- Seismic data play an essential role in sediment, structure, surface and fault modelling, which is critical for the reservoir geometry, but difficult to be quantified for dynamic simulation.

- Fluid properties and well-test analysis results are vital inputs for the dynamic simulation of the fluid flow in the reservoir.

In conclusion, all the input data from different disciplines serve as a value for the geostatistical modelling; however, not all variables can be quantified for history matching.

The established relationship between engaged properties can be quantified through two main input groups in the model: the core and well log data and the results of the SCAL. It is well represented in Fig. 2.3 that these input parameters directly take place in the dynamic simulation. The data here, which can be quantified and described mathematically, are the effective porosity, absolute permeability, relative permeability and capillary pressure functions. The rock type or facies is the parameter that can bind all of these properties and quantify the established relationships. Consequently, the geostatistical modelling, including rock typing or so-called facies modelling, is the most significant part of the closed-loop reservoir characterization, which is jointly the interest of this research.

Chapter 3 Rock Typing

The spatial statistics carries one of the most significant values in the proposed extension of the history matching workflow. Therefore, it needs to be clarified what facies and rock types mean in the context of improved geologically consistent history matching. This Chapter provides an overview of geostatistical modelling and covers the different methods for facies/rock type modelling and the flow parameters that are significantly dependent on the rock types.

3.1 Geostatistical modelling and the importance of facies modelling in improved geologically consistent history matching workflow

The importance of facies modelling or rock typing, as a part of geostatistical modelling, for the implemented workflow extension has been previously mentioned in Chapter 2. If the maintenance of the geologically consistent reservoir model during and after history matching is desired, several factors need to be clarified.

The factors are:

- The process of geological/geostatistical modelling.
- The meaning of geological consistency.
- The parameters and functions that are crucial to be honoured.

3.1.1 Geostatistical modelling

The reservoir mode utilised in any history matching post-processing workflow is always constructed using geostatistical tools. Therefore, it is essential to understand how geostatistical modelling is performed. Fig. 3.1 shows a general overview of the geostatistical modelling workflow. Geostatistics itself is a tool for supporting reservoir characterization. The facies can be modelled after establishing stratigraphic layering and large-scale modelling within the reservoir characterisation process. The facies modelling is primarily done by geostatistical methods, such as e.g. sequential Gaussian simulation. Within the formerly identified facies or rock types, each facies has its porosity distribution, generated by geostatistical methods with the support of core and well-log data. Then, within each of the facies, the co-dependent parameter is defined, which is the permeability distribution that comes from pre-established porosity-permeability ($\boldsymbol{\phi}$-k) relationships. The $\boldsymbol{\phi}$-k function is also used to determine or identify the different rock types.

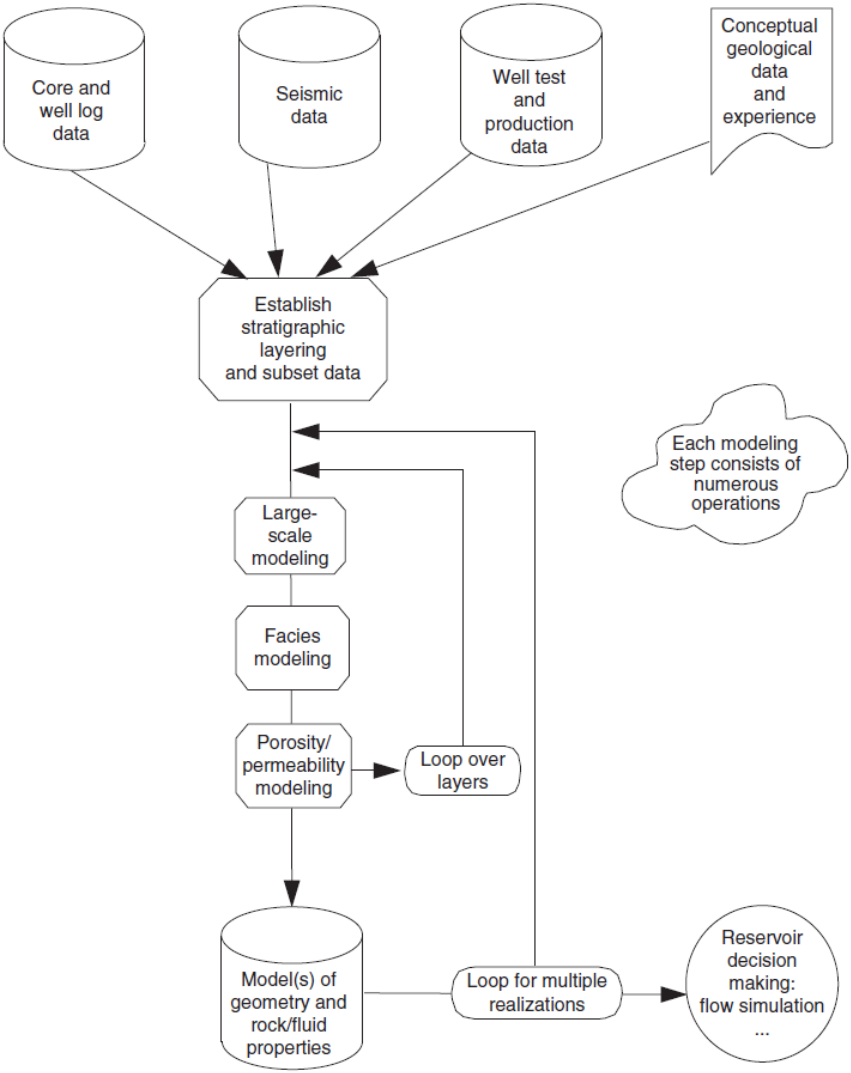

Fig. 3.1: General overview of the geostatistical modelling workflow

Each of the modelling steps shown in Fig. 3.1 consists of numerous operations and can be completed simultaneously and iteratively. The rock types can also be determined with closer attention to the parameters of the constitutive equations, which are the relative permeability and capillary pressure functions. These two functions are essential in determining the fluid flow in a multiphase system within subsurface porous media.

Consequently, the interest in modelling rock type extends to the level of details satisfying the proper distinction between the different rocks in terms of flow properties. From the geological point of view, there can be many facies depending on the composition, compaction, geological age, depositional environment, and other factors. However, the rock type modelling should cover only those facies that affect the dynamic properties, thus, the dynamic simulation. Therefore, geological modelling needs to be conducted within a multidisciplinary group of geoscientists to finalise a comprehensive, sophisticated and relevant model.

3.1.2 **Facies Modelling**

The two different methods that could be adapted for facies modelling (Pyrcz, 2018a) are multiple point or object-based simulations. Two concerns are bound to be countered during the reservoir characterization process. Specifically, these are the definition of the facies and the characterization of their importance in reservoir modelling.

Facies helpfully categorise a rock for subsurface fluid flow calculations. It can be termed the reservoir rock classification method that allows us to better understand it for further numerical simulations for field studies. Facies modelling supports the characterisation of the subsurface formation and in parameter prediction away from the well locations. (Pyrcz and Deutsch, 2014)

Generally, the overall workflow of the categorical simulation (Pyrcz, 2018a) entails that the categorical facies are simulated before creating multiple different realisations. These different realizations should honour the data and the concept of spatial continuity of categorical facies. Then, continuous simulation, such as Sequential Gaussian Simulation, is carried out to create the porosity distribution of the model. The trends of spatial statistics and the spatial continuity within each facies need to be maintained.

Porosity, trends of spatial statistics, spatial continuity, porosity transitions - higher to lower or lower to higher, build up some realization within the facies. Co-simulation is applied for another continuous property modelling, which is permeability that is correlated to porosity. The correlation means that permeability is dependent on the porosity values. They have a bivariate relationship, which is honoured during the property simulation. In a model, there are facies, and within the facies, there are porosity and permeability variations (Pyrcz and Deutsch, 2014; Pyrcz, 2018).

The Multiple Point Simulation (MPS) (Pyrcz, 2018) technique employs training images and captures heterogeneous spatial pattern distribution. The training images present no exact location or specific information, and the wells cannot be inserted there. It does not have coordinates; it cannot be identified within a specific location at the reservoir. The training image is only a pattern, and it has the same scale as the reservoir model. There is no local information in there; there is nothing constrained by local data. It is not conditioned to data, and it is simply a set of patterns extracted and modelled. Instead of modelling a variogram, an image is created, applied, and built into the model. The algorithm scans the training image with known and unknown information and then predicts the conditional probability density function (Pyrcz and Deutsch, 2014; Pyrcz, 2018).

Of course, both methods have advantages and disadvantages; compared to their final models, the results can be very close to each other.

3.2 Definition of Facies

Many different types of facies can be recognized. The main differences between these groups are their scale and the criteria of interest.

The most typical facies categories within subsurface modelling are:

- the lithofacies,

- the depofacies,
- the seismic facies.

The lithofacies are the different types of sediments that are distinctly different in their petrophysical properties. They can be distinguished within the group based on porosity and permeability. Examples of the subcategories are - sandstone, shale, dolomite, limestone. The lithofacies do not provide information about the geometry and the parameter prediction away from the well location. They do not have a good correlation, consequently meaning that they might change too often and too fast within one formation. Therefore, a larger scale of facies is needed for that, which are the depofacies. The lithofacies are sometimes used within depofacies to capture the crucial heterogeneity at points of interest. The distribution of the lithofacies is a highly uncertain parameter because it is challenging, if not impossible, to measure precisely.

The second category is the most commonly used depofacies or depositional facies. It can be composed of a mixture of different kinds of lithofacies. The depofacies provide information about geometry. Examples of depofacies are channels or sheets. Subsequently, this facies category provides a better level of understanding in three-dimensional space in terms of shape and geometry. Therefore, it can provide a better idea of spatial distribution further away from the well location, and thus, predictions of better quality can be eventually made.

Seismic facies, another facies category, use seismic information, such as acoustic impedance or elastic property. This type of facies tries to directly map the rock types based on seismic information.

The hierarchical model includes different facies categories within one model. This structure in a model implies that the facies data are sorted under a hierarchy of different scales. As such, the highest-level scale concerning reservoir structure is characterised by seismic facies. These, in turn, may include depofacies. Furthermore, as previously mentioned, depofacies are composed of various lithofacies that have different porosity-permeability distributions and their correlations consecutively. A typical example of the identification of facies based on the porosity-permeability relationship is presented in Fig. 3.2.

The facies modelling is conducted as a part of geostatistical modeling. Therefore one of the vital parameters, which is the uncertainty of each facies group, needs to be known. The uncertainty level of each category plays an essential role in geologically consistent history matching. It defines the level of freedom during model parameter modification, affecting rock type distribution.

The higher the uncertainty is - the more significant deviation in the distribution is accepted; the lower the uncertainty is - the minor deviation is tolerated, meaning that the original rock type distribution needs to be honoured to the highest extent. In the former case, history matching is geologically consistent with more extensive modifications in

the rock type distribution. While, in the latter case, it is highly recommended to include the facies distribution in the objective function to quantify the quality in geological consistency.

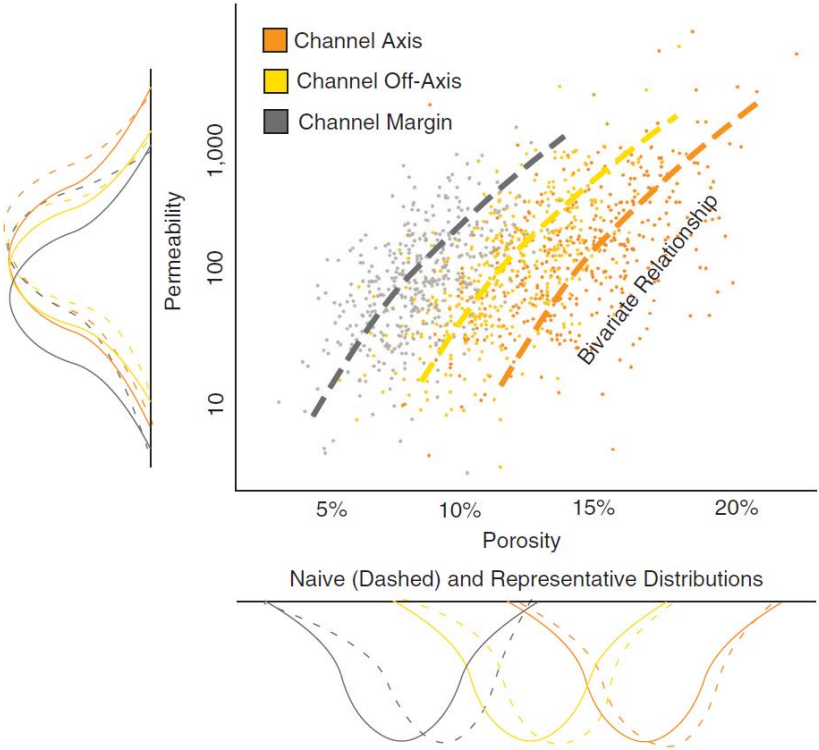

Fig. 3.2: Typical porosity-permeability diagram of different rock types and the individual parameter distributions within the reservoir (Pyrcz and Deutsch, 2014)

To be more specific, the uncertainty of the depofacies is lower than that of the lithofacies. Their distribution should be honoured to the fullest extent. The high certainty of the distribution is not true for the case of lithofacies since their distribution away from the wells is difficult to predict.

The ultimate goal of facies modelling within the reservoir characterization workflow is to have a realistic geological model to run the dynamic simulation. The facies must improve the subsurface prediction. Otherwise, it is of no value to the model. Therefore, it needs to be categorised and chosen carefully and jointly in order to make it worthwhile for dynamic modelling. The number of the facies, mainly, should be carefully chosen. If the model is too detailed, it becomes over-complicated and unnecessarily too complex, while if the number of facies is too tiny, essential details are grouped and, therefore, missed. The decision of the level of complexity is always unique in every field case. The detail of facies modelling always depends on the focus and the goal of the model.

Various methods exist for modelling facies/rock types, but the following criteria should be considered when designing the facies scheme. The suggested criteria for identifying the valuable facies that can benefit the subsurface model is based on the investigations of Michael Pyrcz (Pyrcz and Deutsch, 2014). The criteria can be divided into four categories (Pyrcz, 2018b):

1) Separation of rock properties

Facies must divide the properties of interest that impact subsurface environmental and economic performance, for example, grade, porosity.

Scatterplot, circles should have distinctly different grouping as far as porosity and absolute permeability. If they overlap entirely, the facies behave precisely the same when it comes to fluid flow. The most important for the flow simulation is why this relationship is chosen to identify the rock types.

2) Identifiable in Data

Facies must be identifiable with the most common data available. For instance, if the particular facies are identifiable only in cores, they would be not helpful if most wells had only log data available. This is due to the fact that core plugs generally cover approximately 5-10 % of the length of the well that transects the reservoir unit, whereas log data is provided over the whole length of interest. However, the facies can be defined when both data sources can identify the same features.

3) "Map-able" away from Data

Facies must be easier to predict away from the data source, i.e. wells, than directly the rock properties of interest. The facies improves/allows prediction of rock properties away from the well. Well-logs must be able to map.

4) Sufficient sampling

In order to be able to assess the spatial distribution of petrophysical properties, a sufficient number of samples is required. In other words, there must be enough data to allow for reliable inference of reliable statistics for rock properties for each facies(Journel and Alabert, 1990).

The parameters essential for fluid flow calculation, such as $\boldsymbol{\phi}$-k correlations (well-log and core data), the relative permeability and capillary pressure, including the residual saturations. The theory of these parameters related to rock types (RT) is further explained in the next session.

3.3 Rock Type dependent reservoir properties (model parameters)

This subchapter introduces and presents the characteristics of the strongly rock-type dependent parameters. These parameters are porosity, absolute permeability, relative permeability and capillary pressure. The properties of discussion can be divided into two groups based on their characteristics. The first group includes the static model parameters implemented into the model through geostatistical modelling. These are the porosity and absolute permeability data, which mainly come from core plugs and well logs. The second group is the saturation functions, which are the relative permeability and capillary

pressure curves. These parameters are the function of fluid saturation. In general, the porosity is more like a volumetric property, while the other three, the absolute and relative permeability and the capillary pressure function, are determinants for fluid flow. Moreover, the fluid flow behaviour can be predicted from the saturation functions, and other vital rock-fluid properties, such as essential fluid saturations (connate water and residual oil saturations), can be interpreted.

3.3.1 Porosity-Permeability (ϕ-k) Diagram

This section describes the established correlation between the two main model parameters. First, a brief introduction of porosity and absolute permeability, in general, can be found. Then, the ϕ-k diagram and its characteristics are explained/introduced.

Porosity (ϕ)

The porosity is deemed one of the essential static parameters, as it defines the fluid volume capacity stored in the porous media. We can differentiate several classifications of porosity. Depending on the formation time, the porosity can be either primary or secondary. Based on the location of the pores, it can also be either inter-granular or intra-granular. Moreover lastly, subject to the pore connectivity, total and effective porosity can also be distinguished. Generally, effective porosity is applied in reservoir engineering calculations, including numerical simulations. Effective porosity is applied because it accounts for only

interconnected pore space in the system, which stores the reservoir fluids and is accessible for fluid flow.

Porosity can be defined as the ratio of pore volume over bulk volume and is written as follows:

$$\phi = \frac{V_p}{V_b} = \frac{V_b - V_s}{V_b}$$

Eq. 3.1

, where:

ϕ – porosity,

V_p – pore volume,

V_b – V_T total or bulk volume of the rock,

V_s – Solid volume of the rock.

In addition, micro and macroporosity in both homogenous and heterogeneous rocks can also be differentiated. These two classifications have a strong dependence on each other. Therefore, the representative elementary volume (REV) has to be introduced. The REV represents a small portion of the volume of the reservoir rock, which resembles the actual behaviour of the reservoir. If the applied volume is not enough, the accurate picture of the reservoir cannot be seen because the

microscopic behaviour dominates. If the used volume is representative enough for the reservoir, then the realistic behaviour of the reservoir in field-scale can be represented. Therefore, the REV can be broadly described as the minimum sample volume, representing and accurately describing the reservoir parameters.

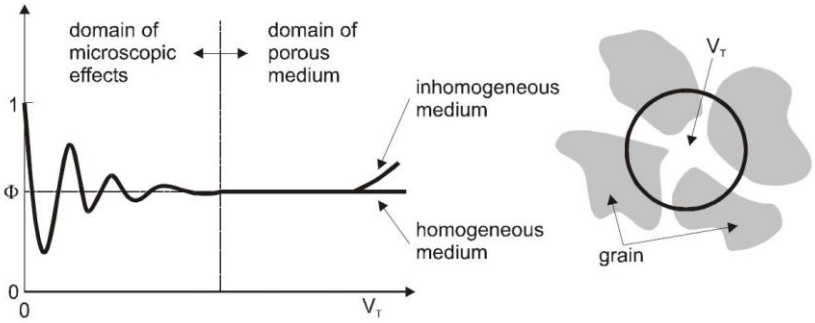

Fig. 3.3: REV (Representative Elementary Volume) in terms of porosity (Bear, 1988)

The porosity is measured through well-logs and core samples. The core should be within the REV dimensions, or otherwise, the measurement is not reliable for the part of the reservoir from where the core sample has been taken. Therefore, after the core sampling and data selection, the second step in the digital rock physics workflow is to obtain the REV. Then, the RCAL and SCAL measurements can be concluded to be representative.

Absolute permeability (k)

The second important parameter is absolute permeability, which is the resistance to the fluid flow in a single-phase system.

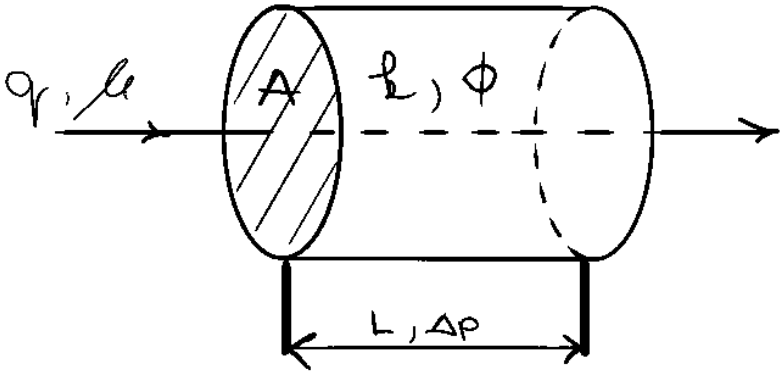

Fig. 3.4: Schematic figure of Darcy´s law (Jenei, 2017)

The widely used formula is called Darcy's law, which is schematically represented in Fig. 3.4. This hypothesis describes the flux along with an L long tube with respect to the ΔP pressure difference.

Darcy´s law is

$$q = -A\frac{k}{\mu}\nabla p = -A\frac{k}{\mu}\frac{\Delta p}{L}$$

Eq. 3.2

the Darcy velocity can be written as

$$v = \frac{q}{A} = -\frac{k}{\mu}\nabla p$$

Eq. 3.3

the formula of the real velocity is

$$v_{real} = v/\phi = \frac{q}{A\phi} = -\frac{k}{\mu\phi}\nabla p$$

Eq. 3.4

, where:

q – volumetric flow rate,

A – cross-sectional area,

k – absolute permeability of the rock,

μ – dynamic viscosity of the fluid,

∇p – pressure gradient along the core,

v – Darcy velocity, v_{real} – real velocity of the fluid,

ϕ – porosity of the core.

The corresponding units of Darcy´s law in Darcy and the SI system can be written as follows.

Darcy units:

$$\left[\frac{cm^3}{s}\right] = \frac{[cm^2][D]}{[cp]}\frac{[atm]}{[cm]}$$

SI units:

$$\left[\frac{m^3}{s}\right] = \frac{[m^2][m^2]}{[Pa.s]}\frac{[Pa]}{[m]}$$

After Henry Darcy, the unit of the permeability is 1 Darcy, which is equal to 9.87×10^{-13} m^2. The core plug has isotropic permeability if the absolute permeability is the same in every direction. In this dissertation, absolute permeability is understood in three dimensions. The two horizontal (k_h) directions are k_x, k_y and in the vertical (k_v) direction as k_z.

Typically, absolute permeability is measured through RCAL experiments, where it can be obtained in all three directions. As a rule of thumb, the following simplification can be applied $k_h=k_x=k_y$ and $k_v=k_z=k_h/10$, where k_h is generally ten times bigger than k_v.

The absolute permeability is assigned to the static models through co-simulation. It is calculated after the assignment of porosity values. It is

calculated based on the preliminarily established relationship between porosity and absolute permeability, so-called ϕ-k diagram/correlation.

Porosity (ϕ) and absolute permeability (k) correlation

A relationship can be established by combining the two main model parameters, namely the porosity and absolute permeability. This relationship is established from the results of the previously described RCAL measurements of rock samples. The methodology is relatively simple - collect all the rock samples with corresponding results and cross-plot the corresponding values. This way, all rock samples have two values: the porosity, and the absolute permeability, which is then indicated on the x- and y-axis. There is a difference in the scale of these two parameters. Therefore the absolute permeability is represented on a logarithmic scale, while the porosity stays linear.

In order to use the ϕ-k function as a part of the history matching process, it needs to be quantified. There are several methods of deriving a correlation between the core porosity and absolute permeability values. In this dissertation, to stay generic, the linear correlation and the corresponding ellipse is used. The ϕ-k diagram then fits a straight line through the "cloud" or cluster of points. This analysis can indicate the different rock types when clearly different clouds can be separated on the diagram.

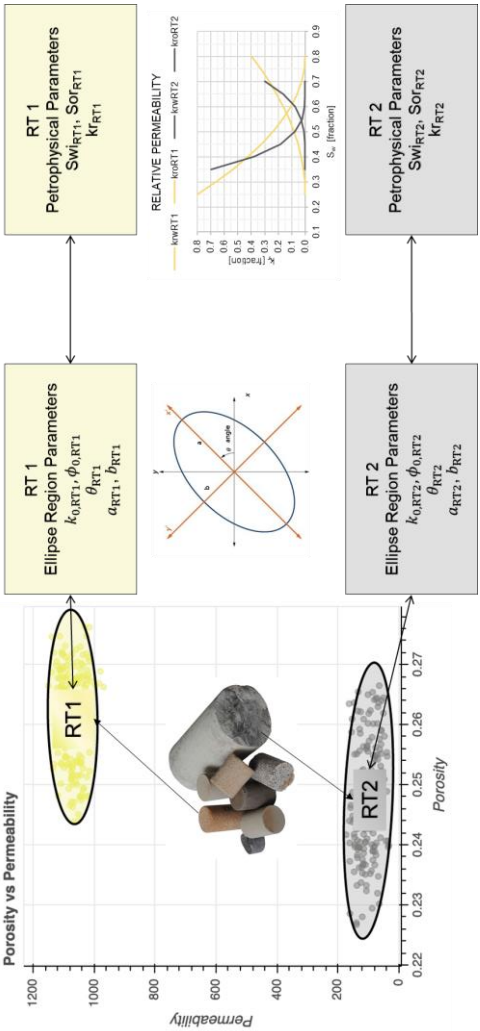

Fig. 3.5: Rock Type dependent parameters and their parameterised connection (Jenei et al., 2020)

Most of the time, porosity and absolute permeability values from different clouds represent different flow behaviour, described by the individual relative permeability and capillary pressure curves. As it was mentioned in the facies modelling section, this is not always the case, but when the focus of the geological model is to perform flow simulations, only those facies or rock types are helpful and need to be identified/separated, where there is a difference in saturation functions; therefore the flow behaviour is affected.

In this dissertation, the applied method is to identify different rock types as the clouds of points, which is technically done by ellipse regions. Fig. 3.5 shows the rock type dependent parameters and their connections. These identified rock types then have corresponding saturation functions, which are, with their characteristics, described in detail within the following section.

3.3.2 Saturation functions (relative permeability and capillary pressure)

The saturation functions are one of the most important parameters with regard to fluid flow. They are taking place in the constitutive equations of extended Darcy's law.

$$q_\alpha = \frac{k \cdot k_{r\alpha}}{\mu_\alpha} \cdot A \cdot \frac{\Delta p_\alpha}{\Delta L}$$

Eq. 3.5

, where,

q_α – flux of phase alpha

k – absolute permeability of the rock,

k_α – relative permeability of the phase α,

μ_α – dynamic viscosity of the phase α,

A - cross-sectional area of the flux,

Δp_α – pressure difference of the phase α

ΔL – the travel length of the fluid

α – different fluid phases can be oil, gas, water.

The reservoir rock's relative permeability and capillary pressure functions for each fluid phase can be measured in a core sample with various special core analysis techniques (SCAL). These SCAL techniques are steady-state, unsteady-state methods for relative permeability values as a function of different saturation values and mercury injection capillary pressure (MICP) and centrifuge methods for capillary pressure measurements. Some of the most commonly used laboratory methods for measuring relative permeability are not described in detail below because this subchapter aims to introduce and

explain the main parameters, characterising different rock types and rock fluid interactions.

Relative permeability

A two-phase or multiphase system implies that two or more fluids co-exist within the porous media. In a multiphase fluid flow system, the flow parameters and the effective permeability of each present phase are reduced due to the reduction of the effective cross-section compared to a single-phase fluid system.

The factor of this reduction can be quantified as relative permeability. It is a dimensionless factor, which describes the influence of the different phases on each other under multiphase flow conditions. The term the relative permeability is solely applicable when at least two fluid phases are present in the system simultaneously. The relative permeability describes the relative flow behaviour of the phases compared to the absolute permeability. Therefore, it can be defined as a ratio between effective permeability and the absolute permeability of the rock, as can be seen in the following formula.

$$k_{r\alpha} = \frac{k_\alpha(S_\alpha)}{k}$$

Eq. 3.6

, where:

$k_{r\alpha}$ – the relative permeability of phase α,

$k_{\alpha}(S_{\alpha})$ – the effective permeability of phase α,

k – the absolute permeability of the rock.

By definition, the sum of the relative permeability cannot be more than one, and the effective permeability should be less than the absolute permeability. This is due to the capillary pressure and the fluids' mutual resistance to each other. However, regarding the latest hypothesis, the relative permeability theoretically can be higher than one. This case happens when the wetting fluid is at immobile saturation and plugs the micro-pores, acting as a lubricant. The continuous and connected wetting phase ultimately allows the other fluid to flow through the rock easier than if just one phase was present(Bear, 1988).

Depending on the rock types, the relative permeability function has significant differences in the characteristics, mostly the shape and form and the immobile and mobile saturation ranges are affected. For example, typically, a low permeability rock has higher immobile fluid saturations, lower end-points and a flatter curve with a higher curvature in comparison to a high permeability class (Felsenthal, 1979). Not only the absolute permeability but many more rock and fluid properties and reservoir conditions can affect the characteristics of relative permeability, which are the following:

- saturation states,
- rock properties, wettability, porosity
- reservoir conditions (overburden pressure, reservoir temperature)
- interfacial tension, fluid density and viscosity,
- initial wetting phase saturation,
- immobile third phase.

Some of these have major, some of them have minor effects, and some of their effects are not independent; the specific relationships are described (Honarpour, Koederitz and Harvey, 1986).

There should be specific attention paid to the wettability of the rock. "Wettability is defined as the tendency of one fluid to spread on or adhere to a solid surface in the presence of another immiscible fluid" (Tarek Ahmed, 2010). Therefore, wettability is an important parameter when the saturation functions are discussed in a multiphase system. The saturation functions can have significant characteristic differences based on the wetting condition. There are different wettability conditions in the case of a two-phase oil-water system, which are: water-wet, oil-wet, intermediate and mixed-wet. Typical examples of relative permeability curves of different wetting systems are illustrated in Fig. 3.6.

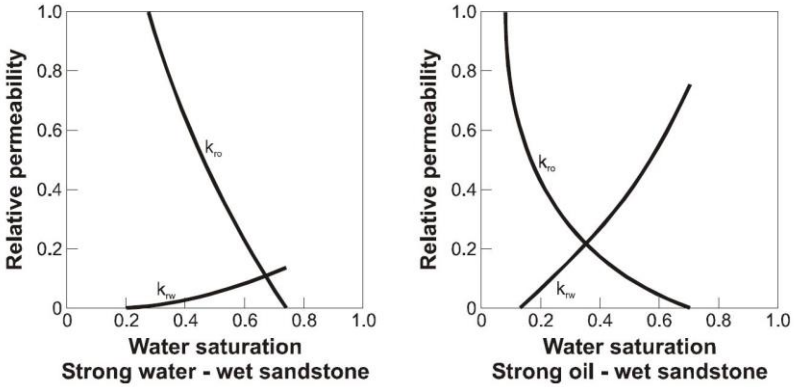

Fig. 3.6: Typical relative permeability curves based on wettability after Craig (Heinemann and Mittermeier, 2013)

In the scope of this research, the saturation function is not used or investigated with regard to wettability. It is essential to raise attention to the fact that the wetting conditions cannot be directly entered in the numerical reservoir simulation. Creative solutions to mimic different wetting conditions during the simulation may be developed in the future. Like in the case of different wet regions within one rock type, the different saturation functions can be considered accordingly. However, this requires further research.

Capillary pressure

The capillary force originates from the pressure difference across the curvature fluid interface and is influenced by the interfacial tension, the wettability and the pore structures. In reservoir simulation, the capillary

pressure is used as a function of water saturation. Fig *3.7* demonstrates an example of a drainage capillary pressure curve as a function of water saturation used in a numerical reservoir simulation. It is considered on the macroscopic level; therefore, the contact angle and the pore structure are included indirectly. This pressure difference is proportional to the density difference. Fig. 3.8 shows the typical characteristic capillary pressure curves for low (flatter) and high (steeper) permeability rock.

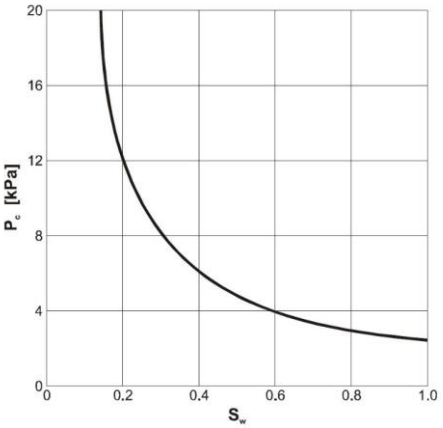

Fig. 3.7: Typical drainage capillary pressure curve as a function of water saturation (Heinemann and Mittermeier, 2013)

$$P_c = p_{nw} - p_w$$

, where:

P_c – capillary pressure,

p_{nw} – hydrostatic pressure of the non-wetting phase,

p_w – hydrostatic pressure of the wetting phase.

If the equilibrium has been assumed on the two-phase interface, the capillary pressure can be the function of the geometry on the micro-scale, as seen in the Young Laplace equation.

$$P_c = \frac{4\sigma_{12}\cos\theta}{d} = \frac{2\sigma_{12}\cos\theta}{r}$$

Eq. 3.7

, where:

P_c – capillary pressure,

σ_{12} –interfacial tension between the wetting and the non-wetting phase,

θ – contact angle of the wetting phase,

d – The diameter of the pore.

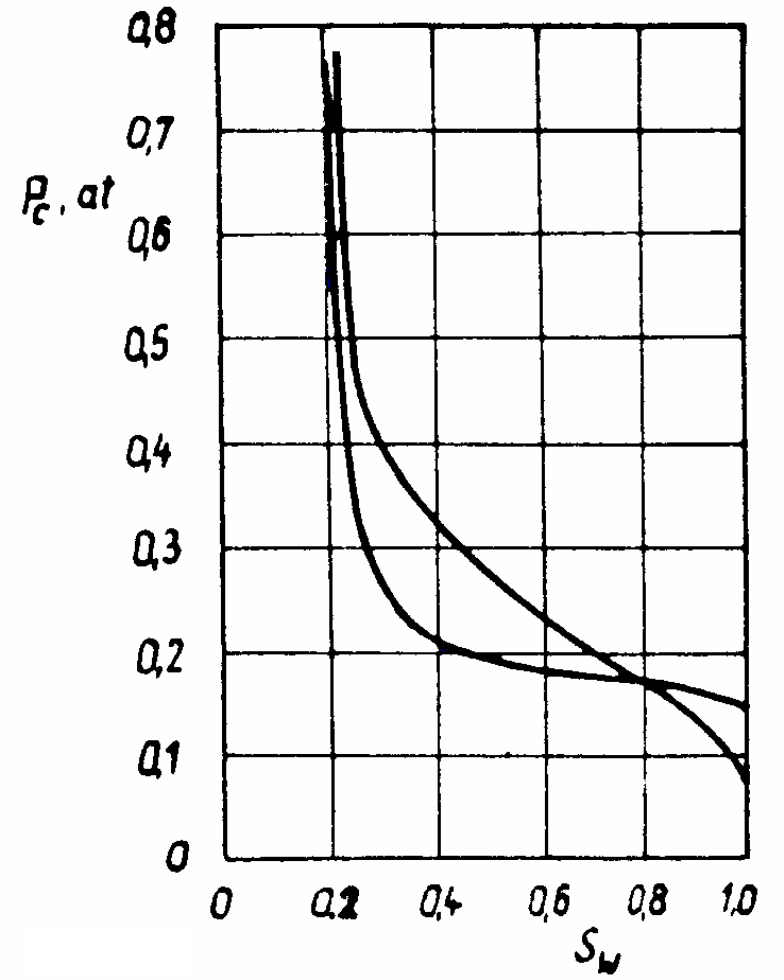

Fig. 3.8: Typical capillary pressure curves for low (flatter) and high (steeper) permeability rock (Bódi, 2006)

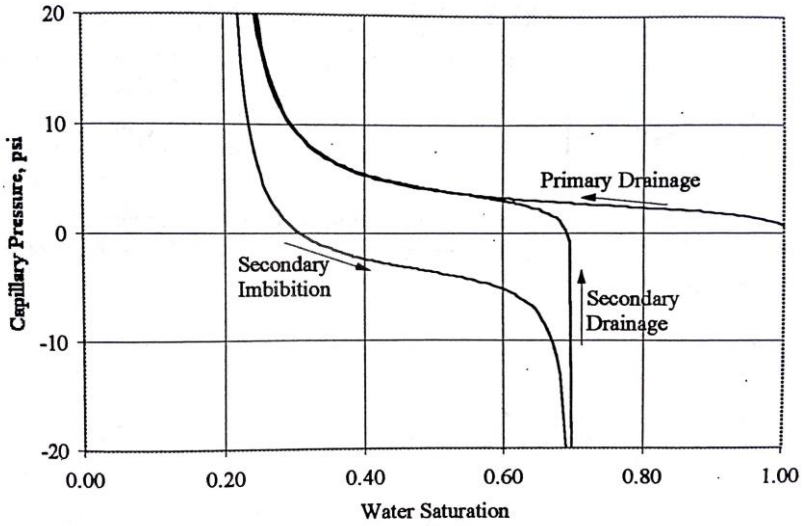

Fig. 3.9: Capillary hysteresis (Christiansen, 2001)

In addition to the capillary behaviour, capillary hysteresis has to be introduced. Because of the capillary hysteresis, two types of reservoir processes have to be marked. One is when the non-wetting fluid displaces the wetting fluid, which is called drainage; the other is when the non-wetting fluid is displaced by the wetting fluid, which is called imbibition. In imbibition and drainage processes, forced and spontaneous parts can be distinguished. These processes can be attached to the actual reservoir conditions; for example, when the reservoir rock is water wet, and the oil is migrating into the reservoir - the process can be called drainage. The other process is spontaneous imbibition when the oil is displaced by water-flooding from a water-wet reservoir. The

wettability of the reservoir rock is an essential parameter; therefore, this property of the rock has to be clarified to know which process is the drainage and which process is the imbibition (Bear, 1988).

The following schematics demonstrate the relationship between the remarkable saturation points.

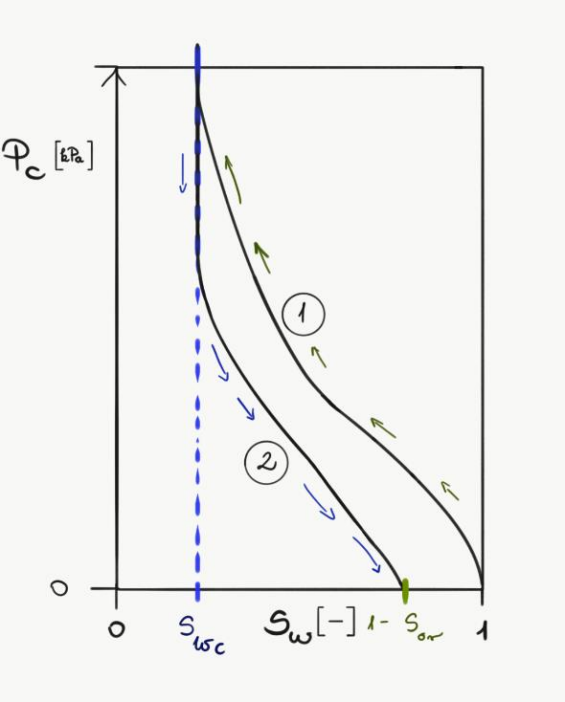

Fig. 3.10: Schematic figure of the capillary hysteresis in a water-wet system, Curve: 1: drainage (water displaced by oil), Curve 2: imbibition (oil displaced by water)

When the reservoir is at the initial stage, the production starts from the end of the first curve, which is the starting point of the second imbibition curve, at the S_{wc} saturation value. The primary drainage capillary curve is used to determine the initial phase distribution in the reservoir, as shown in Fig. 3.11.

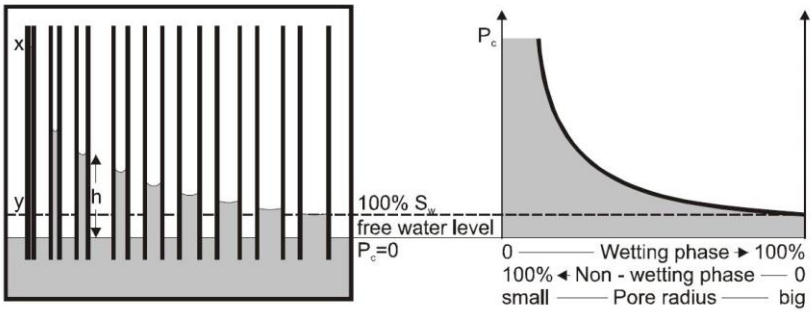

Fig. 3.11: Equilibrium between gravity and capillary forces (Heinemann and Mittermeier, 2013)

3.3.3 Parameterization of saturation functions (relative permeability and capillary pressure)

Commonly, when the relative permeability and the capillary pressure functions are used in any flow calculations in porous media, these functions are parameterised. There are several different parametrisation methods established. In ECLIPSE and tNavigator, these functions are provided in the tabulated form of the forward simulation. These parameterisations are essential for history matching when these

functions are matching parameters. The supported parameterisations are the Corey function, the Eq. 3.8 and Eq. 3.9 for relative permeability accordingly. The capillary pressure function can be parameterized as well with several different functions, for example, the widely used Leverett J function, which helps determine different rock types. Generally, these functions must be the last resort to change in history matching.

Relative Permeability

Several relative permeability correlations are proposed, such as the Burdin method (Burdine, 1953), LET correlation (Lomeland, Ebeltoft and Thomas, 2005), Corey (Corey, 1994) and Brooks-Corey parametrisation (Brooks and Corey, 1966). These correlations can describe the shape of the relative permeability curves if we show them as a function of saturation. In this thesis, the most commonly used Corey correlation has been adapted.

The general Corey approach can be written for oil and water system in the water-wet reservoir rock, as a form of the following equations:

$$k_{rw}(S_w) = k_{rwn} \cdot \left(S_{weff}\right)^{n_w} = k_{rwn} \cdot \left(\frac{S_w - S_{wc}}{1 - S_{or} - S_{wc}}\right)^{n_w}$$

Eq. 3.8

$$k_{ro}(S_w) = k_{ron} \cdot (1 - S_{weff})^{n_{nw}} = k_{ron} \cdot (\frac{1 - S_w - S_{or}}{1 - S_{or} - S_{wc}})^{n_{nw}}$$

Eq. 3.9

, where:

S_w – Given saturation of the water phase,

S_{weff} – Effective saturation of the water phase,

$k_{rw}(S_w)$ – Relative permeability of the water phase at the given saturation,

$k_{ro}(S_w)$ – Relative permeability of the oil phase at the given saturation,

k_{rwn} – The endpoint of the water phase relative permeability curve,

k_{ron} – The endpoint of the oil phase relative permeability curve,

S_{wc} – Connate water saturation,

S_{or} – Residual oil saturation,

n_w – Corey´s exponent of the water phase,

n_o – Corey´s exponent of the oil phase.

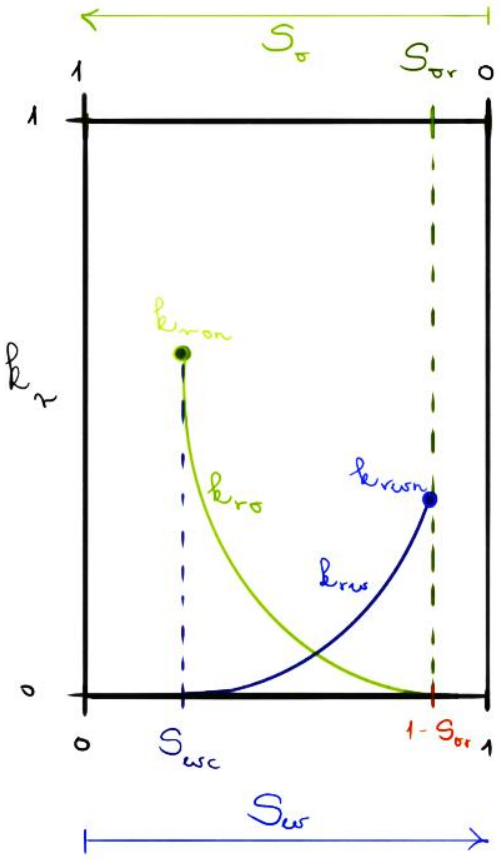

Fig. 3.12: Typical relative permeability curves of oil and water in a water-wet system(Jenei, 2017)

Fig. 3.12Fig 3.12 shows typical relative permeability curves in a water-

wet system when the oil and water phases are present. If the system is water-wet, the cross-section point of the relative permeability curves is above 50 % of water saturation. The other points on the relative permeability curves that significantly affect the flow behaviour in the reservoir are the S_{wc}, S_{or} k_{rwn}, k_{ron}, and the exponents n_w, n_o. These parameters are enough to describe the relative permeability curves. Theoretically, the S_{wc} refers to the unmovable water saturation; thus, it can be attached to the k_{ron}, the endpoint of the oil relative permeability curve, where the oil relative permeability can reach the highest value.

On the other hand, this is the starting point of the water relative permeability curve. Increasing the S_w continuously and gradually decreases the oil relative permeability, whilst the water relative permeability increases.

The cross-section point must be highlighted before the water relative permeability curve reaches the highest point and the oil relative permeability curve at the lowest point. The cross-section point is very remarkable because, at different phase saturations, there can be the same relative permeability of the phases. Furthermore, the system has the lowest total mobility value at this point.

Capillary pressure

Leverett J function (Leverett, 1941) is a sufficient dimensionless representation of capillary pressure curve; it is widely used in industry and research. It can be applied to identify different rock types as well.

The Leverett J function can be calculated with the following equation:

$$J(S_w) = \frac{P_c}{\sigma_{12} \cos \Theta} \sqrt{\frac{k}{\phi}}$$

Eq. 3.10

, where

$J(S_w)$ – Dimensionless Leverett J value as a function of water saturation,

P_c – capillary pressure,

σ_{12} – interfacial tension between fluid 1 and 2,

Θ – contact angle,

k – absolute permeability,

ϕ- porosity.

The representation of the Leverett J function is shown in Fig. 3.13.

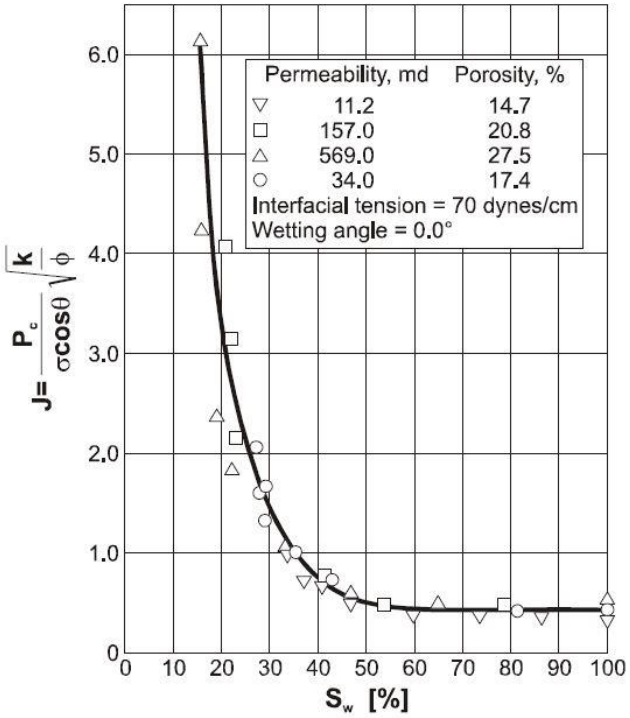

Fig. 3.13: Leverett J function after Leverett (Heinemann and Mittermeier, 2013)

As the above-described function shows clearly, the idea of identifying different rock types should consider the porosity and absolute permeability values is not new. The $\frac{k}{\phi}$ variable can also be used as rock quality index (RQI) (Amaefule et al., 1993; Guo et al., 2007; Chandra

et al., 2015). The rock types can be qualified based on the RQI and sometimes based on the flow zone indicator (FZI). The flow zone indicator is the ratio of the rock quality index and the normalised porosity (Guo et al., 2007).

$$\phi_n = \left(\frac{\phi_{eff}}{1-\phi_{eff}}\right)$$

Eq. 3.11

$$FZI = \frac{RQI}{\phi_n}$$

Eq. 3.12

As an example for parameterization of capillary pressure, the Extended Corey correlation for the capillary pressure curves can be seen in the equation below.

Extended Corey correlation for Pc curves:

$$Pc = \begin{cases} A_w \cdot \left(1 - \dfrac{S_w - S_{wc}}{S_{wd} - S_{wc}}\right)^{cw} + S_{wd} \cdot r_i + b_i \\ S_w \cdot r_i + b_i \\ A_o \cdot \left(1 - \dfrac{1 - S_w - S_{or}}{1 - S_{od} - S_{or}}\right)^{co} + S_{od} \cdot r_i + b_i \end{cases}$$

Eq. 3.13

Assumptions: $$S_{wc} \leq S_w < S_{wd}$$

$$S_{wd} \leq S_w \leq S_{od}$$

$$S_{od} < S_w \leq 1 - S_{or}$$

, where:

A_w , A_o – Height of curve pc area near water and oil zone correspondingly,

r_i – Slope of the linear part (plateau).

$$S_w: S_{wc} < S_{wd} < S_{od} < 1 - S_{or}$$

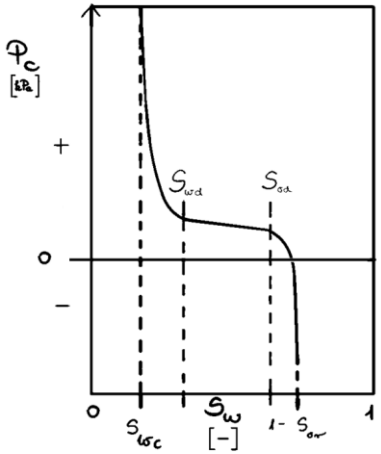

Fig. 3.14: Remarkable points of the Extended Corey function on the capillary pressure curve

3.3.4 Different Facies and Rock Typing in numerical reservoir simulation

The parameter or so-called “keyword” used to identify the different rock types in the simulation software is the SATNUM.

The SATNUM keyword has to be placed in the REGIONS section of the keywords in the simulation deck, and it is connected to the saturation functions. The keyword should be followed by one integer for every grid block in the current input box, specifying the saturation function region to which it belongs. The region number should not be less than one or greater than NTSFUN (set in the TABDIMS keyword). The saturation function region number specifies which set of saturation functions (input using SGFN, SOF3 and related keywords in the PROPS section) should be used to calculate relative permeability and capillary pressures in each grid block.

The data of the TABDIMS keyword consists of some or all of the following items, which describe the sizes of saturation and PVT tables used in the run and the number of fluid-in-place regions. The data must be terminated by a slash(/).

1. NTSFUN. The number of saturation tables entered using SGFN, for example. (Different saturation tables may be used in different parts of the reservoir - see SATNUM.)

The SWOF keyword may be used in runs containing both oil and water as active phases. It may also be used to input tables of water relative permeability, oil-in-water relative permeability and water-oil capillary pressure as functions of the water saturation. If gas is also an active phase in the run, the gas/oil saturation functions must be input with either keyword SGOF or SLGOF.

The data comprises NTSFUN (set in the TABDIMS keyword) tables of water/oil saturation functions, each terminated by a slash (/).

Each table consists of three columns of data. The first column is the water saturation, the second is the corresponding water relative permeability, and the third is the corresponding oil relative permeability. When only oil and water are present, the last column is the corresponding water-oil capillary pressure.

Other parameters identified with the different rock types are porosity, absolute permeability, and connate water and residual oil saturation.

When there are different rock types, different numbers under the SATNUM keyword are used to identify each one of them. For each different SATNUM value, there should be a corresponding SWOF table defined under the PROPS section.

These keywords are valid for both ECLIPSE and tNavigator software because the ECLIPSE keywords are fully supported in tNavigator. (Schlumberger, 2020a; Rock Flow Dynamics, 2021).

Chapter 4 Methodology and Rock Typing Workflow

This Chapter contains a thorough description of the methodology applied in this dissertation, followed by the developed workflow.

In order to achieve the objectives of this research and prove the validity of the concept, two primary stages are performed. The first stage is to apply the traditional history matching method with the available tools on a semi-synthetic model. The second stage aims to perform a history matching with the application of the novel, extended rock typing workflow. Then, a comprehensive comparison of the rock typing workflow results from the second stage and the so-called conventionally-matched results achieved through the first stage can be made.

The details and the realisation procedure of the rock typing workflow are described thoroughly, explaining the applied fundamentals, including the rock type validation and correction steps with the applied distance calculation. The applied distance calculation is described, including the Mahalanobis distance, the utilised confidence interval and their calculation.

4.1 Methodology

As the "truth" model, a synthetic model with the spatial distribution of the petrophysical properties of the reservoir is generated. Two different rock types based on absolute permeability and porosity classes are defined. Consequently, the rock types have a different porosity-permeability relationship (ϕ-k function), relative permeability (k_r), and capillary pressure (P_c) curves with different irreducible fluid saturations, which are connate water (S_{wc}) and residual oil saturation (S_{or}). Simulation of the created "truth" model generates the observed data set, i.e., observed history, which can then be extracted and further utilised in the base case. In order to create a base case model for simulation, the distributions of rock type, porosity and absolute permeability from the "truth" model need to be used to obtain a different realisation.

Construction of simple synthetic simulation cases

Construction and design of a synthetic model with its simulation run deck of the "truth" model provides the observed data set for history matching. This step is then followed by creating a base case with modifying the truth model.

History matching is conducted conventionally as the first attempt, with the original adjoint-based optimization, honouring constraints independently, until a good match within an acceptable range is

achieved. In contrast, the second attempt is conducted with the help of the extended and rock type adjusting workflow, honouring the geological constraints and maintaining the established petrophysical link between the different geological information with respect to the different rock types. The sequence of this proof of concept method is listed and described below.

Proof of Concept

0. Initial rock type distribution, where the relevant petrophysical information is assumed.

1. History matching the base case conventionally using base workflow: changing the model parameters with adjoint driven assisted history matching procedure.

2. History matching with integrated model validation on rock type consistency using the extended workflow: adjusting the rock types according to the model parameter changes.

    a. Iterative parameter changes with rock type adjustments.

    b. When the history matching is satisfactory - finish the loop.

    c. Final history matched model: the model represents the realistic reservoir behaviour with maximum achievable geological consistency.

3. Comparison of the two different history matching results, based on several criteria.

The criteria of comparing the results of the two different history matching workflows are extended. Typically, only the simulated results and objective functions would be compared to analyse the quality of the history matching. Here, the aim is to preserve the geological and geophysical features. Therefore, the success lies within keeping the global parameter distributions while the spatial distributions move closer to the "truth" model, preserving the established connections.

Therefore, the divergence from the "truth" and base case is analysed in additional parameters in both final results. These are the rock type distribution in space, the histogram of rock type, the porosity and absolute permeability distributions, and the correlation between porosity and the permeability (***ϕ-k*** diagram).

The above-described workflow was conducted on a 2D simple model to prove the workflow's concept. Then, the used simple model was altered for sensitivity analysis on the effect of different model parameters on the performance of the extended workflow. The simple synthetic model and its variations are described in Chapter 5, the results of the different model variations are summarised in Chapter 6.

External workflow development with extended constraints

There are two workflows, sensitivity calculation with modification of the parameters and the improved workflow. The geologically consistent history matching is only possible if the changes of the parameters indicate a corresponding change with the other parameters based on their relationship. The changes mentioned above are performed for different properties, such as rock type. The first modification of the parameters is done based on the sensitivity calculation internally; the second modification is done based on the relations externally. The first modifications are conducted under the assisted history matching tool control with the set conditions, while the second modifications are under external control. The rock type adjusting workflow honours the link between the different constraints and is compatible with the most widely used commercial tools, ECLIPSE and tNavigator, as previously described in Chapter 2. The parameters are not modified independently, meaning that after a specific iteration, when the absolute permeability is moved into a different rock type category, the rock type of the cell is changed into the correct category. The rock types are defined before any modifications and have different petrophysical parameters. With the rock type change, the corresponding parameters are also changing automatically, for instance, relative permeability and capillary pressure, while the parameter distributions do not change significantly. In order to evaluate the new tool's capabilities, a benchmark should be performed between the history matching achieved with the available assisted

history matching tool (standard workflow) and with the help of the developed external workflow (rock typing workflow).

Optimization and workflow implementation

The external assisted history matching workflow script is written in a generic way in Python language in order to integrate it into various graphical interfaces according to its new functionalities. The prominent Python script couples and uses the functionalities of SenEx. It executes the individual steps of the history matching workflow. It does not only work with them but several extensions are implemented independently and inserted between the steps of the conventional workflow. The entire workflow is wrapped up in a flexible way, not as one piece; it breaks certain functionalities into steps in order to make them accessible for alterations. In the rock type adjusting workflow, the sequence of the SenEx loop is slightly modified without the interruption of the initial approach. One of the significant extension steps is, for example, the automated multiple setup combination, the identification of different rock type regions and the export of a new set of the array for SATNUM. The detailed overview is written under sub-chapter 4.2 and 4.3.

4.2 The Rock Type Adjusting History Matching Workflow

The rock-type driven extended history matching workflow has three main parts. The first part is the available computer-assisted adjoint driven history matching approach. The second part is the rock type adjustment, which serves as the main contribution of this dissertation. The third part and also the innovative detail is the automation of multiple setup combinations. The idea of performing computer-assisted history matching employing a post-processing tool is not new. The base workflow with detailed insight into the adjoint-based approach is described in Chapter 2. The main focus of this subchapter is to introduce the extension of the adjoint-based history matching approach. The base approach is shown in Fig. 4.1 as the black vertical part (Almuallim *et al.*, 2010) of the workflow representation utilized in the rock typing workflow. The extended workflow has been developed using and improving the adjoint-based tool in terms of geological consistency. In Fig. 4.1, the left blue part (Jenei *et al.*, 2020) represents the rock typing extension, which is one of the vital parts of this work. The rock typing workflow aims to improve the geological consistency of the assisted history matching results.

On top of that, the invisible feature, the automated multiple setup combination, allows the workflow to run through all the history matching sequences without human interaction. This means that the extended workflow can be executed multiple times with different

optimization setups automatically. The Rock Type Adjusting History Matching Workflow is as follows (Jenei *et al.*, 2020):

I) Model Preparation and Identification of Rock Type Regions

II) Extended optimization setup (model parameter limits and objective function weights)

    1) Sensitivity Explorer Loop (one optimization iteration)

        1. Initialize Sensitivity Explorer Case

        2. Simulation

        3. Mismatch calculation (Objective Function)

        4. Sensitivity coefficients calculation (with respect to model parameters)

        5. Model parameters modification

    2) Adjustment of Rock Type

        1. Rock type number (SATNUM) identification

        2. Rock type number (SATNUM) update

III) Multiple-setup combinations

The first point (I) is emphasised because of automatically identifying rock types from the base case with the extended workflow and the confidence ellipse definition. The identification of rock type regions is conducted before running any numerical calculations.

The second point (II) is the extended optimisation setup. This step is conducted as a part of the conventional workflow, where the weights, limits and the desired parameters for modification are set up. The Sensitivity Explorer Loop lists and includes the functions and steps conducted within one iteration. Several iterations can take place within one optimization setup. In order to apply new weighting factors and emphasise different parameters and set different limits, a new setup needs to be prepared. Within the Optimisation Setup, one of the main contributions of this research is the Adjustment of Rock Type. The first step within the rock type adjustment is identifying rock type number (SATNUM) driven by the new absolute permeability and porosity values. The criteria are based on the pre-defined rock type regions in ϕ-k space, with the application of Mahalanobis distance to the centre of the confidence ellipse or interval. The second step is updating the rock type number (SATNUM) according to the previous step, which then implies a change in the used corresponding rock physics functions (k_r, P_c). Different SATNUM leads to the application of different saturation function tables.

The third point (III) is multiple setup combinations, which can automatically execute several optimization setups with different

sequences. The applied and combined setup series are based on the typical history matching phases. For example, first, focus on the global values and match the overall energy in the reservoir through the static reservoir pressure, then focus on the global fluid production rates. Finally, focus on the more tedious part with the local rates(individual well-rates), then fine-tune it for the breakthrough times.

4.2.1 Adjustment of Rock Type

The workflow for adjusting rock types is based on newly generated porosity and absolute permeability values (ϕ, k). It consists of two main steps. The first step is the validation, followed by the required correction in the second step. Fig. 4.1 shows the rock-typing extension of the workflow presented in Fig. 2.2.

First step/Validation: The purpose of the validation step is to identify whether the porosity-permeability values of an individual cell still honour the currently assigned rock type. The corresponding feasibility region characterises each rock type in the ϕ-k diagram. The feasibility region is the space where a particular rock type is defined based on petrophysical studies, core sample and log data, as well as established correlations (Pyrcz and Deutsch, 2014). In the case where ϕ-k values of a particular cell are inside the feasibility region, the rock type does not change. However, if the ϕ-k values of a cell fall out of the current rock type region, the correction step is applied.

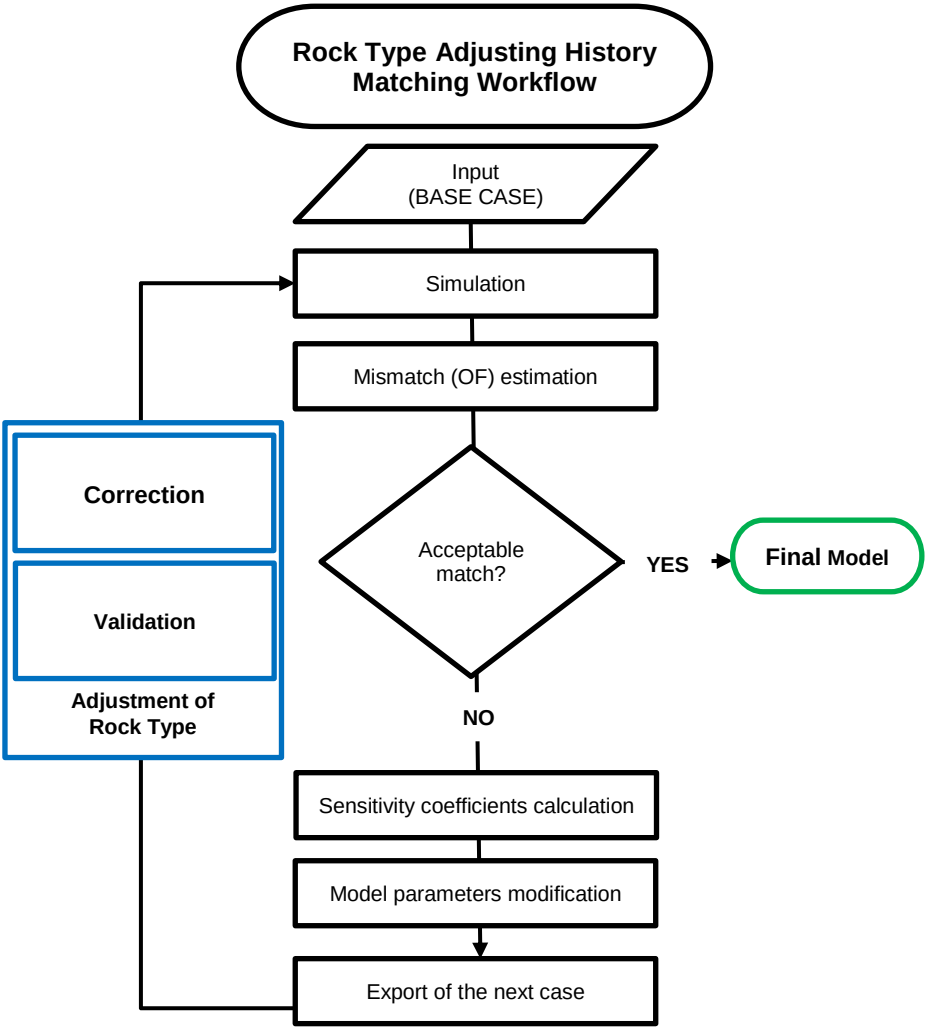

Fig. 4.1: The Rock Type Adjusting History Matching Workflow (Jenei et al., 2020)

Second step/Correction: The correction step assigns the "correct" rock type to the cells based on the statistical measure, called Mahalanobis distance, defined in standard deviation units. The distance is calculated between the given ϕ-k value of the cell and every available rock type region in the ϕ-k diagram. This distance functions as a basis for deciding which rock type should be assigned to the individual cells. The closest rock type regarding the above distance measure is then assigned to the given cell. This way, the ϕ-k point is uniquely identified in the ϕ-k space between the feasible regions associated with the corresponding rock types.

The identification of rock type is unique even when the rock type regions overlap. In nature, or in realistic scenarios, that is fairly often the case. In the presented approach, the uniqueness is ensured because as long as the ϕ-k value is inside the feasibility region, the rock type does not change.

Nevertheless, the ϕ-k point from the overlapping area can still take different rock type values throughout the history matching process by travelling from one feasibility region to another. This way, the history matching process advances towards exploring the best fit within the initially assigned rock type region. Only when the sensitivities suggest that a better fit can be achieved outside of the original rock type, then the algorithm move the ϕ-k point out and continue the search for the best fit consistently and uniquely.

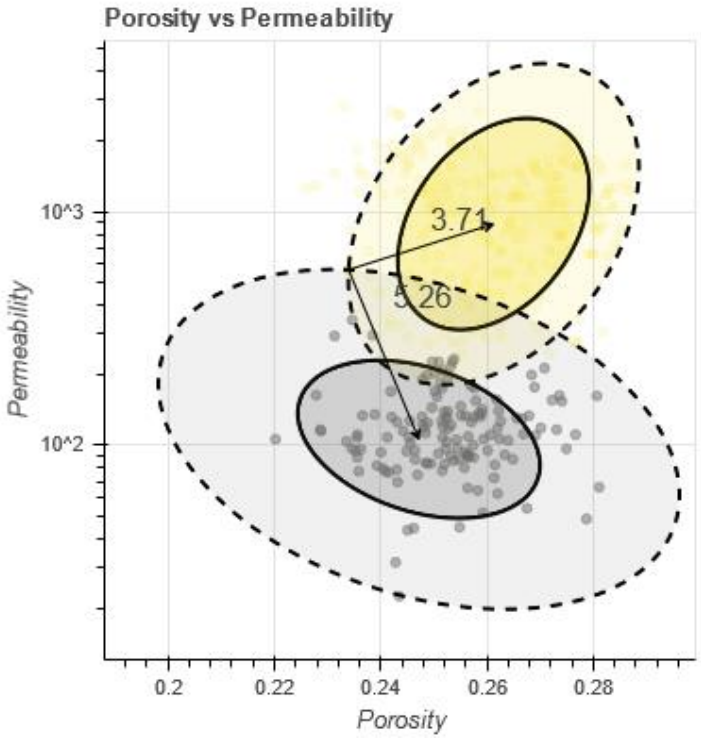

Fig. 4.2: A representation of Mahalanobis distance calculation for the validation and the correction step

The two ways of rock type correction are possible the confidence interval based method and the confidence ellipse region-based method. These are described in further detail in the following section.

4.2.2 Automation of multiple setup combinations

As previously explained in Chapter 2, the history matching procedure has a typical and standard sequence, where the advantage can be taken when the process needs to be automatized. The developed workflow allows us to conduct this effortlessly. Nonetheless, it gives a great value in terms of optimization of the history matching steps and saving time for the reservoir engineer in charge. As it is well known, the final results can be even more precise in cases where the visual judgement of the engineer is not involved, but the precise numbers are considered. Indeed, in the end, excellent engineering judgment is required. However, in a well-constrained multiple set-up combination, a successful history match can be conducted with good quality and within a reasonable amount of iterations. The automation gives considerable value to the rock type adjusting workflow and the original application of the adjoint approach without rock type adjustments. The example can be a more straightforward case when different rock types are either unavailable, not necessary to use, or simply not present in a given case. Since the rock type adjustment is not applicable in such reservoirs, one might note that there is no use of the extended workflow. It is not precisely the case because the automation part can generally be utilised in favour of the history matching procedure. The setups can be varied based on the modifying parameters and the targeted matching parameter, and, therefore, several different multiple set-up combinations can be created. A representative example is shown in the Workflow part of this chapter.

4.3 AIDA: Rock typing workflow extension (Python)

Python is chosen to extend and automate the adjoint-based conventional history matching process. It provides a rich selection of libraries for scientific purposes. Python is a widely accepted programming language by most reservoir modelling software, such as tNavigator, INTERSECT or CMG Software Suite. The core functionality of Sensitivity Explorer, a so-called API (application programming interface), is used to perform the main steps of the history matching procedure, such as defining optimization and objective function setup, performing sensitivity calculations, evaluating an objective function, updating the simulation deck with new grid property values. A thorough description of the workflow is listed below.

Identification of regions

The first important step in performing the history matching is setting up the search space and feasibility region; hence the necessary model parameter constraints must be defined. The pre-processing step is done using the Python script, using the porosity and permeability data from the base case. The parameters of respective confidence ellipses are calculated by establishing the correlation between porosity and absolute permeability of corresponding rock types.

History matching setup files

Since the optimization goal is to minimize the objective function, corresponding objective function weights must be well defined. In addition, the optimization algorithm has its specific settings, such as the maximum number of iterations to be performed and desired tolerance of objective function to be reached. All these settings are defined in the setup file, which Sensitivity Explorer uses. With Python script, the history matching process is further extended and automated by exploiting several setup files, each representing main optimization settings for the specific history matching stage described above.

Simulation and sensitivity calculations

After identifying the regions, using the desired setup file, the typical history matching steps are performed by calling the functionality of Sensitivity Explorer through Python. That includes running the simulation with current model parameters, calculating an objective function mismatch and sensitivity coefficients, and finally exporting the new model parameter arrays (porosity and absolute permeability).

Adjustment of rock types (new SATNUM array)

Once new parameter arrays are defined, rock type regions are validated with Python script. If for some grid cells with new ϕ-k values, currently assigned rock type – SATNUM number with corresponding saturation functions, no longer valid, the selection of correct rock type is performed

with the script, applying the Mahalanobis distance and confidence ellipse definition, associated with corresponding rock types. After adjusting the rock types, the simulation deck is updated with the new SATNUM values using Python script. After that, the described loop continues until one of the conditions is reached, either when the maximum iteration to be performed for the corresponding setup file is achieved, or the objective function is reached to the desired tolerance.

Automation of multistage history matching

If more history matching stages were assigned to be performed, then the procedure repeats using a dedicated optimization setup file for each stage till no more stages are scheduled.

The automated setup combinations are represented in Fig. 4.3 as an extension of the history matching workflow, including all the functionalities described above.

Overall, it is worth pointing out that the extended workflow allows to include different optimization algorithms and different optimization software due to general and flexible implementation.

Post-processing of results

The visualization is also done in Python to analyse further and compare obtained results and corresponding statistics, exploiting the Bokeh library (Bokeh Development Team, 2021).

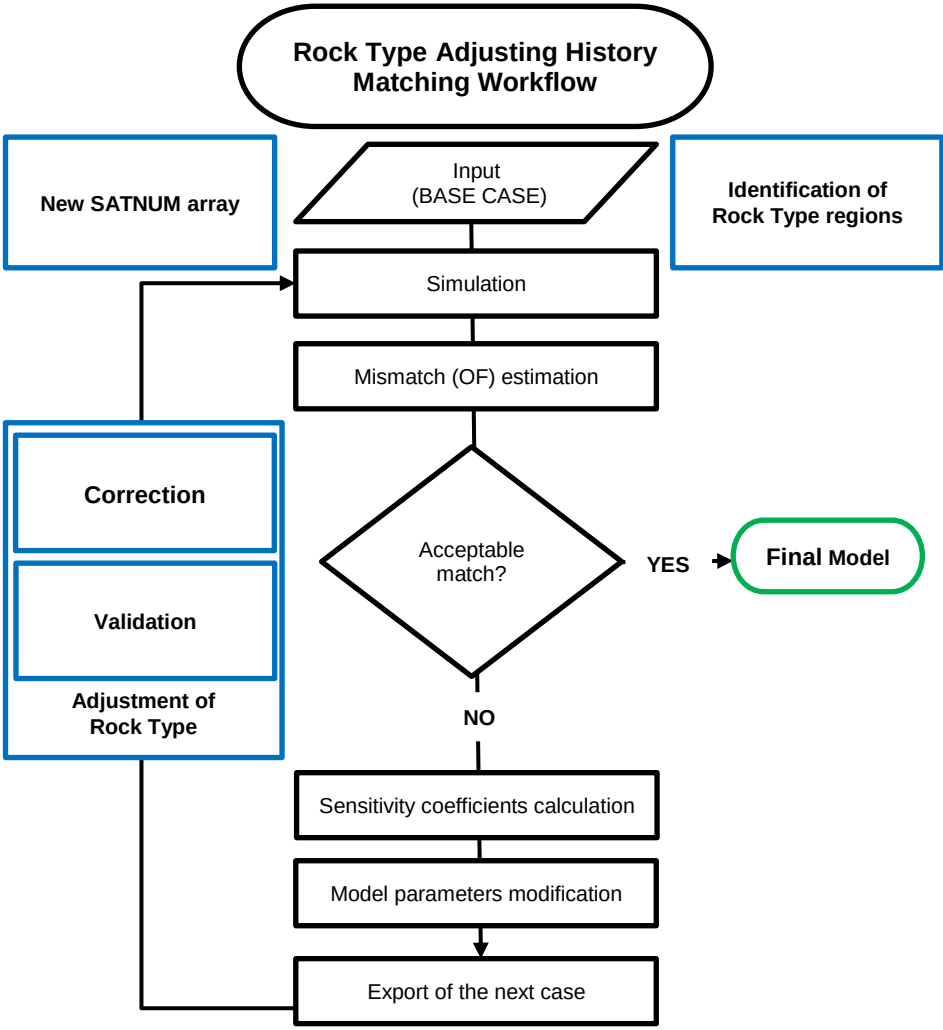

Fig. 4.3: AIDA: Rock typing workflow extension

4.4 The Mahalanobis-distance calculation

In order to understand the Mahalanobis distance calculation (Mahalanobis, 1936) better, the fundamental equations of circle and ellipse need to be introduced first. After introducing the used algebraic equations, the Mahalanobis distance calculation with the definition and calculation of a confidence interval is explained. A review of all tessellation cases are listed, and in the end, the rock typing with the detailed selection logic is described, illustrating an example.

4.4.1 Equation of Circle and Ellipse

First, for simplicity, the starting point is the equation of a circle:

$$X^2 + Y^2 = R^2$$

Eq. 4.1

$$\frac{X^2}{R^2} + \frac{Y^2}{R^2} = 1$$

Eq. 4.2

It describes the locus (set of points) of the points equidistance from the origin $(0,0)$ on the distance R :

$$R = \sqrt{X^2 + Y^2}$$

Eq. 4.3

If one wants to use the above circle as the reference, then all the points located on the distance $l = d \cdot R$ from the origin $(0,0)$, with $d = \frac{l}{R}$, can be described by the following form of the equation of a circle:

$$X^2 + Y^2 = l^2$$

Eq. 4.4

$$X^2 + Y^2 = (d \cdot R)^2$$

Eq. 4.5

$$\frac{X^2}{R^2} + \frac{Y^2}{R^2} = d^2$$

Eq. 4.6

, where $d = \frac{l}{R}$ is scaled distance of points located at the distance $l = d \cdot R$ from the origin $(0,0)$. d is an analogue of the Mahalanobis distance in this case. If $d = 1$, the points are located at the reference circle of radius R; if $d < 1$, the points lie inside the reference circle; if $d > 1$, the points lie outside the reference circle. Therefore, for any point p there is a circle of radius R_p centred at origin $(0,0)$ that goes through this point with the analogue of Mahalanobis distance $d_p = \frac{R_p}{R}$.

Similarly, the canonical equation of an ellipse aligned with the coordinate axes centred at the origin $(0,0)$ can be written as follows:

$$\frac{X^2}{a^2} + \frac{Y^2}{b^2} = 1$$

Eq. 4.7

, where a is the semi-major axis, and b is the semi-minor axis, i.e. $a \geq b$.

Taking the above ellipse as the reference, all the points located on the scaled version of this ellipse with semi-major axis $l = d \cdot a$, $m = d \cdot b$ can be written using the following form of the equation of ellipse:

$$\frac{X^2}{l^2} + \frac{Y^2}{m^2} = 1$$

Eq. 4.8

$$\frac{X^2}{(d \cdot a)^2} + \frac{Y^2}{(d \cdot b)^2} = 1$$

Eq. 4.9

$$\frac{X^2}{a^2} + \frac{Y^2}{b^2} = d^2$$

Eq. 4.10

, where $d = \frac{l}{a} = \frac{m}{b}$ is the scaled distance of the points located on the scaled version of the reference ellipse "d" is an analogue of the Mahalanobis distance in this case. If $d = 1$, the points are located at the

reference ellipse; if $d < 1$, the points lie inside the reference ellipse; if $d > 1$, the points lie outside the reference ellipse. Therefore, for any point p there is an ellipse with a semi-major axis a_p, and semi-minor axis b_p, centred at the origin $(0,0)$ that goes through this point with the analogue of Mahalanobis distance $d_p = \frac{a_p}{a} = \frac{b_p}{b}$.

In the general form, the ellipse centred at (x_C, y_C) and rotated counterclockwise by the angle θ from the positive direction of x axis toward semi-major axis a takes the form:

$$\frac{\big((x - x_C) \cdot \cos\theta + (y - y_C) \cdot \sin\theta\big)^2}{a^2} + \frac{(-(x - x_C) \cdot \sin\theta + (y - y_C) \cdot \cos\theta)^2}{b^2} = 1$$

Eq. 4.11

The equation is obtained by translation of the original coordinate system (x, y) to the centre (x_C, y_C) and by rotation with angle θ in the counter-clockwise direction:

$$\begin{pmatrix} x \\ y \end{pmatrix} = \begin{pmatrix} x_C \\ y_C \end{pmatrix} + \begin{pmatrix} \cos\theta & -\sin\theta \\ \sin\theta & \cos\theta \end{pmatrix} \cdot \begin{pmatrix} X \\ Y \end{pmatrix}$$

$$x = x_C + X \cdot \cos\theta - Y \cdot \sin\theta$$

$$y = y_C + X \cdot \sin\theta + Y \cdot \cos\theta$$

Using reverse transformation, one gets the above equation of rotated and shifted ellipse:

$$X = (x - x_C) \cdot \cos\theta + (y - y_C) \cdot \sin\theta$$

$$Y = -(y - x_C) \cdot \sin\theta + (y - y_C) \cdot \cos\theta$$

The locus of points located at the Mahalanobis distance d can be written then as:

$$\frac{\big((x - x_C) \cdot \cos\theta + (y - y_C) \cdot \sin\theta\big)^2}{a^2} + \frac{(-(x - x_C) \cdot \sin\theta + (y - y_C) \cdot \cos\theta)^2}{b^2} = d^2$$

Eq. 4.12

, where (x_C, y_C) is the centre of the reference ellipse, a is the semi-major axes, and b is the semi-minor axes, i.e. $a \geq b$; θ is the angle of rotation measured from the positive x axis direction to corresponding ellipse semi-major axis. d is an analogue of the Mahalanobis distance. Therefore, for any point p there is an ellipse with a semi-major axis a_p, and semi-minor axis b_p, centred at (x_C, y_C) and rotated counterclockwise by angle θ, that goes through this point with the analogue of Mahalanobis distance $d_p = \frac{a_p}{a} = \frac{b_p}{b}$.

In the vector form, the equation of circle can be rewritten as follows:

$$\boldsymbol{x}^T \cdot \boldsymbol{x} = (x \quad y) \cdot \begin{pmatrix} x \\ y \end{pmatrix} = x^2 + y^2 = R^2$$

Eq. 4.13

It represents the Euclidean distance.

Similarly, the analogue of the Mahalanobis distance in the vector form for the reference circle can be rewritten as:

$$\frac{x^2}{R^2} + \frac{y^2}{R^2} = d^2$$

Eq. 4.14

$$\boldsymbol{x}^T \cdot A \cdot \boldsymbol{x} = (x \quad y) \cdot \begin{pmatrix} 1/R^2 & 0 \\ 0 & 1/R^2 \end{pmatrix} \cdot \begin{pmatrix} x \\ y \end{pmatrix} = d^2$$

Eq. 4.15

In the case of reference ellipse, the analogue of the Mahalanobis distance in vector form can be written as:

$$\frac{x^2}{a^2} + \frac{y^2}{b^2} = d^2$$

Eq. 4.16

$$\boldsymbol{x}^T \cdot A \cdot \boldsymbol{x} = (x \quad y) \cdot \begin{pmatrix} 1/a^2 & 0 \\ 0 & 1/b^2 \end{pmatrix} \cdot \begin{pmatrix} x \\ y \end{pmatrix} = d^2$$

Eq. 4.17

Similarly, in the general case of the reference ellipse located at the centre (x_C, y_C) and rotated counterclockwise by the θ angle, the vector form can be written as:

$$\frac{\big((x - x_C)\cdot\cos\theta + (y - y_C)\cdot\sin\theta\big)^2}{a^2} + \frac{(-(x - x_C)\cdot\sin\theta + (y - y_C)\cdot\cos\theta)^2}{b^2} = d^2$$

$$\boldsymbol{x}^T \cdot A \cdot \boldsymbol{x} = (x - x_C \quad y - y_C) \cdot \begin{pmatrix} \frac{\cos^2\theta}{a^2} + \frac{\sin^2\theta}{b^2} & \left(\frac{1}{a^2} - \frac{1}{b^2}\right)\cdot\cos\theta\cdot\sin\theta \\ \left(\frac{1}{a^2} - \frac{1}{b^2}\right)\cdot\cos\theta\cdot\sin\theta & \frac{\sin^2\theta}{a^2} + \frac{\cos^2\theta}{b^2} \end{pmatrix} \cdot \begin{pmatrix} x - x_C \\ y - y_C \end{pmatrix} = d^2$$

$$\boldsymbol{x}^T \cdot A \cdot \boldsymbol{x} = \boldsymbol{x}^T \cdot R \cdot D \cdot R^T \cdot \boldsymbol{x} = (x - x_C \quad y - y_C) \cdot \begin{pmatrix} \cos\theta & -\sin\theta \\ \sin\theta & \cos\theta \end{pmatrix} \cdot \begin{pmatrix} 1/a^2 & 0 \\ 0 & 1/b^2 \end{pmatrix} \cdot \begin{pmatrix} \cos\theta & \sin\theta \\ -\sin\theta & \cos\theta \end{pmatrix} \cdot \begin{pmatrix} x - x_C \\ y - y_C \end{pmatrix} = d^2$$

, where $R = \begin{pmatrix} \cos\theta & -\sin\theta \\ \sin\theta & \cos\theta \end{pmatrix}$ is the rotation matrix and $D = \begin{pmatrix} 1/a^2 & 0 \\ 0 & 1/b^2 \end{pmatrix}$ is a diagonal scaling matrix.

To get the canonical form of the equation of an ellipse, one needs to multiply matrix A from left and right by R^{-1} and R^{-T} correspondingly.

Using the property of rotation matrix $R^{-1} = R^T, R^{-T} = (R^T)^{-1} = (R^T)^T = R$ one gets:

$$A = R \cdot D \cdot R^T \Longrightarrow R^{-1} \cdot A \cdot R^{-T} = (R^{-1} \cdot R) \cdot D \cdot (R^T \cdot R^{-T}) = D$$

Eq. 4.18

$$D = R^T \cdot A \cdot R$$

Eq. 4.19

4.4.2 Distance Calculation - Application of Mahalanobis distance

The correlation between porosity and absolute permeability and statistical data variance in principal directions for each rock type should be considered. Therefore, instead of Euclidean distance, the Mahalanobis distance in ϕ-k space is chosen for identifying the closest rock type from the given point. It allows defining statistical distance utilizing standard deviations in the principal direction of correlated data. The Mahalanobis distance between point $\mathbf{x}(\phi,k)$ and the mean $\boldsymbol{\mu}_{RT}(\phi,k)$ of the rock type, can be written as follows:

$$d_{M,RT}(\boldsymbol{x}, \boldsymbol{\mu}_{RT}) = \sqrt{(\boldsymbol{x} - \boldsymbol{\mu}_{RT})^T \boldsymbol{\Sigma}_{\mathrm{RT}}^{-1} (\boldsymbol{x} - \boldsymbol{\mu}_{RT})}$$

Eq. 4.20

, where $\boldsymbol{\Sigma}_{\boldsymbol{RT}}^{-\mathbf{1}}$ is the inverse covariance matrix of corresponding ϕ-k data of the rock type.

After finding principal directions (x', y') from eigenvalues and eigenvectors, the inverse covariance matrix takes diagonal form, with corresponding variances $\left(\sigma_{x'}^2, \sigma_{y'}^2\right)$ along with the principal directions:

$$\widetilde{\boldsymbol{\Sigma}}_{\boldsymbol{RT}}^{\boldsymbol{-1}} = \begin{pmatrix} 1/\sigma_{x'}^2 & 0 \\ 0 & 1/\sigma_{y'}^2 \end{pmatrix}$$

Eq. 4.21

In the new coordinate system, along with the principal directions, ellipse equation Eq. 4.20 takes the canonical form:

$$(x' \quad y') \cdot \begin{pmatrix} 1/\sigma_{x'}^2 & 0 \\ 0 & 1/\sigma_{y'}^2 \end{pmatrix} \cdot \begin{pmatrix} x' \\ y' \end{pmatrix} = \left(\frac{x'}{\sigma_{x'}}\right)^2 + \left(\frac{y'}{\sigma_{y'}}\right)^2 = d_{M,RT}^2$$

Eq. 4.22

Two feasibility region shapes are considered based on the underlying data statistics associated with the rock type: interval and ellipse. In case of the dominant variance only in one of the ϕ or k directions, the interval is chosen as the representative region of the related rock type. The ellipse region is used if there is notable variance in both ϕ and k values associated with the rock type.

Confidence Interval

The common frequentists approach defines the confidence interval to estimate the unknown population parameters derived from the sample data (Pyrcz, 2018). Hence, the range of values is proposed instead of

calculating one single value for the unknown population parameter. Therefore, the estimation is presented in the form of the interval, known as the confidence interval. In our case, the population mean is the subject of the estimation. The key in calculating the confidence interval is in defining the confidence level of the interest. Typically, the 95% confidence level is used. It needs to be noted that the 95% level does not imply that there is a 95% chance that the proposed interval contains the true population parameter value (population mean in this case). Instead, it states that in 95% cases, the calculated interval, in other words, 95% of intervals, contain the actual population parameter value. Thus, for each sample, there is a different confidence interval to be calculated, and from all these intervals, only 95% contain the true population estimate. Therefore, the confidence level provides the confidence in the calculated interval, not in the estimated value.

The length of the confidence level depends on the sample size, and the narrower it is, the more precise is the estimation, in a statistical sense.

The calculated population mean of the normally distributed population is normally distributed under the assumption that the standard deviation of the underlying population is known. It is the result of the Central Limit Theorem (Gnedenko and Kolmogorov, 1954; James, G., Witten, D., Hastie, T., Tibshirani, 2013). In case if the standard deviation of the population is unknown, the sample standard deviation s is used instead. The calculated population mean gets then the

Student's t-distribution. Hence the estimation of the population mean can be written as follows:

$$\bar{x} \sim N\left(\mu, \frac{\sigma}{\sqrt{n}}\right)$$

Eq. 4.23

$$s^2 = \frac{1}{n-1} \cdot \sum_{i=1}^{n} (x_i - \bar{x})^2$$

Eq. 4.24

$$\mu = \bar{x} \pm z_{\alpha/2} \frac{\sigma}{\sqrt{n}} \approx \bar{x} \pm t_{\alpha/2} \frac{s}{\sqrt{n}}$$

Eq. 4.25

, where $z_{\alpha/2}$- z-score and $t_{\alpha/2}$ is the t-score. This tells us how many standard deviations are required to capture a specified alpha level. In the case of a two-tailed test, when the z is 5%, it means 2.5-2.5% on the lower and upper tail.

For the confidence level of 95% the $z_{\alpha/2} \approx 1.96$. Student's t-distribution is the function of the sample size. The bigger the sample size, the closer the Student's t-distribution to the Normal distribution. It is generally considered that if the sample size is more than or equal to 30 ($n \geq 30$), it is acceptable to use Normal distribution instead of Student's t-distribution.

The theory of confidence interval can be used for a broad range of problems. This dissertation serves the purpose of creating a base for a more geologically consistent history matching tool.

The parameters of the distribution need to be known. The confidence interval theory is used in a reversed form to specify the acceptable range for parameter changes on the porosity-permeability diagram.

4.4.3 Application of Confidence Ellipse Calculation

The boundaries of the feasibility region can be chosen in a way that it includes all the data points associated with the rock type or by specifying certain confidence levels, which result in confidence region or confidence interval, correspondingly. Typically, a confidence level of 95% (P=0.95) is chosen to adequately present the boundaries of the confidence region (James, G., Witten, D., Hastie, T., Tibshirani, 2013).

The confidence ellipse can be generated based on either the χ_k^2 chi-squared statistic with k=2 degrees of freedom, in a case when sufficient data samples are provided ($n \geq 30$), or with Hotelling's $T_{k,n-1}^2$ t-squared statistic with k=2 degrees of freedom for the case with a small amount of n data samples ($n < 30$) (James, G., Witten, D., Hastie, T., Tibshirani, 2013). Corresponding confidence regions can be written as follows:

$$P\left((\boldsymbol{x}-\boldsymbol{\mu}_{RT})^T\cdot\boldsymbol{\Sigma}_{\mathrm{RT}}^{-1}\cdot(\boldsymbol{x}-\boldsymbol{\mu}_{RT})\leq CDF_{\chi_2^2}^{-1}(1-\alpha)\right)=1-\alpha=0.95$$

Eq. 4.26

$$P\left((\boldsymbol{x}-\boldsymbol{\mu}_{RT})^T\cdot\boldsymbol{\Sigma}_{\mathrm{RT}}^{-1}\cdot(\boldsymbol{x}-\boldsymbol{\mu}_{RT})\leq CDF_{T_{2,\mathrm{n}-1}^2}^{-1}(1-\alpha)\right)=1-\alpha=0.95$$

Eq. 4.27

, where α is the statistical significance for the one-tail test.

The confidence interval is used in the case of the dominant variance in ϕ or k direction. In the case of a sufficient amount of data samples ($n > 30$), the standard normal distribution is used $\mathcal{N}(0,1)$, the so-called z-statistic. Otherwise, if a small amount of n data samples ($n \leq 30$) is given, then the Student's t_{n-1} t-statistic is applied (James, G., Witten, D., Hastie, T., Tibshirani, 2013). Corresponding confidence intervals can be written as follows:

$$P\left(\mu_{RT}-t_{n-1,\frac{\alpha}{2}}\cdot\sigma_{RT}\leq x\leq\ \mu_{RT}+t_{n-1,\frac{\alpha}{2}}\cdot\sigma_{RT}\right)=1-2\cdot\frac{\alpha}{2}=0.95$$

Eq. 4.28

$$P\left(\mu_{RT}-z_{\frac{\alpha}{2}}\cdot\sigma_{RT}\leq x\leq\ \mu_{RT}+z_{\frac{\alpha}{2}}\cdot\sigma_{RT}\right)=1-2\cdot\frac{\alpha}{2}=0.95$$

Eq. 4.29

, where $\alpha/2$ is the statistical significance for the two-tail test.

The representation of the 68-95-99 rule is shown in *Fig 4.4*.

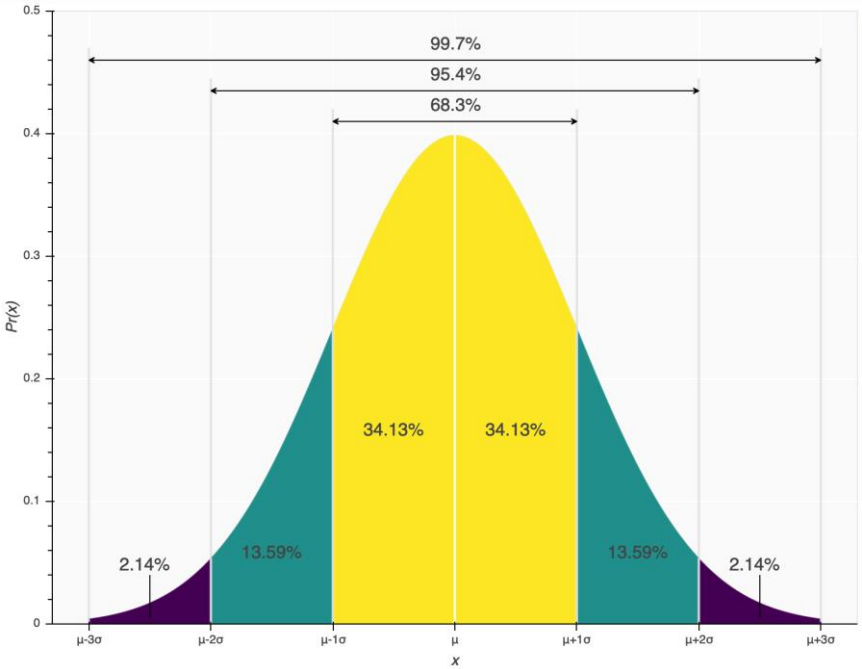

Fig. 4.4: Representation of the confidence interval based on probability

4.4.4 **Rock Type Selection**

The rock type adjustment process is done by exploiting Eq. 4.26 - Eq. 4.29 and Eq. 4.20. First, from Eq. 4.26 - Eq. 4.29, the standard deviation score is calculated for every rock type to establish the boundaries of feasibility regions. Then, Eq. 4.20. is applied to determine the Mahalanobis distance to corresponding confidence ellipses/intervals at any given point from the dataset. If the distance at the ϕ-k point of

interest is smaller than the standard score of the confidence region, the given point belongs to the currently assigned rock type (validation). In case if the distance is higher, the ϕ-k point falls out from the particular region, then the rock type with the smallest distance is assigned (correction). The representation of confidence regions and Mahalanobis distance from a ϕ-k point to corresponding rock types is illustrated in Fig. 4.5.

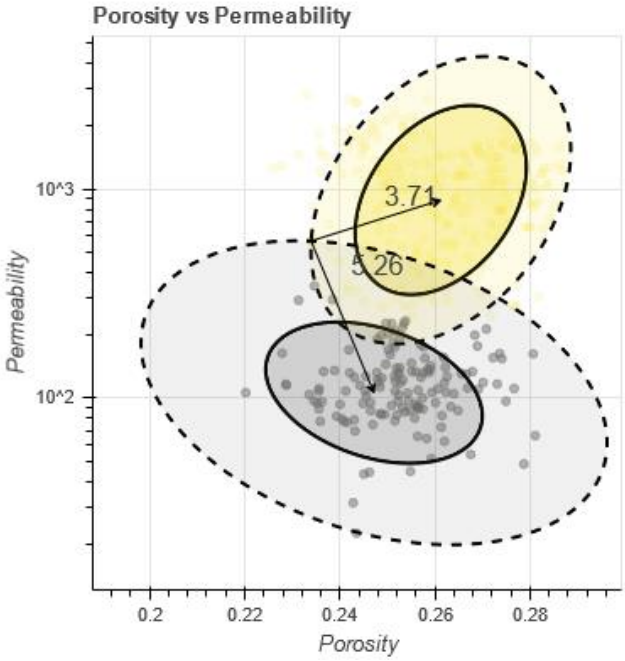

Fig. 4.5: Representation of Mahalanobis-distances and confidence intervals

4.5 Application of the Mahalanobis distance - Rock-type regions tessellation

Identification of a rock type employing Mahalanobis distance can produce cases when rock type regions form non-contiguous sets (unrealistic scenarios). The equidistant points between rock type regions need to be identified to establish the separation of rock types in a contiguous manner.

4.5.1 Rock-type regions tessellation produced by Mahalanobis distance

In order to separate the rock type precisely using mathematical approaches, the equidistant points between the different rock type regions need to be identified. The different rock types and the used distance calculation (Mahalanobis distance) are represented with the ellipse equation.

Therefore the equidistant points can be determined by solving the equation of Mahanlobis distance from one rock type being equal to Mahanlobis distance from another rock type.

The Mahalanobis distance from the rock type region i can be written as follows:

$$\frac{\left((x - x_i) \cdot \cos\theta_i + (y - y_i) \cdot \sin\theta_i\right)^2}{a_i^2} + \frac{(-(x - x_i) \cdot \sin\theta_i + (y - y_i) \cdot \cos\theta_i)^2}{b_i^2} = d_i^2$$

Eq. 4.30

, where (x_i, y_i) is the centre of the ellipse i, a_i is the semi-major axis and b_i is the semi-minor axis, when $a_i \geq b_i$, and the θ_i is the angle of rotation measured from the positive x axis direction to the corresponding ellipse semi-major axis.

Therefore, the equation for equidistant points between rock type 1 and 2 can be written as $d_1^2 = d_2^2$.

After rearranging the equation to the right side, the final equation is a general equation of the quadratic form of the conic section:

$$A \cdot x^2 + 2 \cdot B \cdot x \cdot y + C \cdot y^2 + 2 \cdot D \cdot x + 2 \cdot E \cdot y + F = 0$$

Eq. 4.31

Using the properties of the second-degree polynomial and taking into account the form of coefficients, which arose from $d_1^2 = d_2^2$, in total, seven different cases can occur. These cases can be split into two groups: degenerate and non-degenerate cases. The three non-degenerate cases

are the ellipse, the hyperbola, and the parabola. The other four degenerate cases are point (degenerate ellipse), intersecting lines (asymptotes of hyperbola), coinciding and parallel lines (degenerate parabolas). All of these mentioned sets of equidistant points are the so-called conic sections. In the general case, a few more degenerate conic sections can be described by the above second-degree polynomial. These cases are imaginary ellipse and imaginary parallel lines, but due to the special form of coefficients, it is proven that such cases cannot occur from the equation $d_1^2 = d_2^2$ (Manasipov, 2021)

Chapter 5 Proof of Concept – Simple Quarter-Five-Spot Model

Before the full-field application of the developed workflow, the algorithm needs to be tested, and the concept needs to be validated on a simple synthetic model. After successfully completing history matching on a simple synthetic case, the extended approach is tested and optimized through several test cases. Chapter 5 reveals the input data and introduces the proposed improvements of the approach. Results of the simulation run in each iteration are analysed. The initialization of these simulation runs may differ according to the rock type changes, which considerably influence the simulation result. Therefore, the workflow needs to be tested and optimized with a sufficient amount of test cases covering the sensitivities of all the parameters used during the development of the approach. In each test case, a thorough analysis has been performed to compare the results gained from the existing assisted history matching tool and the application of the new extended workflow.

This chapter contains the model description for the synthetic proof of concept model. Both truth and base models are described with the applied parameter distributions. On top of that, it lists the different scenarios for the detailed sensitivity study of each parameter, namely

porosity, absolute permeability, relative permeability and capillary pressure functions. The different alterations of each model are discussed and explained. This chapter is followed by the representation and discussion of the results of each case.

5.1 Model description – "Truth" Model

The simple synthetic model is a 2D realization with one layer. The model size is 200m*200m in the x-, y-direction and 10 m in the z-direction. The mesh contains 400 identical cells. The "truth" model with rock type distribution and wells is shown in Fig. 5.1. The fluid system contains two phases, one aqueous and one oleic phase. The well configuration follows a quarter of a five-spot, including one injector at the bottom left corner (blue circle) and one producer (green circle) at the top right corner of the mesh.

5.1 Parameterization

The static model also requires proper and consistent parameterization in advance. Two different rock types (RT) are defined: Rock Type 1 (RT1-yellow) represents a high permeability class; Rock Type 2 (RT2-grey) represents a low permeability class. The porosity distribution of the two rock types is also within different ranges. The assigned

parameters of each facies are realistic and consistent according to the rock type categories.

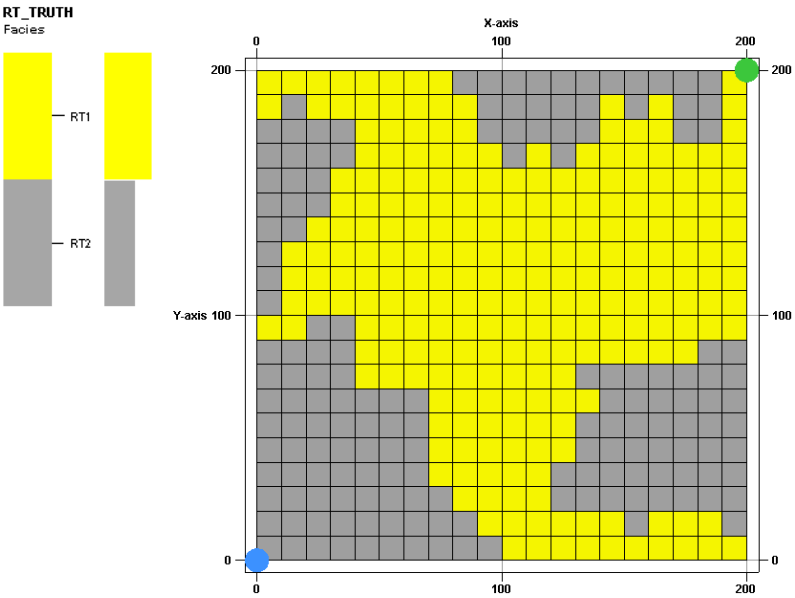

Fig. 5.1: The "truth" model rock type distribution RT1 – 60%, RT2 – 40%

Characteristic relative permeability and capillary pressure functions are generated according to the different rock types. Porosity is normally distributed (Eq. 5.1), while absolute permeability follows a log-normal distribution (Eq. 5.2).

$$\phi \sim \mathcal{N}(\mu_\phi, \sigma_\phi^2)$$

Eq. 5.1

$$\log k \sim \mathcal{N}(\mu_k, \sigma_k^2)$$

Eq. 5.2

Tab. 1 contains the summary of the assigned parameters of both rock types. It shows their porosity, absolute permeability ranges, minimum (min), maximum (max), mean values (mean), and standard deviation (SD).

Tab. 1: Overview – Summary of the characteristic rock type properties (porosity, absolute permeability, saturations)

RT	**Porosity**				**Absolute permeability**			
	min	max	mean	SD	min	max	mean	SD
#	[%]	[%]	[%]	[%]	[mD]	[mD]	[mD]	[mD]
RT1	23	30	25	8	200	2000	1100	320
RT2	20	27	25	3	20	200	110	32

Tab. 2 demonstrates the proposed and followed characteristic parameters of oil and water relative permeability (k_r) curves with the connate water (S_{wc}), residual oil (S_{or}) saturations and the Corey exponents for oil (n_o), water (n_w). Accordingly, it contains the characteristic entry pressure (pentry) values for both rock types.

Tab. 2: Summary of the characteristics of relative permeability curves based on rock type

RT	**Saturation**		**Relative-Permeability**				**P_{cow}**
	Swc	Sor	k_{roend}	k_{rwend}	n_o	n_w	p_{entry}
#	[fraction]	[fraction]	[-]	[-]	[-]	[-]	[bar]
RT1	0.25	0.20	0.80	0.40	2	2	0.02
RT2	0.35	0.30	0.70	0.30	4	4	0.1

The corresponding relative permeability curves are shown in Fig. 5.2. The "truth" model's porosity and absolute horizontal permeability distribution are shown in Fig. 5.4 and Fig. 5.5, respectively. The used capillary pressure curves for both low and high permeability rock types can be seen below in Fig. 5.3.

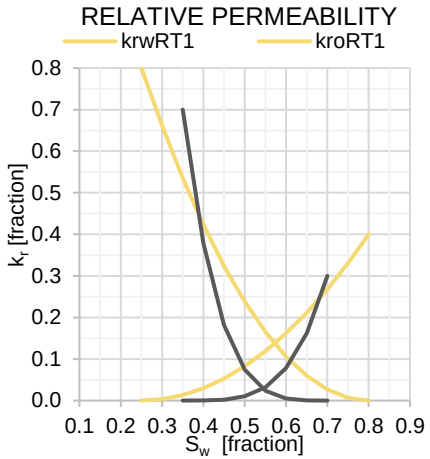

Fig. 5.2: Relative permeability functions of RT1 (yellow) and RT2 (grey)

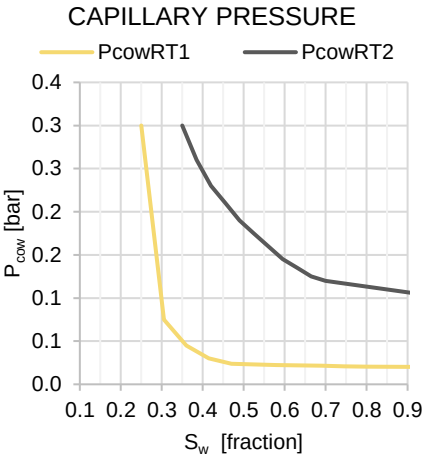

Fig. 5.3: Capillary pressure functions of RT1 (yellow) and RT2 (grey)

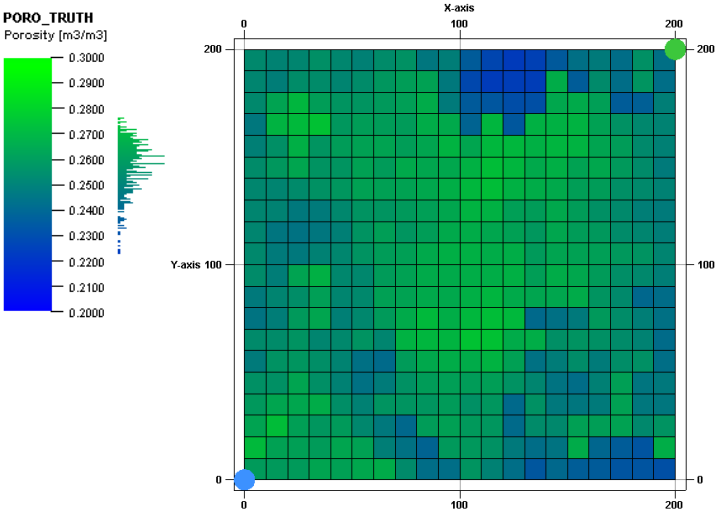

Fig. 5.4: The "truth" model's porosity distribution

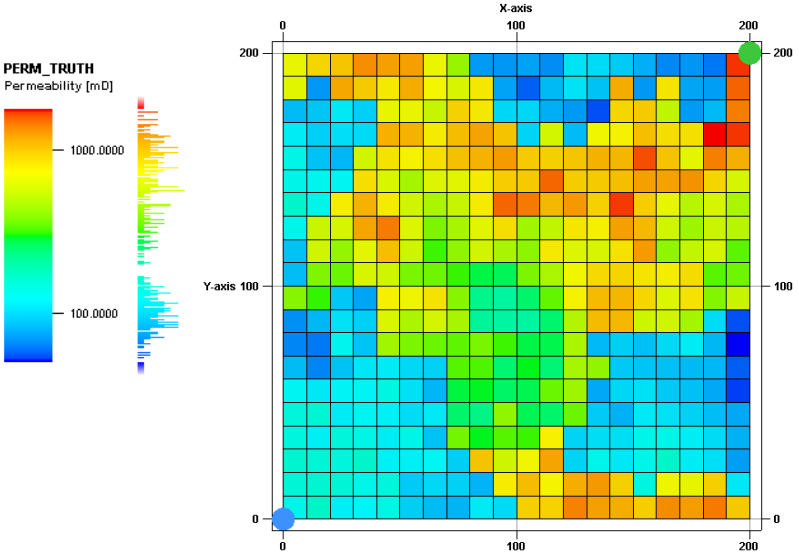

Fig. 5.5: The "truth" model absolute horizontal permeability distribution

The synthetic model variations are established with the above-described parameter distributions and characteristics shown in Tab. 1 and Tab. 2. The synthetic model, which contains both absolute permeability and porosity distributions, is used for the simulation with varying relative permeability and capillary pressure functions identified by the rock types. Before the history matching, the simulation is first conducted on the "truth" model with the history setup as validation in all cases. The validation is needed to avoid inconsistencies in the base case model due to incorrect simulation control.

5.2 Base Case Model

In order to generate the base model for the base case during history matching, the initial rock type distribution of the "truth" model has been slightly modified. Different realization of the predefined parameter distribution was used as an initial guess. The base case model's initial rock type and parameter distribution in the case of different parameter distributions for the different rock types and in the case of the same parameter distribution for the different rock types are shown in Fig. 5.7, Fig. 5.8, Fig. 5.9 and Fig. 5.10 accordingly.

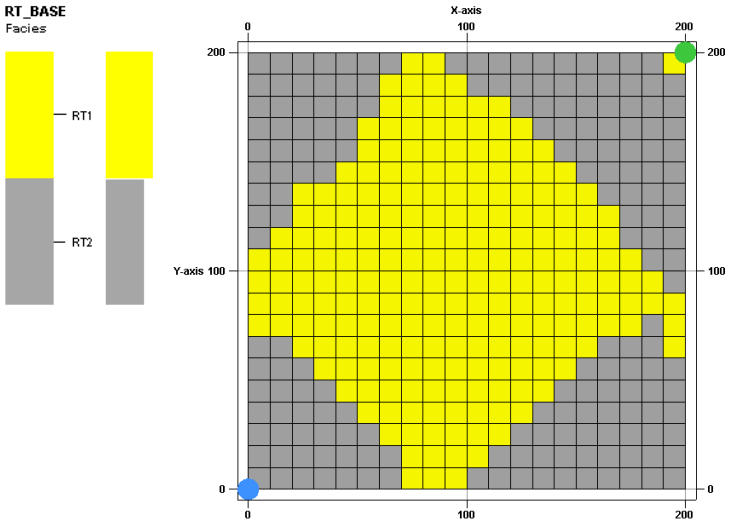

Fig. 5.6: The base model's rock type distribution (RT1-55%, RT2-45%)

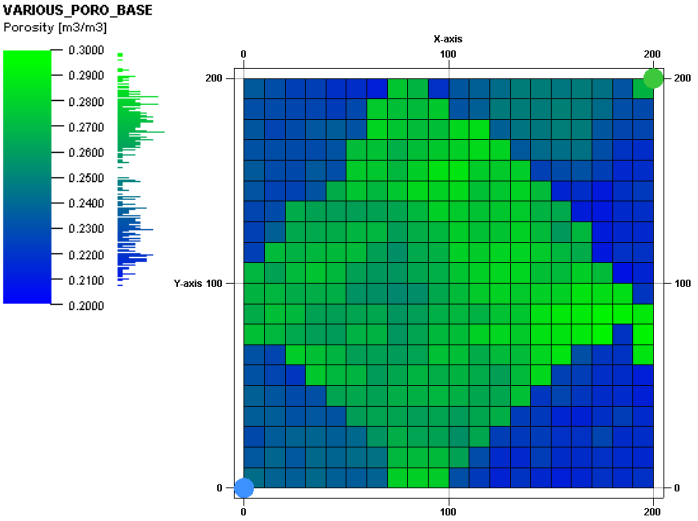

Fig. 5.7: The base model's porosity distribution (varying between the rock types)

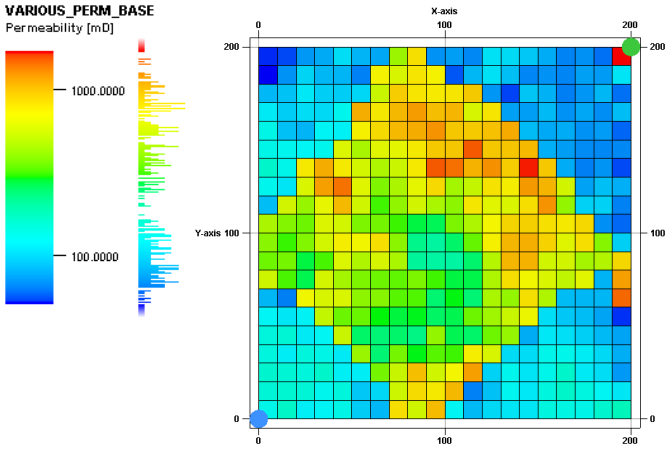

Fig. 5.8: The base model's absolute horizontal permeability distribution (varying between the rock types)

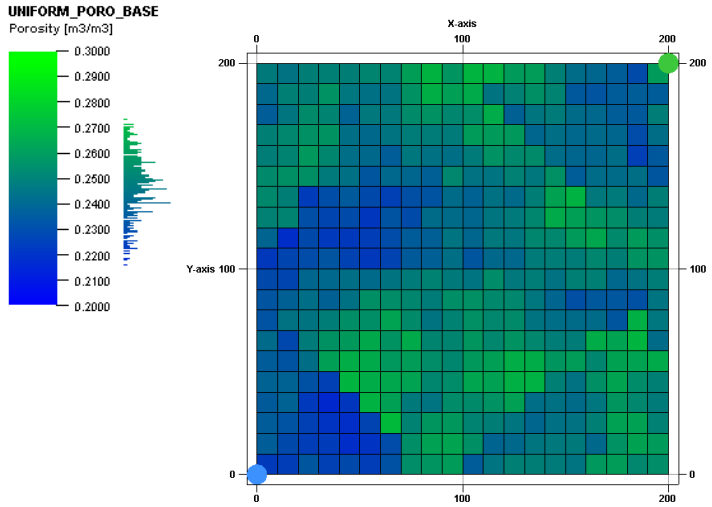

Fig. 5.9: The base model's porosity distribution (identical in both rock types)

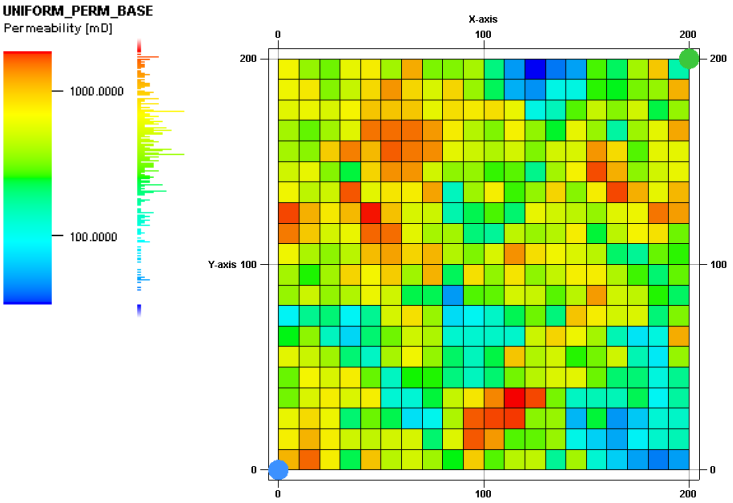

Fig. 5.10: The base model's absolute horizontal permeability distribution (identical in both rock types)

5.2.1 Initial and Boundary Conditions

The model is a closed system with no flow boundaries. The connate water saturation is used to determine the initial fluid saturation distribution, and the initial reservoir pressure is set at a reference depth of the model. In order to generate the production history of the synthetic model, the simulation controls in the "truth" case are constant water injection rate (q_{winj}=constant) at the injector and constant liquid production (q_{liq}=constant) with bottom-hole-flowing pressure limit (p_{wf_prod}=constant) at the producer. The base case simulation model is controlled by a constant injection rate (q_{winj}=constant), the production control is the observed liquid rate (q_{liq}) generated and extracted from the truth model simulation.

5.3 Summary of Models

In order to analyse the effect of individual model parameters on the rock-type driven history matching workflow, three different realizations of the model are created with a total number of nine simulation cases. The primary model is established with the above-described parameter distributions and properties shown in Tab. 1 and Tab. 2., which is represented as the most complex case highlighted with blue in Fig. 5.11. Then, two other models are introduced with the alteration of the primary model.

The first modified version kept the absolute permeability variation but took only one single uniform porosity distribution, which is the mean of the porosity distribution of the two rock types from the primary model. The rock types share the same porosity distribution. The porosity values vary for both rock types within the same ranges. The model was created to capture the effect of rock type change based only on the absolute permeability driven history matching.

The second alteration of the primary model kept the porosity variation and used only one single uniform absolute permeability distribution, which is the mean of the absolute permeability distribution of the two rock types from the primary model. The reason for keeping the absolute permeability distribution identical for both rock types and using only the different porosity distribution is to investigate the effect or significance of porosity driven history matching on the rock typing workflow.

After investigating these two modified scenarios, a reliable conclusion can be drawn on the complex simulation case conducted with the primary model, which contains both variable absolute permeability and porosity distributions.

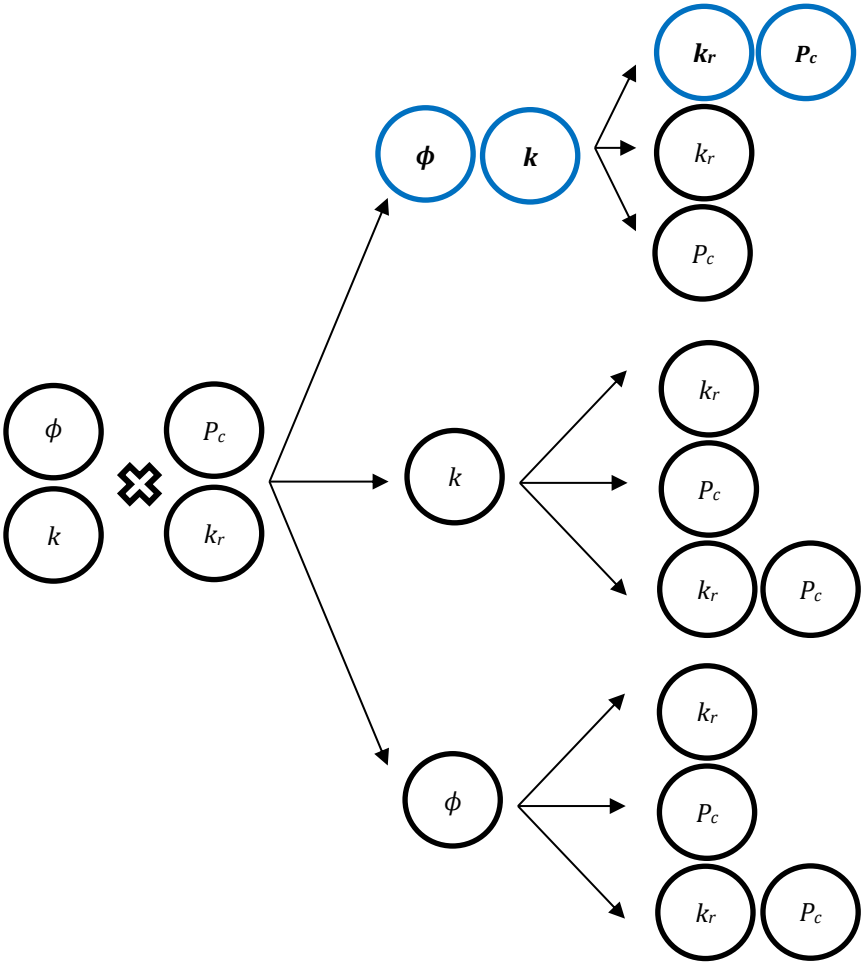

Fig. 5.11: The combination of different parameters in the representative models for sensitivity analysis

All the variations of models with the combination of simulations conducted are listed in the following Fig. 5.11. Each model is simulated for three different scenarios, which are described in Fig. 5.11. The first simulation setup is conducted with varying relative permeability where the capillary pressure is neglected. The second setup has different capillary pressure and identical relative permeability values for both rock types. The third case is the complex setup where both saturation functions (k_r, P_c) vary from rock type to rock type.

Tab. 3: Summary of the cases for sensitivity analysis

Model	Rock Type dependent parameter		Simulation Case	ID
	Static property	Saturation function		
1	k	k_r	Case 1.1	PERMKR
		P_c	Case 1.2	PERMPC
		k_r , P_c	Case 1.3	PERMPCKR
2	ϕ	k_r	Case 2.1	POROKR
		P_c	Case 2.2	POROPC
		k_r , P_c	Case 2.3	POROPCKR
3	ϕ , k	k_r	Case 3.1	POROPERMKR
		P_c	Case 3.2	POROPERMPC
		k_r , P_c	Case 3.3	POROPERMPCKR

The reason for running and analysing the first and second setup with all three models is to investigate the individual significance of relative permeability and capillary pressure in the rock type-driven history matching workflow. Last but not least, coupling the variation of relative permeability and capillary pressure functions can be analysed together in a third advanced simulation setting. The summary of the cases for sensitivity analysis is shown in Tab. 3 with their parameters and identifiers.

5.4 Sensitivity study

In order to prepare the different models and simulation cases, the logical order must be set. The available static properties are the variable and uniform absolute permeability and porosity distributions. The saturation functions also have two variations for both relative permeability- and capillary pressure functions. There are variable (different) and uniform (average) relative permeability curves and variable and neglected (P_c=0) capillary pressure functions available.

The number of combinations would be sixteen different simulation cases, but some of the combinations would not make sense physically; therefore, the practical conclusion could not be drawn. Therefore the eliminated cases are when both the porosity and the absolute permeability of different rock types are identical and when the relative

permeability and the capillary pressure has no variety within the different rock types.

Practically, if the rock types have the same porosity and absolute permeability distribution, it will make no difference in the flow calculations to distinguish between rock types. The rock type adjustment workflow does not affect the history matching results if the relative permeability and capillary pressure are the same for both rock types. The facies modelling section describes the appropriate rock type selection and modelling in more detail. Therefore, after eliminating the inappropriate ones, the number of the examined simulation cases is reduced to nine (Tab. 3), calculated with the following formula (Eq. 5.3).

$$\left(2^{2=|\{k,\phi\}|}-1\right)\times\left(2^{2=|\{k_r,p_c\}|}-1\right)=9$$

Eq. 5.3

, where

k,ϕ - parameters driving rock type change,

k_r, p_c – parameters influencing flow behaviour within each rock type.

The adjustments of these parameters have a different effect on model behaviour. The porosity (ϕ) is responsible for present hydrocarbon volume; the absolute permeability (k) influences flow path (pattern) and rate. The relative permeability (k_r) has the same effect on flow dynamics as absolute permeability, but it also has phase-specific dominance. The

capillary pressure (P_c) influences the initialisation, affecting the initial fluid distribution. It has competition with gravity force in the case of a 3D model.

The following sub-chapters give a detailed overview of the nine simulation cases chosen to test the rock type adjusting workflow.

5.5 Model 1: Uniform porosity, variable absolute permeability distribution

The first model has uniform porosity and variable absolute permeability distribution. The goal of performing history matching on the simulation cases conducted through Model 1 is to test the sensitivity of the RT adjusting workflow to absolute permeability driven history matching setup. The porosity values are unified over the two different rock types in order to avoid interference. Model 1 has three different simulation setups, and these cases are listed below.

5.5.1 Case 1.1: PERMKR

The simulation case called PERMKR has rock-type dependent absolute permeability distribution, and the relative permeability is set to be rock type dependent.The capillary pressure is neglected in this case to focus only on the sensitivity for relative permeability.

5.5.2 Case 1.2: PERMPC

The simulation case called PERMPC has the rock-type dependent absolute permeability distribution, but the relative permeability is simplified, and both rock types have the same relative permeability functions. The capillary pressure is introduced as a rock type dependent function, where both rock types have well-distinguished values. The goal of the history matching of this model is to investigate the sensitivities for only capillary pressure, neglecting the relative permeability differences in a porosity and absolute permeability driven history matching setup.

5.5.3 Case 1.3: PERMPCKR

The simulation case called PERMPCKR has not only rock-type dependent absolute permeability distribution, but also rock-type dependent saturation functions are applied. Both the relative permeability and the capillary pressure are set to be rock type dependent functions. The capillary pressure is not neglected in this case but varies between different rock types with relative permeability functions.

5.6 Model 2: Variable porosity, uniform absolute permeability

In the second model, the main target parameter is the porosity.

The goal was to test the sensitivity of the RT adjusting workflow to another main model parameter, which is the porosity. Therefore this model variation is parameterized with the simplified uniform absolute permeability distribution and different (variable) porosity distribution based on different rock types. Model 2 also has three different simulation setups, and these cases are listed below.

5.6.1 Case 2.1: POROKR

The first simulation case with a variable porosity model is the POROKR, which focuses on the porosity-driven workflow's sensitivity to the relative permeability. Therefore the effect of the capillary pressure is neglected, so it is set to zero.

5.6.2 Case 2.2: POROPC

The simulation case called POROPC has the rock type-dependent porosity distribution, and not only the absolute permeability but the relative permeability is simplified, and both rock types have the same relative permeability functions. The capillary pressure is introduced as a rock type dependent function, where both rock types have well-distinguished values. The goal of the history matching of this model is to investigate the sensitivities for capillary pressure, neglecting the relative permeability differences.

5.6.3 Case 2.3: POROPCKR

The simulation case called POROPCKR has not only rock-type dependent porosity distribution but also rock type-dependent saturation functions are applied. Both the relative permeability and the capillary pressure functions are set to be rock type dependent. The capillary pressure is not neglected in this case but varies between different rock types with relative permeability functions.

5.7 Model 3: Variable porosity and absolute permeability distribution

After a detailed sensitivity analysis of the history matching workflow to different parameters, the last combined model is examined. The last model is Model 3, which has the most complex static features. This model is parameterized for both static model properties (porosity and absolute permeability) with their variable distributions based on the rock types. It means that both model parameters are significantly rock type dependent. Model 3 has as well three different simulation setups, and these cases are listed below.

5.7.1 Case 3.1: POROPERMKR

The simulation case called POROPERMKR has rock type-dependent porosity and absolute permeability distributions, but also, the relative

permeability is set to be rock type dependent. In this case, the capillary pressure is eliminated to focus only on the sensitivity of the porosity and absolute permeability driven history matching workflow for relative permeability.

5.7.2 Case 3.2: POROPERMPC

The simulation case called POROPERMPC has the rock-type dependent porosity and absolute permeability distributions, but the relative permeability is simplified, and both rock types have the same relative permeability functions. The capillary pressure is introduced as a rock type dependent function, where both rock types have well-distinguished values. The goal of the history matching of this model is to investigate the porosity and absolute permeability driven history matching workflow sensitivities for capillary pressure, eliminating the effect of different relative permeability functions.

5.7.3 Case 3.3: POROPERMPCKR

This case, called POROPERMPCKR, is the most complex simulation case within the simple synthetic models, where the porosity and absolute permeability distribution varies, including variable saturation functions within each rock type. This case is the most representative one for reality, where all the variations of the parameters are coupled. This simulation model gives a complex and comprehensive conclusion on all the possible parameters driving the history match.

Chapter 6 Results of the Simple Quarter-Five-Spot Model

This chapter represents and discusses the results of the simple model's different simulation cases and summarises the significant conclusions of the sensitivity study. The model description can be found in Chapter 5, with all the necessary details, such as parameter distribution and alterations.

All nine cases have the same history matching setup during the matching process so that a comprehensive comparison can be drawn based on the same conditions. The results of two different multiple setup combinations are shown and analysed. The shown setup combinations are the BESTPARENT and the ITERNUM.

The detailed results and analysis of the history matching procedure are shown through the case “PERMKR” conducted with the standard and rock typing workflow through the BESTPRENT setup combination.

The results are represented and summarized comparatively; in this sequence, each case compares the main parameters for the truth, the base, the history matched case without, and with the rock type

adjusting workflow. In order to compare the efficiency of the rock typing workflow, the history matching results of the nine cases are compared to the conventional workflow.

General History Matching Setup

The history match in all of the nine cases is conducted with the help of the previously described assisted history-matching tool in two attempts with two different approaches. The first attempt is where the model parameters were modified within the defined minimum and maximum constraints, applying only the conventional history matching workflow driven by the adjoint approach. Then the second attempt is where the adjoint-based history matching workflow is applied with the rock type adjusting extension. The in-house created external workflow was used to adjust the rock types according to the calculated sensitivities of the model parameters (porosity and absolute permeability).

During the history matching procedure of all nine cases, the matching parameters are the same, the field pressure (p_{static}), bottom-hole-flowing pressure (p_{wf}), oil (q_o) and water (q_w) rate, as well as water-cut (WCUT). The observed data is generated and extracted from the "truth" model.

The monitored parameters are the ϕ-k relationship, histograms of rock type, absolute permeability, porosity, the absolute and relative difference in STOIIP and objective function changes. Different weighting factors are assigned to each desired matching parameter

during the minimisation of the objective function, depending on the different history matching stages (setup) within the typical sequence.

BESTPARENT: Combines three matching stages with four conditions. The stages are the overall match with big steps, emphasised rates, overall match with small steps. The conditions are minimum and maximum objective function values, a maximum number of iterations and start from the best case. The best case is identified with the smallest number of the total objective function.

ITERNUM: Combines three matching stages with one condition. The stages are the overall match with big steps, emphasised rates, overall match with small steps. The condition is only the maximum number of iterations.

The conditions are applied between two different setup stages. A detailed explanation can be found, coupled with the result analysis.

6.1 History Matching Results of PERMKR (Case 1.1 with Model 1)

In the presented test case called PERMKR, porosity and absolute permeability are the only directly modified parameters. In the case of PERMKR, the rock types are only distinguished through absolute and relative permeability. The different rock types share the same porosity distribution, and the capillary pressure is neglected.

6.1.1 Base Case Simulation

Fig. 6.1 illustrates the base case simulation results of the oil (green) and the water (blue) rate, indicating an excellent initial guess.

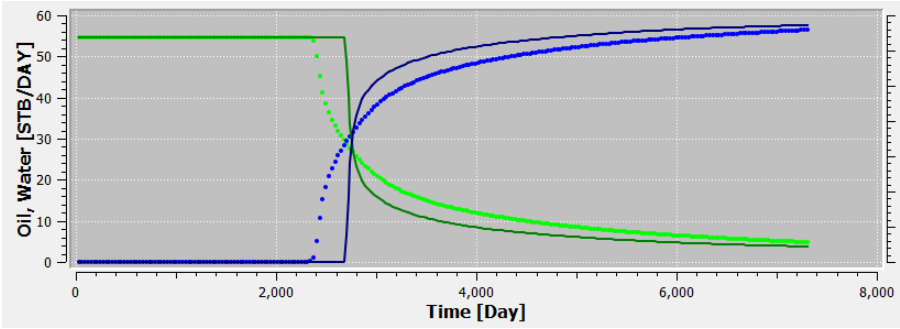

Fig. 6.1: The "truth" model observed (dotted lines) production history (oil-green, water-blue) compared to the base case simulation results (solid lines)

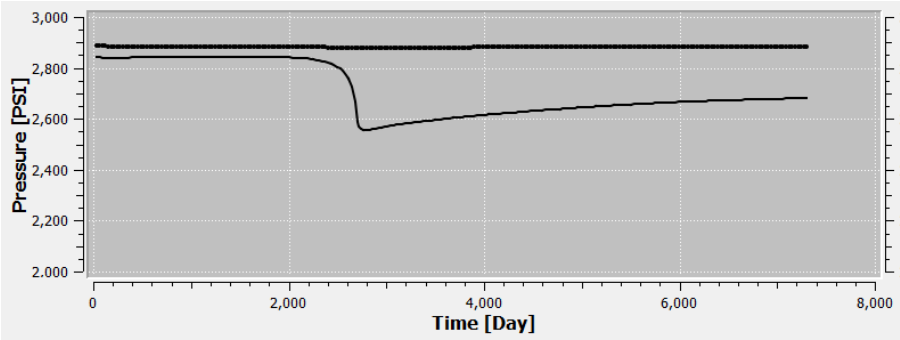

Fig. 6.2: The "truth" model observed (dotted thick black line) bottom-hole flowing pressure compared to the base case simulation results (solid thin black line)

Fig. 6.2 shows the historical and calculated bottom-hole flowing pressure. According to the simulation results, improvement in the pressure match and water breakthrough is still required. The simulated cumulative oil and water production volume (solid lines) are already close to the historical values (dotted lines). In order to find the optimal solution utilizing the gradient approach, a good enough initial guess is required. Therefore the presented base case is an appropriate starting point for the history match.

6.1.2 History matching without the Adjustment of Rock Type (the conventional way)

A conventional history matching is performed with the previously shown test case PERMKR (Case 1.1) as a first attempt. Fig. 6.3 illustrates the history matching results of the oil (green) and the water (blue) rate, indicating an acceptable match. Although the bottom-hole-flowing pressure match is achieved relatively quickly and easily, cumulative rates and water breakthrough improvement are still required.

The history matching results shown in Fig. 6.3 are achieved using the same weights in the applied objective function as in the rock-type adjusting workflow setup. The identical history matching setups assure that the capabilities and results of the two workflows can be consistently and comprehensively compared. However, the results of conventional workflow can be further improved.

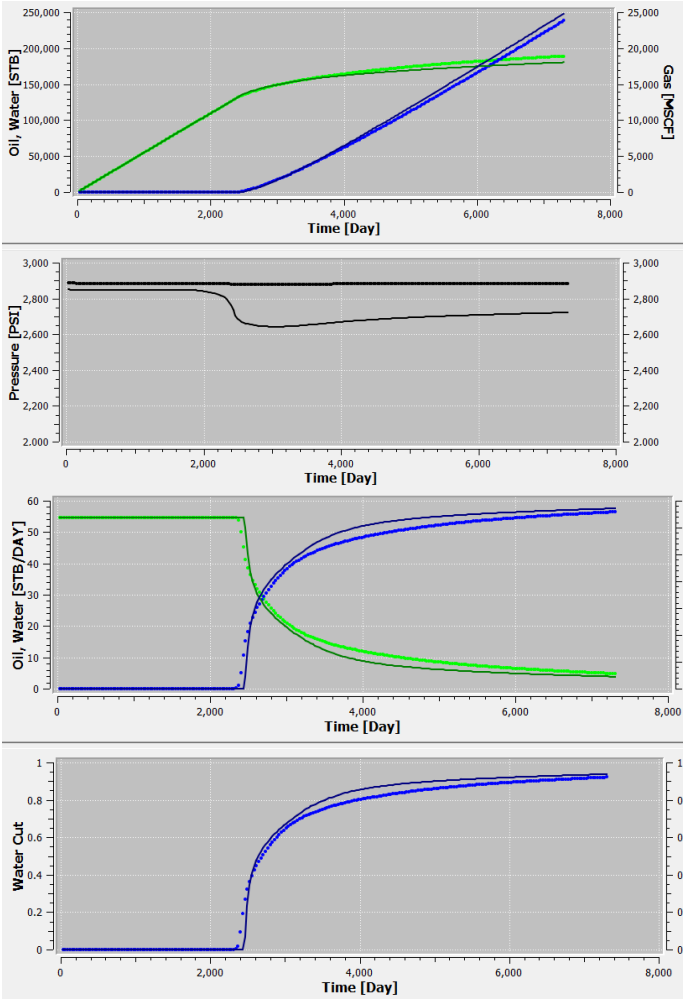

Fig. 6.3: The "truth" model observed (dotted lines) production history (oil-green, water-blue) compared to the final model simulation results (solid lines) achieved without Adjustment of Rock Type

A further improved match could be achieved by adjusting the objective function weights in the different stages. Nevertheless, the history match is satisfactory to a certain level and could not be further improved with the used setup combination. One of the main reasons for not achieving a better match is that the correct initial fluid saturations must be assigned to the individual cells to get the right fluid volumes into the wells at the right time. In order to achieve that, the common practice is to scale the capillary pressure curves or the relative permeability curves as a last resort. The residuals are determined from the corresponding rock type's saturation functions. Since the rock type is not adjusted in this workflow, the rock type indicator does not change, so the initially assigned saturation functions are used; therefore, it is impossible to achieve the correct initial fluid distribution without violation of the model. Arriving at a better match requires more radical parameter changes, but it means some kind of sacrifice needs to be taken. Either stop further matching the model with a higher OF value or violate the geological model, where the minimum and maximum constraints are maintained over the history matching procedure; however, the overall geological consistency would be lost because the rock types are not assigned correctly for the given ϕ-k values, even in the presented case, as shown in Fig. 6.11.

Fig. 6.4 and 6.5 represent the model's porosity and absolute horizontal permeability distribution after the conduction of the history matching with the standard workflow.

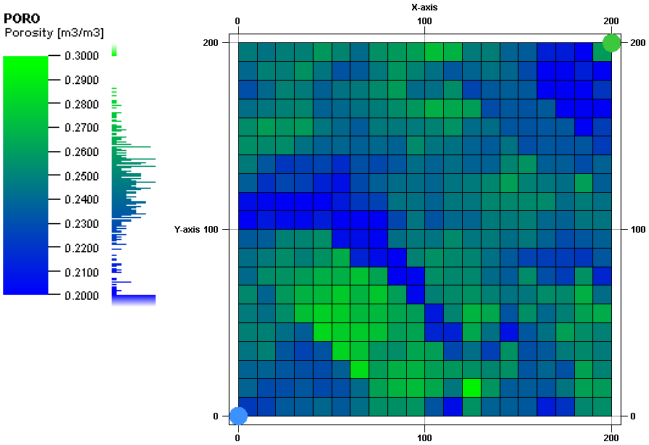

Fig. 6.4: The final model's porosity distribution using the adjoint approach without rock-typing

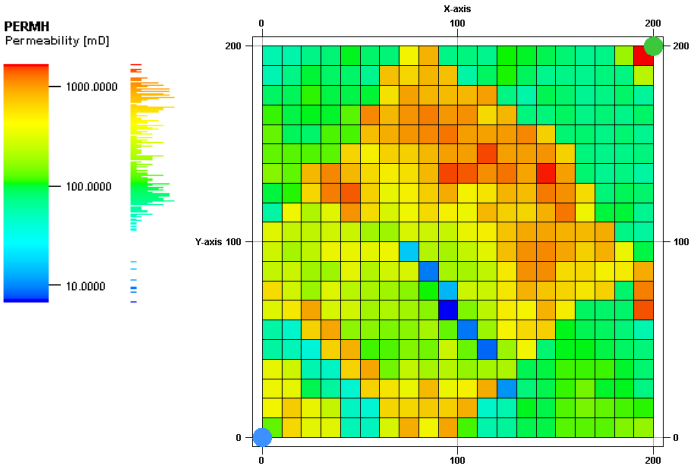

Fig. 6.5: The final model's absolute horizontal permeability distribution using the standard workflow without rock-typing

The history matching is conducted by utilising the extended workflow as a second attempt. The results of the rock-typing workflow are presented in the next section.

6.1.3 History matching with the Adjustment of Rock Type (extended workflow)

In this second history matching attempt, the parameters were not modified independently. After a particular iteration, when the absolute permeability (ϕ-k point) moved into a different rock type category according to the Mahalanobis distance, the rock type of the cell has been changed into the correct category. The rock types are defined as preliminary and have different petrophysical parameters. Both rock types are identified within ellipse regions in ϕ-k space. With changing rock types, the corresponding parameters are automatically changed as well; for instance, the relative permeability, while the parameter distributions have not changed significantly. Therefore, the simulation achieved the observed production volumes, driven by the correction of initial saturations due to the rock type adjustment. Fig. 6.6 illustrates the history matching results of the oil (green) and the water (blue) rate, indicating a perfect match. Improvements in the pressure and cumulative rates, as well as water breakthrough, are not required. The history match is satisfactory. Therefore the rock type adjusting history matching workflow arrived at the final model.

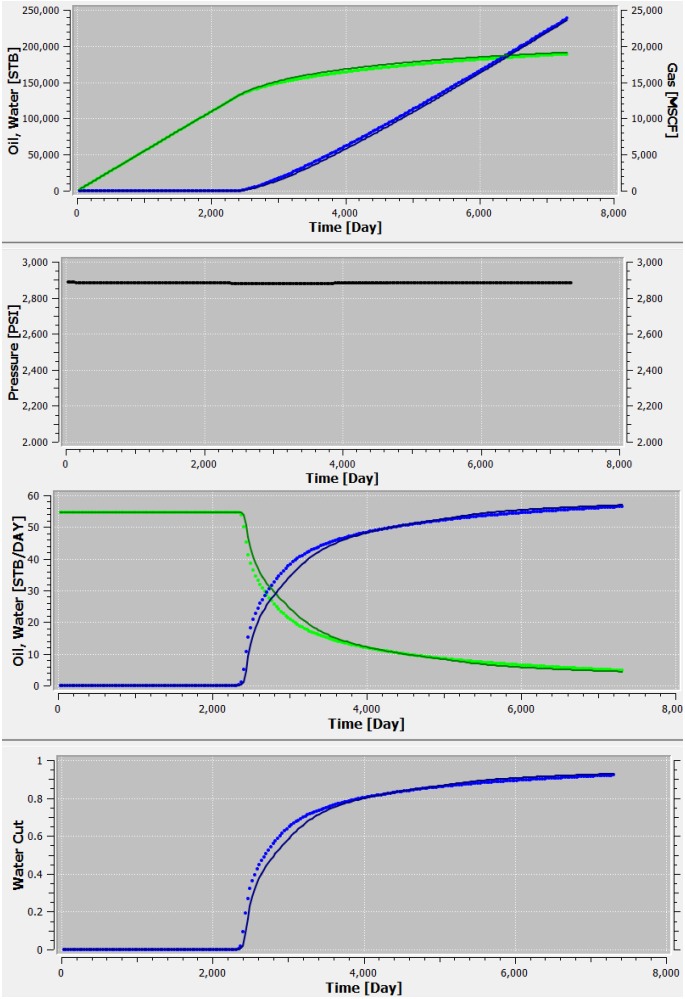

Fig. 6.6: The "truth" model observed (dotted lines) production history (oil-green, water-blue) compared to the final model simulation results (solid lines) achieved with rock type adjusting history matching workflow

These results show the proof of concept on a synthetic two-dimensional model, where essential conclusions can be drawn. The history match is achieved by applying multiple optimization setups (three-stage) under ten iterations without violating the model. Fig. 6.7, Fig. 6.8 and Fig. 6.9 show the final model's porosity, absolute horizontal permeability and rock type distribution accordingly. The minimum and maximum geological constraints are maintained, preserving the petrophysical consistency. The ϕ-k relationship and the STOIIP have not changed significantly. The rock type distribution of the final model is shown in Fig. 6.9.

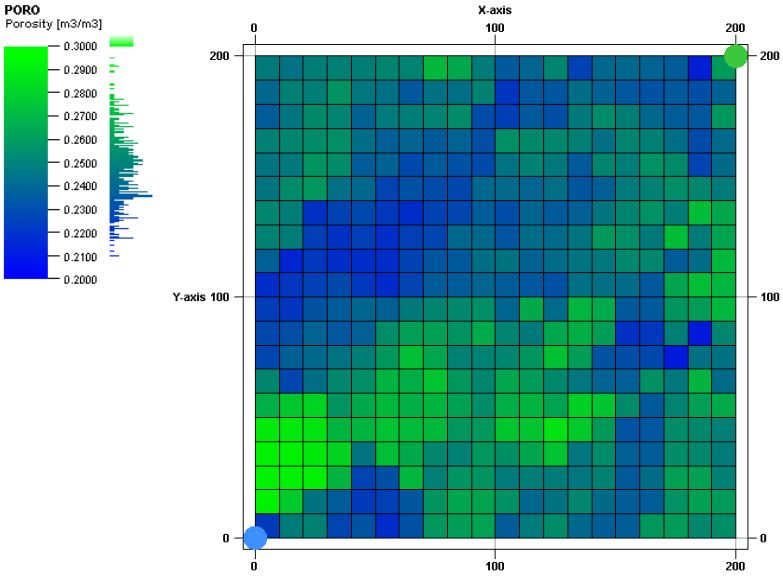

Fig. 6.7: The final model's porosity distribution using the Rock Typing (RT) workflow

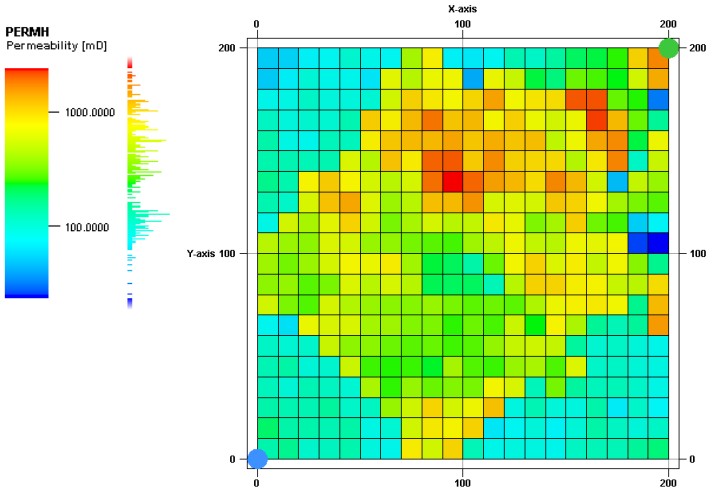

Fig. 6.8: The final model's absolute horizontal permeability distribution, using the RT workflow

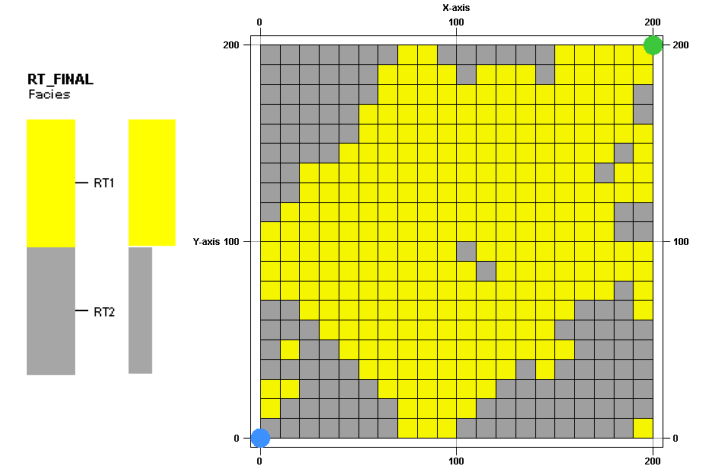

Fig. 6.9: The final model's rock type distribution utilising the Rock Type Adjusting History Matching Workflow

In terms of preserving the original rock type distribution, the geological consistency could not be reached to the greatest extent; which means that the rock type distribution (RT1-RT2) in the "truth" model is 60%-40%, in the base case model, it is 55%-45%, and in the final model it is 65%-35% accordingly. Fig. 6.10 compares the porosity, the absolute horizontal permeability and rock type distribution of each model. The comparison between the "truth", base and final model's rock type distribution is illustrated from top to bottom. The first column is the spatial porosity distribution the second and the third columns are the average absolute horizontal permeability and rock type spatial distribution accordingly. The first row shows the "TRUTH" model, the second row represents the base, and the last two rows show the history-matched final models. Fig. 6.10 demonstrates the alteration of the rock type into the "truth" direction around the producer well in the upper right corner of the final model. The overall conclusion is that the adjoint-based algorithm finds the "correct" direction of the parameter changes in the producer area, which is already a significant achievement.

Fig. 6.11 shows a comparative comparison of the ϕ-k correlation, porosity, absolute permeability and rock type distribution in the TRUTH, BASE and FINAL models without and with rock type adjustments, respectively.

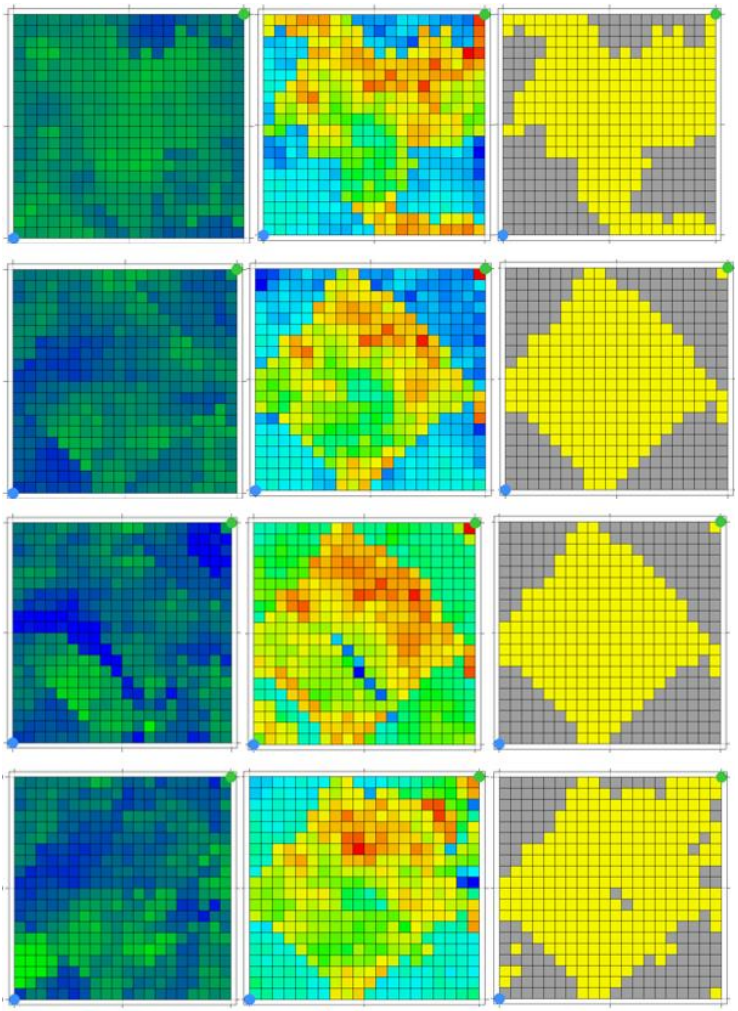

Fig. 6.10: Comparison of porosity, absolute horizontal permeability and rock type distribution in the "truth", base and final history matched models without ($n_{iteration}$=111) and with rock type adjustments ($n_{iteration}$=9), respectively

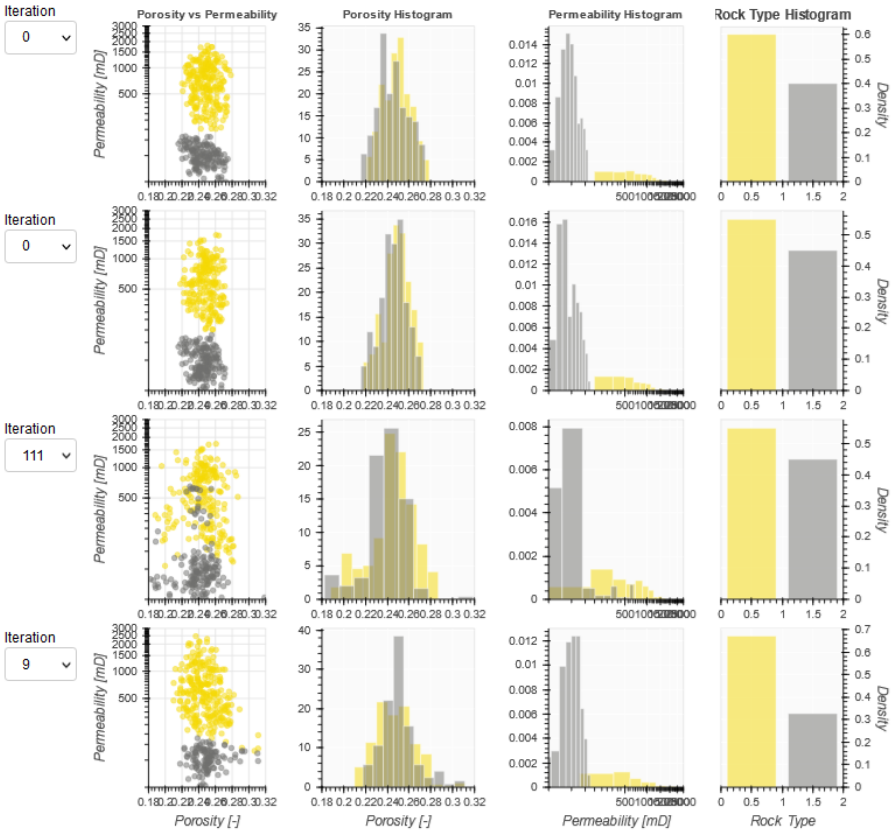

Fig. 6.11: The comparison of ϕ-k correlation, porosity, absolute permeability and rock type distribution in the "TRUTH", BASE and FINAL models without ($n_{iteration}$=111) and with rock type adjustments ($n_{iteration}$=9), respectively

The integrated extension of rock-type adjustments into the workflow helps keep the model physically consistent, resulting in a faster history

matching process requiring fewer iterations and model parameter changes in the case of porosity and absolute permeability driven history match with only varying relative-permeability functions within rock types.

6.2 Further cases

The following cases have been studied, and their results are summarised and compared in sub-chapter 6.3.

History Matching Results of PERMPC (Case 1.2)

In the presented test case, porosity and absolute permeability were the only modified parameters. In the case of PERMPC, the rock types are only distinguished through absolute permeability and capillary pressure.

History Matching Results of PERMPCKR (Case 1.3)

In the presented test case, porosity and absolute permeability were the only modified parameters. In the case of PERMPCKR, the rock types are only distinguished through absolute and relative permeability and capillary pressure.

History Matching Results of POROKR (Case2.1)

In the presented test case, porosity and absolute permeability were the only modified parameters. In the case of POROKR, the rock types are only distinguished through porosity and relative permeability.

History Matching Results of POROPC (Case2.2)

In the presented test case, porosity and absolute permeability were the only modified parameters. In the case of POROPC, the rock types are only distinguished through porosity and capillary pressure.

History Matching Results of POROPCKR (Case2.3)

In the presented test case, porosity and absolute permeability were the only modified parameters. In the case of POROPCKR, the rock types are only distinguished through porosity and relative permeability and capillary pressure.

History Matching Results of POROPERMKR (Case3.1)

In the presented test case, porosity and absolute permeability were the only modified parameters. In the case of POROPERMKR, the rock types are distinguished through all possible static model parameters (porosity, absolute permeability) and relative permeability.

History Matching Results of POROPERMPC (Case3.2)

Porosity and permeability were the only directly modified parameters in the presented test case. In the case of POROPERMPC, the rock types are distinguished through all possible static model parameters (porosity, absolute permeability) and capillary pressure.

History Matching Results of POROPERMPCKR (Case3.3)

Based on the calculated sensitivities in both history matching attempts of the presented test case, the porosity and absolute horizontal permeabilities (k_x, k_y,) were the only directly modified parameters. In the second attempt, the rock types are also adjusted; therefore, the corresponding parameters are changing: relative permeability and capillary pressure. The relative permeability and capillary pressure are not scaled or matched, meaning no changes to the defined curves. In the case of POROPERMPCKR, the rock types are distinguished through all possible parameters, namely porosity, absolute and relative permeability and capillary pressure. This case couples all the rock-type related features; therefore, this is the simple model's most complex, realistic and most comprehensive simulation scenario.

6.3 Results of the sensitivity analysis of the different parameters in rock type adjusting history matching workflow

History matching aims to improve the reservoir simulation model under given assumptions, constraints, and constitutive laws within predetermined feasibility regions, defined by relevant measurements. In general, while history matching a newly created model matches the observations, but violating the constraints and the established link between model parameters. The new model moves away from assumptions and initially gains knowledge from history matching. In order to measure if the changes are acceptable, there are geological consistency indicators introduced.

6.3.1 Geological consistency indicators

The used objective function (OF) described in the literature review is a suitable measure of how successful and satisfying the match is. The OF is calculated in the used adjoint-based optimisation application, which minimises the objective function, where it only contains the dynamic variables, such as pressures and fluid rates. Since this dissertation focuses on and improves geological consistency, some kind of indicator needs to be introduced to measure the deviation in static parameters. In order to not only rely on a visual judgment about the changes of the static properties, the geological consistency needs to be quantified. The

chosen parameter is the fraction of variance unexplained (FVU), which can be written through the definition of generalised R^2 for measured (calculated) variable f and observed variable y:

$$R^2 = 1 - \frac{SS_{res}}{SS_{tot}}$$

Eq. 6.1

$$FVU = 1 - R^2 = \frac{SS_{res}}{SS_{tot}}$$

Eq. 6.2

$$FVU[\%] = 100 \cdot FVU$$

Eq. 6.3

$$SS_{res} = \sum_i (y_i - f_i)^2$$

Eq. 6.4

$$SS_{tot} = \sum_i (y_i - \bar{y})^2$$

Eq. 6.5

, where SS_{res} is the sum of squares of residuals, and the SS_{tot} is the total sum of squares of measured difference with its mean. The FVU is used in this dissertation in the form of a percentage.

The FVU applied for porosity and absolute permeability grid properties can be written as:

$$FVU_{\phi}[\%] = 100 \cdot \frac{\sum_i (\phi_i^{true} - \phi_i)^2}{\sum_i (\phi_i^{true} - \bar{\phi}^{true})^2}$$

Eq. 6.6

$$FVU_{k}[\%] = 100 \cdot \frac{\sum_i (k_i^{true} - k_i)^2}{\sum_i \left(k_i^{true} - \bar{k}^{true}\right)^2}$$

Eq. 6.7

$$FVU_{\log_{10} k}[\%] = 100 \cdot \frac{\sum_i (\log_{10} k_i^{true} - \log_{10} k_i)^2}{\sum_i \left(\log_{10} k_i^{true} - \overline{\log_{10} k}^{true}\right)^2}$$

Eq. 6.8

, where ϕ_i, k_i are the grid block porosity and absolute permeability correspondingly, from a given model (final model), while $\phi_i^{true}, k_i^{true}$ are the properties from the "TRUTH" model. There is a luxury of comparing the final model to the "TRUTH" model in the case of the simple synthetic cases. Unfortunately, this is not an option in the usual practice, as the "TRUTH" model is unknown, and we can only refer to the base case.

The extended version of FVU for two sets of variables ϕ, k can be written as follows:

$$FVU_{\phi,k}[\%] = 100 \cdot \frac{\sum_i (\phi_i^{true} - \phi_i)^2 + \sum_i (k_i^{true} - k_i)^2}{\sum_i (\phi_i^{true} - \bar{\phi}^{true})^2 + \sum_i \left(k_i^{true} - \bar{k}^{true}\right)^2}$$

Eq. 6.9

$$FVU_{\phi,\log_{10} k}[\%] = 100 \cdot \frac{\sum_i(\phi_i^{true} - \phi_i)^2 + \sum_i(\log_{10} k_i^{true} - \log_{10} k_i)^2}{\sum_i(\phi_i^{true} - \bar{\phi}^{true})^2 + \sum_i\left(\log_{10} k_i^{true} - \overline{\log_{10} k}^{true}\right)^2}$$

Eq. 6.10

The results approved that the used adjoint workflow to be geologically consistent with and without the rock typing part on a global scale. The calculated FVU of the static model parameters independently and in their correlation in all of the nine tested cases were below 1% or equal to it. That means the R^2 is 99% or higher. These results are more proving a concept than being practical.

On the one hand, the FVU values are average globally, so this indicator cannot detect the details and local deviations. On the other hand, in the case of an actual field, the geological model is available only; it tries to mimic the underlying reservoir as much as possible; in the case of the simple model, it is the "TRUTH". Therefore in practice, validation of the final history matched model can only be through the base case. Therefore other factors need to be monitored for crosschecking the validity of the final matched model. It is vital to mention that, in history matching, the only available model which contains all the known (measured) information of the reservoir is the product of the geostatistical modelling. Therefore, maintaining the geological consistency in the final model means honouring the established relations between different model parameters in the static model, so the base case.

During the history matching process, the static model is adjusted to the dynamic data through the reservoir engineering part of the reservoir characterisation process while maintaining the information gathered and interpreted in the geostatistical modelling process. The chosen parameters are the geological consistency measures compared to the BASE case. Two new variables are introduced as geological consistency indexes: the rock type's validity and the Mahalanobis distance's validity.

Valid Rock Type (VRT)

The VRT shows the percentage of all the grid blocks which are located within the initial confidence interval. This number counts what percentage of grid blocks with rock types are inside the initially established confidence interval.

$$VRT\ [\%] = \frac{n_{FINAL}}{n_{BASE}} \cdot 100$$

Eq. 6.11

, where

n_{FINAL} – the number of cells (phi-k values) inside of the original ellipse in the final model,

n_{BASE} – the number of cells phi-k values inside the original ellipse in the base model.

Valid Mahalanobis Distance (VMD)

The second parameter for rock type validation is the VMD. It shows what percentage of all the grid-block belong to the correct rock type employing Mahalanobis distance. This indicator's estimation uses the validation step from the rock-typing workflow and counts the correct rock types. Theoretically, it should be 100% valid, but the results show on average between 90-100 % in most cases. This is possible and correct because of two reasons. This deviation is because the rock types can have overlapping areas during the history matching and because of an extra condition applied between the validation and correction step. As described in the rock typing workflow section, the additional condition is used to not just jump from rock types back and forth without control. The correction step is only applied in case of overlapping rock-types if the phi-k point already moved out from the ellipse of one rock type; until it does not happen, the phi-k point will not be assigned to the other rock type even if the calculated Mahalanobis distance would suggest that. This additional condition assures that the optimization is the least disturbed and that the changes are more consistent with the original model. Without the extra condition, the phi-k points could just shuffle back and forth without some sort of a path or logic. In this way, it is controlled and smooth.

This crosscheck is not applied for the calculation below because it would bias the results. Depending on the magnitude of the error, the overlap of the rock types can be interpreted. The bigger the deviation is, the

more significant the overlap or, in other words, the more valid the model based on the VMD indicator, the smaller the overlap is, so they smash into each other less.

$$VMD\ [\%] = \frac{n_{valid}}{n_{total}} \cdot 100$$

Eq. 6.12

, where

n_{valid} – number of grid blocks (phi-k points) with valid rock type,

n_{total} –the total number of grid blocks (phi-k points).

6.3.2 Summary of the nine test cases

The conventional or so-called standard (STD) and the rock-typing workflow (RT) were tested and compared during this research. The testing was carried out on synthetic test cases (in total 9) described in Chapter 5 through different history matching setups.

The two most significant and representative setup combinations are included in this dissertation. The first presented setup combination is the "BESTPARENT", and this is an automated combination of different setups, where three stages are applied. The first and the last

stage focuses on the overall match. The second stage emphasises the individual fluid rates.

The difference between the first and last stage is the scale of the maximum allowed parameter modifications within one iteration. The first stage starts with more flexible steps (more extensive range), and the last stage is intended for fine-tuning with the small range of maximum allowed changes.

The important detail of this automated setup combination is that four conditions are applied to change from one history matching setup to another one. The first condition is the sufficient minimum of the objective function (lower bound); the second condition is the maximum number of iterations; the third condition is the maximum of the objective function (upper bound). Then the fourth condition is a practical requirement, which ensures that every new setup stage starts from the best case within the previous iterations. This condition is intended to achieve better convergence rates and avoid overshooting, or in simple words, to prevent divergence (stepping out) from a good optimization track (path). The resemblance can be found in optimization procedures known as line search, when instead of applying the full optimization step suggested by the gradient, the algorithm estimates the objective function based on smaller steps in the same direction (stepping backwards) and chooses a step based on the best objective function value.

In an idealistic case, within the iterations, the objective function is minimized, and according to the first setup, when it reaches the desired sufficient minimum value, the next setup would be applied. This is not always the case, and during the iterations, if the starting case is not good enough or if the history matching setup is not adequately set, the OF might not reach the desired value or can be wrecked. Therefore, it is necessary to introduce secondary conditions. If the OF minimum is not reached, then a maximum number of iterations is applied as a second condition. Then in case of a failed match, when the history matching is entirely off, a maximum value for OF is applied in case not to waste time on false iterations. Once it goes in the wrong direction, it will never find back the way to the correct path. The third condition is to stop the iterations when the OF is invalid and move to the next setup.

There is also an important addition which is the search of the best parent case; since there can be inconsistencies introduced during the automated setup combination, it is not sufficient to start the new setup purely from the last iteration because it is not guaranteed that it started new setup because the desired minimum OF is reached. Therefore the automation needs to be controlled. The condition is always to start the new setup from the best case.

Best parent case history matching multiple setup combination

Tab. 5 summarizes the result of the applied BESTPARENT setup combination through standard and rock typing workflow accordingly.

BESTPARENT STD: Best parent case selection setup with the standard history matching workflow.

Tab. 4: Summary of the OF values in the FINAL models of the sensitivity analysis, history matched with the BESTPARENT setup combination through the standard (STD) workflow

ID	Iteration	Objective Function			
		Total	Oil rate	Water rate	BHP
PERMKR	111	0.1964	0.0859	0.0859	0.0246
PERMPC	120	0.7612	0.3800	0.3800	0.0012
PERMPCKR	127	0.6971	0.3441	0.3441	0.0090
POROKR	34	0.7581	0.3622	0.3622	0.0337
POROPC	82	0.6993	0.3434	0.3434	0.0124
POROPCKR	128	0.7709	0.3366	0.3366	0.0977
POROPERMKR	33	0.4581	0.2287	0.2287	0.0006
POROPERMPC	20	0.7819	0.3891	0.3891	0.0037
POROPERMPCKR	126	0.6997	0.3490	0.3490	0.0018

Tab. 4 shows the number of iterations and the objective function (OF) values in each case achieved through the standard workflow.

Tab. 5 shows the results of the geological consistency (GC) values for each case matched with the standard workflow.

Tab. 5: Summary of the GC values in the FINAL models achieved through the standard workflow

ID	Iteration	Geological Consistency	
		VRT	VMD
PERMKR	111	75.50	92.25
PERMPC	120	24.75	72.25
PERMPCKR	127	68.75	83.50
POROKR	34	93.75	100.00
POROPC	82	87.50	97.25
POROPCKR	128	88.50	100.00
POROPERMKR	33	54.25	79.75
POROPERMPC	20	62.75	87.75
POROPERMPCKR	126	44.25	81.75

BESTPARENT RT: Best parent case selection setup with the rock typing history matching workflow.

Tab. 6 and 7 show the number of iterations and the objective function (OF) values, and the results of the geological consistency (GC) values for each case achieved with the rock typing (RT) workflow.

Tab. 6: Summary of the OF values in the FINAL models of the sensitivity analysis, history matched with the BESTPARENT setup combination through the rock typing workflow

ID	Iteration	Objective Function			
		Total	Oil rate	Water rate	BHP
PERMKR	9.00	0.1311	0.0407	0.0407	0.0497
PERMPC	13.00	0.2352	0.1152	0.1152	0.0048
PERMPCKR	12	0.0918	0.0456	0.0456	0.0005
POROKR	33	0.7572	0.3618	0.3618	0.0337
POROPC	25	0.5326	0.2635	0.2635	0.0057
POROPCKR	128	0.7709	0.3366	0.3366	0.0977
POROPERMKR	9	0.8284	0.4016	0.4016	0.0252
POROPERMPC	22	0.1708	0.0851	0.0851	0.0006
POROPERMPCKR	15	0.0489	0.0244	0.0244	0.0001

Tab. 7: Summary of the GC values in the FINAL models achieved through the rock typing workflow

ID	Iteration	Geological Consistency	
		VRT	VMD
PERMKR	9.00	84.00	96.25
PERMPC	13.00	94.50	98.75
PERMPCKR	12	96.00	99.00
POROKR	33	93.75	100.00
POROPC	25	91.75	99.50
POROPCKR	128	88.50	100.00
POROPERMKR	9	63.75	90.00
POROPERMPC	22	74.25	93.50
POROPERMPCKR	15	37.25	90.25

Multiple history matching setup combination with the maximum number of iterations

The simplest multiple setup combination results are presented in this section for standard and rock-typing workflow as well. Here, the applied conditions were only the number of maximum iterations at each setup stage, and the stages were the same as in the BESTPARENT setup combination

These results serve as the basis for the optimised setup combination presented above. The results show an obvious need for smarter conditions for each stage, such as monitoring lower and upper bound objective function values and selecting the best parent case.

In this case, the results are not as good as in the BESTPARENT history matching setup, but already show improvements with the rock typing workflow compared to the standard workflow. In most cases, the iteration number and objective function are improved; the porosity dependent cases were neither successful with this setup combination.

Tab. 8, 9, 10 and 11 summarise the history matching result achieved using the ITERNUM multiple setup combination. The summary shows the number of iterations and the objective function (OF) values and as well as the results of the geological consistency (GC) values for each case achieved with the standard (STD) and the rock typing (RT) workflow accordingly.

ITERNUM STD: Maximum iteration number setup with the standard history matching workflow.

Tab. 8: Summary of the OF values in the FINAL models of the sensitivity analysis, history matched with the ITERNUM setup combination through the standard workflow

ID	Iteration	Objective Function			
		Total	Oil rate	Water rate	BHP
PERMKR	15	0.6088	0.3043	0.3043	0.0001
PERMPC	67	0.5569	0.2531	0.2531	0.0508
PERMPCKR	62	0.7530	0.3593	0.3593	0.0344
POROKR	33	0.2143	0.1043	0.1043	0.0057
POROPC	30	0.6341	0.3160	0.3160	0.0021
POROPCKR	21	0.7158	0.3564	0.3564	0.0030
POROPERMKR	62	0.4683	0.2125	0.2125	0.0432
POROPERMPC	63	0.3963	0.1814	0.1814	0.0335
POROPERMPCKR	12	0.7628	0.3569	0.3570	0.0489

Tab. 9: Summary of the GC values in the FINAL models achieved through the standard workflow

ID	Iteration	Geological Consistency	
		VRT	VMD
PERMKR	15	75.25	47.50
PERMPC	67	79.25	38.50
PERMPCKR	62	93.75	88.25
POROKR	33	89.75	64.00
POROPC	30	99.25	90.75
POROPCKR	21	94.25	73.75
POROPERMKR	62	72.00	25.00
POROPERMPC	63	74.50	48.50
POROPERMPCKR	12	87.25	78.25

ITERNUM RT: Maximum iteration number setup with the rock typing history matching workflow.

Tab. 10: Summary of the OF values in the FINAL models of the sensitivity analysis, history matched with the ITERNUM setup combination through the rock typing workflow

ID	Iteration	Objective Function			
		Total	Oil rate	Water rate	BHP
PERMKR	49	0.1196	0.0589	0.0589	0.0019
PERMPC	12	0.0972	0.0377	0.0377	0.0219
PERMPCKR	10	0.2766	0.1321	0.1321	0.0124
POROKR	1	1.0469	0.4543	0.4543	0.1383
POROPC	28	0.6484	0.3203	0.3203	0.0079
POROPCKR	17	0.4744	0.2337	0.2337	0.0071
POROPERMKR	69	0.1465	0.0548	0.0548	0.0368
POROPERMPC	52	0.0152	0.0075	0.0075	0.0001
POROPERMPCKR	35	0.0260	0.0130	0.0130	0.0000

Tab. 11: Summary of the GC values in the FINAL models achieved through the rock typing workflow

ID	Iteration	Geological Consistency	
		VRT	VMD
PERMKR	49	93.75	47.75
PERMPC	12	99.50	88.75
PERMPCKR	10	99.25	95.75
POROKR	1	100.00	93.50
POROPC	28	100.00	91.00
POROPCKR	17	99.00	86.25
POROPERMKR	69	85.50	45.50
POROPERMPC	52	89.75	47.50
POROPERMPCKR	35	92.50	47.00

6.3.3 Summary of the analysis of the different parameters in rock type adjusting history matching workflow

The geological inconsistencies can be easily missed out after getting a good match because a complex model with rich parameter space can mimic the behaviour of the reservoir with original assumptions but with an unphysical combination of parameter values. That is fundamentally incorrect and will lead to the wrong prediction of future flow behaviour.

The sensitivity analysis on the presented nine cases shows that each of the properties can have its own severity effect on the quality and consistency of the matched final model.

On the side of the physical meaning, the properties have mathematical characteristics and representation as scalar value (magnitude), direction, linear/non-linear function. Depending on the position in each equation, those properties can have an effect of simple shift or scale too. In other words, the parameters which take a more significant place in the conservation equations (equation term, e.g. Darcy velocity, storage term) can introduce more flexibility to match the observations, but with the risk of violating the feasibility of the model itself. Porosity appears in the storage term, influencing the fluid content in the grid cell, while absolute permeability, relative permeability and capillary pressure are part of the Darcy velocity term, which affects the magnitude and direction of the flow. Absolute permeability and relative permeability

are responsible for the advective part of total and phase flow correspondingly, while capillary pressure is associated with the diffusive part of the flow.

Therefore, it can be seen that porosity being present only in storage and having less freedom of mimicking other characteristics of flow cannot by itself solve the issue of an insufficient history match. Hence the rock type adjustment workflow is absolutely vital for achieving better history matching results and reproducing correct dynamic reservoir behaviour.

On the other hand, absolute and relative permeabilities have a more superior position in the model structure, the darcy velocity, controlling the path and speed of flow (advective part of the flow). Absolute and relative permeability appear in darcy velocity together as a product, which is called effective permeability $k_{eff} = k \cdot k_r$. A change in absolute permeability affects all phases, and a change in relative permeability affects only the selected phase. Effective permeability can mimic a wider variety of reservoir fluid flow behaviour but at the same time have more significant risks of violating the original assumptions and introducing more geologically apparent inconsistencies. That can give a wrong impression on the model nature and change the view on the reservoir without the knowledge-proven basis; in other words, it can present a reservoir engineer with an unfeasible predictive scenario.

Capillary pressure has a significant effect on the initial – "static" saturation distribution (local fluid volumes), and being also a part of

darcy velocity affects the flow path (the diffusive part of the flow). Therefore, it can also mimic a wide variety of flow patterns. In addition, in the case of wrongly assigned rock type, the volumetric part of the cell can be compensated by unfeasible porosity values, which achieves the goal of the matching (primarily for pressure), but introduces the wrong model with incorrect fluid volumes spatially, which is not supported by relevant measurements.

It is important to mention that the analysed models consist of only one layer in this work. Therefore the influence of capillary and gravity forces is not present to the fullest extent. In addition, it is of general knowledge that when the history period does not have an injection phase, capillary pressure has a larger effect on history matching. However, if the prediction phase is dominated by injection, then capillary pressure plays a minor role, and the viscous forces prevail. Therefore, in the viscous dominated regime, the fluxes are proportional to a pressure gradient (pressure difference) between production and injection wells, and the flow direction is given from injection to production well.

Chapter 7 Summary

This chapter summarises the main findings and outcomes, including the proposed workflow's benefits, completed objectives and lack of features, and the suggested possible improvements.

7.1 Conclusion

This dissertation focuses on improving the conventional gradient-based assisted history matching procedure by developing an external workflow. This novel approach is meant to adjust the rock types to reach a better geological consistency level and automate the history matching setup sequence. The latter implies that the emphasis would be automatically switched from one dynamic variable to another, e.g. when the fluid rates match within an acceptable level, the emphasis will switch to pressure match.

7.1.1 Concluding remarks

Geological consistency:

One of the primary objectives was to improve the geological consistency to a higher level than it can currently be achieved. The geological consistency is proven to be maintained through rock type definition. In this new workflow, including the correlations, the rock type binds all of the geological properties together, where every parameter iteratively changes consistently. The porosity and absolute permeability cannot define the rock type by themselves independently. Treating each grid block's porosity and absolute permeability values as one data point through their correlation in the ϕ-k space proves success in solving this issue.

The Mahalanobis distance calculation and confidence interval integrate all properties with their probability ranges; the porosity and absolute permeability values are not examined separately. Integrating the Mahalanobis distance calculation for the rock type validation and correction has successfully proved to keep the model away from physical and geological inconsistencies without sacrificing the matching of dynamic properties.

Automated-extended workflow:

The designed general workflow is robust and can be applied to any simulation software to perform automated history matching. It is easily adaptable to other assisted history matching tools.

- Proof of Concept Model: The developed synthetic two-phase 2D model serves the fundamental purpose of proving the concept within realistic data ranges and distributions. The built simple model is a quarter of a five-spot model, with one oil producer and water injector. The model includes two rock types, representing a relatively good and a poorer quality rock with their characteristic petrophysical parameter distributions. The test cases prove the concept and highlight the necessity of improved history matching in terms of linked petrophysical properties through the rock type definition. The suggested changes in porosity and absolute permeability drive the rock type change in the workflow. The used method allows for independent porosity and absolute permeability changes in each grid block. The proposed algorithm results show significant improvements while keeping the model geologically consistent.

- Sensitivity Analysis: The performance of the extended workflow concerning the parameters which characterise different rock types, namely porosity, absolute permeability,

relative permeability, and capillary pressure functions, is analysed. The advantages of the created workflow over the standard adjoint approach are demonstrated through the different history matching cases with different scenarios. The sensitivity analysis provides a comprehensive comparison of the significance of each model parameter on the rock type adjusting history matching workflow. The results subsequently conclude the necessity of rock type validation and correction. On top of that, it can also be concluded that a "smart" well-constrained automation is beneficial for achieving maximum efficiency and quality.

7.1.2 Summary

In conclusion, the rock typing workflow shows more favourable results than the conventional method by itself. The history match with the same quality could not be achieved with only the absolute permeability and porosity change (the standard conventional way). The success of the rock type validation and correction lies in the details because the rock typing workflow can indirectly adjust the relative permeability and capillary pressure. Compared to absolute permeability, relative permeability has a more dynamic nature since it is a fluid phase and saturation dependent. From the initialization point of view, in order to have the right amount of fluid in place, the rock type properties should be honoured. On the one hand, the connate water saturations are taken from the corresponding saturation functions. On the other hand, the

capillary pressure function significantly impacts the correct spatial distribution of the fluid saturations and, therefore, the correct fluid volumes.

Overall, the novel approach improves the geological consistency of the models during the history matching process, thereby improving the quality and reliability of the reverse simulation. Moreover, this extension includes workflow automation, which is a great standalone achievement that can potentially reduce the work hours previously required for the iterations to find the right set of data.

7.2 Future work

The following future investigations are suggested to be done in order to develop the tool for further improved history match: (i) Application of constrained optimization with provided feasibility regions for rock types on the porosity-permeability diagram and (ii) extending the objective function with multiobjective optimization to preserve the rock type distribution. (iii) Execution of the rock typing workflow on a full-field model and comparison to the standard workflow. (iv) Testing the rock typing workflow in the case of different wetting regions within one rock type, where the different saturation functions can be considered accordingly.

References

[1] Aanonsen, S. I. *et al.* (2009) 'The Ensemble Kalman Filter in Reservoir Engineering--a Review', *SPE Journal*, 14(03), pp. 393–412. doi: 10.2118/117274-PA.

[2] Almuallim, H. *et al.* (2010) 'SPE 131627 History-Matching With Sensitivity-Based Parameter Modifications at Grid- Block Level', *Paper presented at the SPE EUROPEC/EAGE Annual Conference and Exhibition, Barcelona, Spain, June 2010.* doi: 10.2118/131627-MS.

[3] Almuallim, H. *et al.* (2018) 'Advanced assisted history matching of a large mature oil field based on a huge number of grid-block level parameters and saturation functions', *Society of Petroleum Engineers - Abu Dhabi International Petroleum Exhibition and Conference 2018, ADIPEC 2018.* doi: 10.2118/192780-ms.

[4] Amaefule, J. O. *et al.* (1993) 'Enhanced reservoir description: using core and log data to identify hydraulic (flow) units and predict permeability in uncored intervals/ wells', *Proceedings - SPE Annual Technical Conference and Exhibition*, Omega(c), pp. 205–220. doi: 10.2523/26436-ms.

[5] Awofodu, D. D. (2019) *Improving Reservoir Characterization using the Adjoint Method in History Matching.* Doctoral Thesis. Clausthal University of Technology. doi: 10.21268/20200407-0.

[6] Awofodu, D. D., Ganzer, L. and Almuallim, H. (2018)

'Revealing Hidden Reservoir Features During History Matching Using An Adjoint Method', *16th European Conference on the Mathematics of Oil Recovery, ECMOR 2018*, 2018(1), pp. 1–18. doi: 10.3997/2214-4609.201802141.

[7] Aziz, K. and Settari, A. (1979) *Petroleum reservoir simulation*. Applied Science Publishers.

[8] Bäck, T. (1996) *Evolutionary Algorithms in Theory and Practice*, *Evolutionary Algorithms in Theory and Practice*. Oxford University Press. doi: 10.1093/OSO/9780195099713.001.0001.

[9] Bear, J. (1988) *Dynamics of Fluids in Porous Media*. Environmental Science.

[10] BeicipFranlab (2021) *CougarFlow Uncertainty Management & Assisted History Matching*. Available at: https://www.beicip.com/uncertainty-management-assisted-history-matching.

[11] Bentley, M. (2016) 'Modelling for comfort?', *Petroleum Geoscience*, 22(1), pp. 3–10. doi: 10.1144/petgeo2014-089.

[12] Bódi, T. (2006) *Rezervoármérnöki alapok*. Miskolc: University of Miskolc.

[13] Bokeh Development Team (2021) 'Bokeh: Python library for interactive visualization'. Available at: https://bokeh.org/.

[14] Brooks, R. H. and Corey, A. T. (1966) 'Properties of Porous Media Affecting Fluid Flow', *Journal of the Irrigation and Drainage Division*, 92(2), pp. 61–88. doi: 10.1061/JRCEA4.0000425.

[15] Bukshtynov, V. *et al.* (2015) 'Comprehensive framework for gradient-based optimization in closed-loop reservoir management', *Computational Geosciences*, 19(4), pp. 877–897.

doi: 10.1007/s10596-015-9496-5.

[16] Burdine, N. T. (1953) 'Relative Permeability Calculations From Pore Size Distribution Data', *Journal of Petroleum Technology*, 5(03), pp. 71–78. doi: 10.2118/225-G.

[17] Caers, J. (2002) 'Geostatistical History Matching under Training-Image Based Geological Model Constraints', *Proceedings - SPE Annual Technical Conference and Exhibition*, pp. 869–884. doi: 10.2118/77429-ms.

[18] Chandra, V. *et al.* (2015) 'Effective integration of reservoir rock-typing and simulation using near-wellbore upscaling', *Marine and Petroleum Geology*, 67, pp. 307–326. doi: 10.1016/j.marpetgeo.2015.05.005.

[19] Chen, Y. and Oliver, D. S. (2010) 'Ensemble-based closed-loop optimization applied to brugge field', *SPE Reservoir Evaluation and Engineering*, 13(1), pp. 56–71. doi: 10.2118/118926-PA.

[20] Christiansen, R. L. (2001) *Two-phase Flow Through Porous Media: Theory, Art and Reality of Relative Permeability and Capillary Pressure*. Golden, Colo. Petroleum Engineering Dept., Colorado School of Mines 2001.

[21] Christie, M., Arnold, D. and Winton, G. (2021) *Raven*. Available at: http://useraven.com/.

[22] Class, H. *et al.* (2009) 'A benchmark study on problems related to CO2 storage in geologic formations', *Computational Geosciences 2009 13:4*, 13(4), pp. 409–434. doi: 10.1007/S10596-009-9146-X.

[23] Computer Modelling Group, C. M. (2021) *CMOST-AI*. Available at: https://www.cmgl.ca/cmost-ai.

[24] Corey, A. T. (1994) *Mechanics of immiscible fluids in porous media*. Water Resources Publications.

[25] Crevillén-García, D. (2018) 'Surrogate modelling for the prediction of spatial fields based on simultaneous dimensionality reduction of high-dimensional input/output spaces', *Royal Society Open Science*, 5(4). doi: 10.1098/RSOS.171933.

[26] Debye, P. (1909) 'Näherungsformeln für die Zylinderfunktionen für große Werte des Arguments und unbeschränkt veränderliche Werte des Index', *Mathematische Annalen 1909 67:4*, 67(4), pp. 535–558. doi: 10.1007/BF01450097.

[27] Dorigo, M. and Gambardella, L. M. (1997) 'Ant colony system: A cooperative learning approach to the traveling salesman problem', *IEEE Transactions on Evolutionary Computation*, 1(1), pp. 53–66. doi: 10.1109/4235.585892.

[28] EMERSON (2021) *Tempest ENABLE*. Available at: https://www.pdgm.com/products/tempest/tempest-enable#.

[29] Ertekin, T., Abou-Kassem, J. H. and King, G. R. (2001) *Basic Applied Reservoir Simulation*. Society of Petroleum Engineers.

[30] Evensen, G. (1994) 'Sequential data assimilation with a nonlinear quasi-geostrophic model using Monte Carlo methods to forecast error statistics', *Journal of Geophysical Research: Oceans*, 99(C5), pp. 10143–10162. doi: 10.1029/94JC00572.

[31] Felsenthal, M. (1979) 'A statistical study of some waterflood parameters.', *JPT*, 31(10), pp. 1303–1304. doi: 10.2118/7666-PA.

[32] Gnedenko, B. V. and Kolmogorov, A. N. (1954) *Limit distributions for sums of independent random variables*. Addison-Wesley.

[33] Guo, G. *et al.* (2007) 'Rock typing as an effective tool for permeability and water-saturation modeling: A case study in a

clastic reservoir in the Oriente basin', *SPE Reservoir Evaluation and Engineering*, 10(6), pp. 730–739. doi: 10.2118/97033-pa.

[34] Harris, C. R. *et al.* (2020) 'Array programming with NumPy', *Nature*, 585(7825), pp. 357–362. doi: 10.1038/s41586-020-2649-2.

[35] Hastings, W. K. (1970) 'Monte carlo sampling methods using Markov chains and their applications', *Biometrika*, 57(1), pp. 97–109. doi: 10.1093/BIOMET/57.1.97.

[36] Heinemann, Z. E. and Mittermeier, G. M. (2013) *TEXTBOOK SERIES VOLUME 1 FLUID FLOW IN POROUS MEDIA*. Leoben.

[37] Helmig, R. (1997) 'Multiphase Flow and Transport Processes in the Subsurface', *Multiphase Flow and Transport Processes in the Subsurface*. doi: 10.1007/978-3-642-60763-9.

[38] Honarpour, M., Koederitz, L. and Harvey, A. H. (1986) 'Relative permeability of petroleum reservoirs', *Relative Permeability of Petroleum Reservoirs*, pp. 1–143.

[39] HOT Engineering (2021) *SENSITIVITY EXPLORER – THE DISRUPTIVE HISTORY MATCHING TOOL*. Available at: https://hoteng.com/reservoir-innovations_senex/.

[40] James, G., Witten, D., Hastie, T., Tibshirani, R. (2013) *An Introduction to Statistical Learning - with Applications in R*. Springer.

[41] Jenei, B. (2017) *Numerical modelling and automated history matching in SCAL for improved data quality*. Master's Thesis. Montanuniversität Leoben.

[42] Jenei, B. *et al.* (2020) 'Geologically consistent history matching honouring rock types driven by adjoint method', *Society of*

Petroleum Engineers - Abu Dhabi International Petroleum Exhibition and Conference 2020, ADIPEC 2020. doi: 10.2118/203231-ms.

[43] Johnson, H. D. (1996) 'Stochastic modeling and geostatistics: Principles, methods, and case studies', *Marine and Petroleum Geology*, 13(7), pp. 859–860. doi: 10.1016/0264-8172(96)83699-3.

[44] Journel, A. and Alabert, F. (1990) 'New method for reservoir mapping', *J. Pet. Technol.*, 42(02), pp. 212–218. doi: 10.2118/18324-pa.

[45] Kalman, R. E. (1960) 'A new approach to linear filtering and prediction problems', *Journal of Fluids Engineering, Transactions of the ASME*, 82(1), pp. 35–45. doi: 10.1115/1.3662552.

[46] Kennedy, J. and Eberhart, R. (1995) 'Particle swarm optimization', *Proceedings of ICNN'95 - International Conference on Neural Networks*, 4, pp. 1942–1948. doi: 10.1109/ICNN.1995.488968.

[47] Levenberg, K. (1944) 'A method for the solution of certain non-linear problems in least squares', *Quarterly of Applied Mathematics*, 2(2), pp. 164–168. doi: 10.1090/QAM/10666.

[48] Leverett, M. C. (1941) 'Capillary Behavior in Porous Solids', *Transactions of the AIME*, 142(01), pp. 152–169. doi: 10.2118/941152-g.

[49] Li, G. and Reynolds, A. C. (2009) 'Iterative Ensemble Kalman Filters for Data Assimilation', *SPE Journal*, 14(03), pp. 496–505. doi: 10.2118/109808-PA.

[50] Liu, D. C. and Nocedal, J. (1989) 'On the limited memory BFGS method for large scale optimization', *Mathematical*

Programming 1989 45:1, 45(1), pp. 503–528. doi: 10.1007/BF01589116.

[51] Liu, N. and Oliver, D. S. (2003) 'Automatic History Matching of Geologic Facies', *Proceedings - SPE Annual Technical Conference and Exhibition*, pp. 5471–5480. doi: 10.2523/84594-MS.

[52] Liu, N. and Oliver, D. S. (2005) 'Ensemble Kalman filter for automatic history matching of geologic facies', *Journal of Petroleum Science and Engineering*, 47(3–4), pp. 147–161. doi: 10.1016/j.petrol.2005.03.006.

[53] Lomeland, F., Ebeltoft, E. and Thomas, W. H. (2005) 'A New Versatile Relative Permeability Correlation', in *Proceedings of the 2005 International Symposium of the SCA, Abu Dhabi, United Arab Emirates, October 31 - November 2*.

[54] Mahalanobis, P. C. (1936) 'On the generalized distance in statistics', *Proceedings of the National Institute of Science of India*, pp. 49–55.

[55] Manasipov, R. (2021) *Unpublished Research Note*.

[56] Marquardt, D. W. (2006) 'An Algorithm for Least-Squares Estimation of Nonlinear Parameters', *SIAM Journal on Applied Mathematics*, 11(2), pp. 431–441. doi: 10.1137/0111030.

[57] Maschio, C., Vidal, A. C. and Schiozer, D. J. (2008) 'A framework to integrate history matching and geostatistical modeling using genetic algorithm and direct search methods', *Journal of Petroleum Science and Engineering*, 63(1–4), pp. 34–42. doi: 10.1016/j.petrol.2008.08.001.

[58] Michael, H. A. and Voss, C. I. (2009) 'Estimation of regional-scale groundwater flow properties in the Bengal Basin of India and Bangladesh', *Hydrogeology Journal 2009 17:6*, 17(6), pp.

1329–1346. doi: 10.1007/S10040-009-0443-1.

[59] Mosser, L., Dubrule, O. and Blunt, M. J. (2019) 'DeepFlow: History Matching in the Space of Deep Generative Models', *arXiv preprint*. Available at: http://arxiv.org/abs/1905.05749.

[60] Nelder, J. A. and Mead, R. (1965) 'A Simplex Method for Function Minimization', *The Computer Journal*, 7(4), pp. 308–313. doi: 10.1093/COMJNL/7.4.308.

[61] Nocedal, J. and Wright, S. J. (2006) 'Numerical optimization', in *Springer Series in Operations Research and Financial Engineering*. doi: 10.1007/978-0-387-40065-5.

[62] Oliver, D. S. and Chen, Y. (2010) 'Recent progress on reservoir history matching: a review', *Computational Geosciences 2010 15:1*, 15(1), pp. 185–221. doi: 10.1007/S10596-010-9194-2.

[63] Oliver, D. S., Reynolds, A. C. and Liu, N. (2008) *Inverse theory for Petroleum Reservoir Characterization and History Matching*. Cambridge University Press.

[64] pandas development team, T. (2020) 'pandas-dev/pandas: Pandas'. Zenodo. doi: 10.5281/zenodo.3509134.

[65] Panfilov, M. (2010) 'Underground Storage of Hydrogen: In Situ Self-Organisation and Methane Generation', *Transport in Porous Media 2010 85:3*, 85(3), pp. 841–865. doi: 10.1007/S11242-010-9595-7.

[66] Pyrcz, M. J. (2018a) *07 Data Analytics: Confidence Interval*. Texas, United States of America. Available at: https://youtu.be/oaXCcTWcU04.

[67] Pyrcz, M. J. (2018b) *15 Data Analytics: Facies Modeling*. Texas, United States of America. Available at: https://youtu.be/vd3A7RLVzA4.

[68] Pyrcz, M. J. (2018c) *Data Analytics and Geostatistics*. Texas,

United States of America. Available at: https://youtu.be/pxckixOlguA.

[69] Pyrcz, M. J. and Deutsch, C. V (2014) *Geostatistical Reservoir Modeling*. Second edi. New York: Oxford University Press. Available at: https://books.google.at/books?id=wNhBAgAAQBAJ.

[70] Resoptima (2021) 'ResX'. Available at: https://resoptima.com/product/resx/.

[71] Ringrose, P. and Bentley, M. (2015) *Reservoir Model Design*, *Reservoir Model Design*. Springer. doi: 10.1007/978-94-007-5497-3.

[72] Rock Flow Dynamics (2021) 'User Manual - TNavigator 21.2'.

[73] Rock Fluid Dynamics (2021) *tNavigator*. Available at: ttps://rfdyn.com/tnavigator.

[74] Romero, C. E. and Carter, J. N. (2001) 'Using genetic algorithms for reservoir characterisation', *Journal of Petroleum Science and Engineering*, 31(2–4), pp. 113–123. doi: 10.1016/S0920-4105(01)00124-3.

[75] Schlumberger (2020a) 'Eclipse Manual 2020.1'.

[76] Schlumberger (2020b) 'Petrel Manual 2020'.

[77] Schlumberger (2021) *MEPO - Multiple Realization Optimizer*. Available at: https://www.software.slb.com/products/mepo#sectionFullWidthTable.

[78] Schulze-Riegert, R. *et al.* (2013) 'Strategic scope of alternative optimization methods in history matching and prediction workflows', *SPE Middle East Oil and Gas Show and Conference, MEOS, Proceedings*, 2, pp. 1472–1485. doi: 10.2118/164337-ms.

[79] Storn, R. and Price, K. (1997) 'Differential Evolution – A Simple and Efficient Heuristic for global Optimization over Continuous Spaces', *Journal of Global Optimization 1997 11:4*, 11(4), pp. 341–359. doi: 10.1023/A:1008202821328.

[80] Streamsim Technologies (2021) *3DSL Simulator*. Available at: https://www.streamsim.com/technology/streamlines/3dsl-simulator.

[81] Tarek Ahmed (2010) *Reservoir Engineering Handbook*. Elsevier Inc. doi: 10.1016/C2009-0-30429-8.

[82] Thiele, M. R. and Batycky, R. P. (2016) 'Evolve: A linear workflow for quantifying reservoir uncertainty', *Proceedings - SPE Annual Technical Conference and Exhibition, UAE, September 2016.*, pp. 26–28. doi: 10.2118/181374-ms.

[83] Tiab, D. and Donaldson, E. C. (2015) 'Petrophysics: Theory and Practice of Measuring Reservoir Rock and Fluid Transport Properties: Fourth Edition', *Petrophysics: Theory and Practice of Measuring Reservoir Rock and Fluid Transport Properties: Fourth Edition*, pp. 1–894. doi: 10.1016/C2014-0-03707-0.

[84] Virtanen, P. *et al.* (2020) 'SciPy 1.0: Fundamental Algorithms for ScientificComputing in Python', *Nature Methods*, 17, pp. 261–272. doi: 10.1038/s41592-019-0686-2.

[85] Wang, L. and Oliver, D. S. (2021) 'Fast robust optimization using bias correction applied to the mean model', *Computational Geosciences*, 25(1), pp. 475–501. doi: 10.1007/s10596-020-10017-y.

[86] Zakirov, E. S. *et al.* (2017) 'Automated geologically-consistent history matching of facies distribution and reservoir properties in inter-well space by adjoint methods', *Society of Petroleum Engineers - SPE Russian Petroleum Technology Conference*

2017. doi: 10.2118/187803-ms.

[87] Zubarev, D. I. (2009) 'Pros and Cons of Applying Proxy-models as a Substitute for Full Reservoir Simulations', *Proceedings - SPE Annual Technical Conference and Exhibition*, 5, pp. 3234–3256. doi: 10.2118/124815-MS.